Current Based Condition Monitoring of Electromechanical Systems

Model-free drive system current monitoring: faults detection and diagnosis through statistical features extraction and support vector machines classification

M.M.A. Bin Hasan BSc, MSc

Submitted for the degree of Doctor of Philosophy

School of Engineering Design and Technology

University of Bradford

2012

Keywords: Predictive maintenance, condition monitoring, induction motor, fault detection, machine learning, support vector machines.

Abstract

A non-invasive, on-line method for detection of mechanical (rotor, bearings eccentricity) and stator winding faults in a 3-phase induction motors from observation of motor line current supply input. The main aim is to avoid the consequence of unexpected failure of critical equipment which results in extended process shutdown, costly machinery repair, and health and safety problems.

This thesis looks into the possibility of utilizing machine learning techniques in the field of condition monitoring of electromechanical systems. Induction motors are chosen as an example for such application. Electrical motors play a vital role in our everyday life. Induction motors are kept in operation through monitoring its condition in a continuous manner in order to minimise their off times. The author proposes a model free sensor-less monitoring system, where the only monitored signal is the input to the induction motor. The thesis considers different methods available in literature for condition monitoring of induction motors and adopts a simple solution that is based on monitoring of the motor current. The method proposed use the feature extraction and Support Vector Machines (SVM) to set the limits for healthy and faulty data based on the statistical methods. After an extensive overview of the related literature and studies, the motor which is the virtual sensor in the drive system is analysed by considering its construction and principle of operation. The mathematical model of the motor is used for analysing the system. This is followed by laboratory testing of healthy motors and comparing their output signals with those of the same motors after being intentionally failed, concluding with the development of a full monitoring system. Finally, a monitoring system is proposed that can detect the presence of a fault in the monitored machine and diagnose the fault type and severity.

Acknowledgments

In the name of Allah, the most gracious, the most merciful.

At the beginning, all thanks and gratitude is to the Almighty Allah for giving me all the courage and assistance to reach this stage.

I would like to express my sincere gratitude to the Libyan Peoples in wide and Ministry of Higher Education, Libya for sponsoring me though out this course in the form of a scholarship.

Special thanks go to both of my supervisors Professor M. K. Ebrahimi and Professor I. Mujtaba for their support and guidance throughout all the phases of this work.

A word of thanks should go to colleague Mr. William Bradley with whom the design and implementation of the whole experiments were carried out.

Switchgear & Instruments Ltd. should be thanked for their financial support in the form of providing the test rig and testing needs.

Another expression of thanks should be extended to Mr. Chib who comes all the way of his work to help in implementing the tests either by ideas or by direct involvement in executing certain works. Not forgetting the staff of the mechanical workshops where most of the tests preparations were made.

Last but not least, special thanks and gratitude to my wife, Entesar, who stood, and still, beside me all the way, who without her patience, help, and encouragement this work wouldn't come to light; and to my family back home for their endless support.

Bradford, November 2012

Table of Contents

List of Figures

List of Tables

Chapter 1. Introduction

Condition monitoring (CM) means the continuous evaluation of the health of plant and equipment throughout its serviceable life [1]. Taking measurements while the machine is operational is called on-line condition monitoring. As a simple fault may lead to very costly damage, the idea of detecting a fault, confronting it and relating it to ideally one cause before it deteriorates is the main concern of engineers and researchers. Hence, the idea of condition monitoring and fault detection has emerged.

Early detection and diagnosis of process faults while the plant is still operating in a controllable region can help avoid abnormal event progression and reduce productivity losses which in turn can help avoid major system breakdowns and catastrophes.

Faults or abnormal conditions, as referred to in industry, can lead to huge loses of monies and time. For example, It is estimated that the petrochemical industry alone in the US incurs approximately 20 billion dollars in annual losses due to poor abnormal event management (AEM) [2]. And hence they have rated AEM as their number one problem that needs to be solved [3]. This explains the considerable interest in this field now from industrial practitioners as well as academic researchers. In some industries, maintenance now is the second highest or even the highest element of operating costs. As a result in the last three decades it has moved from almost nowhere to the top of the league as a cost control priority [4].

1.1 Maintenance Approach

All maintenance schemes have contained two types of works [1, 5]; the first of which is an immediate reaction to plant failures (breakdown or reactive) maintenance. The other is the fixed time interval or preventive maintenance, which is performed during fixed times where engineers take the advantage of slow production cycles to carry out such tasks. A third type of maintenance has emerged recently which is based on monitoring (condition based maintenance) of the process condition [1, 5, 6]. It involves fault detection and diagnosis. The main advantage of such method is increasing machine availability and performance, reducing sequential damage, increasing machine life, and reducing spare parts inventories [5]. An efficient CM scheme is capable of providing warning and predicting faults at early stage [7]. Table 1.1 shows a comparison between the three types of maintenance.

1.2 Fault Detection and Diagnosis Tasks

Fault detection and diagnosis (FDD) involves the following tasks:

- Fault Detection: to tell whether there is a fault or everything is functioning well.
- Fault Isolation: to determine the location of the fault and which part has become faulty.
- Fault Evaluation: where the size and type or nature of fault has been estimated.

Table 1.1 Maintenance Types [4]

	Reactive Maintenance	Preventive Maintenance	Predictive Maintenance
Advantages	No Upfront costs i.e. equipment, training. Seen as an easy option	Maintenance is planned and helps prevent unplanned breakdowns	Risk of unexpected breakdowns are reduced
		Fewer catastrophic failures resulting in expensive secondary damage	Equipment life is extended
		Great control over inventory	Reduce inventory and labour costs
			Maintenance can be planned and carried out when convenient
			Risk of Health& safety &Environmental incidents are reduced
			Opportunity to understand why equipment has failed and improve efficiency
Disadvantages	High risk of catastrophic failure or secondary damage. High repair and replacement costs	High replacement costs: parts replaced too early	High upfront costs including equipment and training
	Loss of key assets due to high down time. Lost production and missed contract deadlines	Risk of early failure-infant mortality. Human error during replacement of repaired or new parts	Additional skills or outsourcing required
	Inventory- high cost of spare parts or replacement equipment	Parts may often have many years of serviceable life remaining	
	High labour cost-overtime, subcontract and due to equipment hiring		
	Increased health and safety risks		
	Environmental concerns		

Though the relative importance of these three tasks are obviously subjective, however detection is an absolute must for any practical system and isolation is almost equally as important.

Fault evaluation, on the other hand, may not be essential. Hence, fault diagnosis is very often considered as fault detection and isolation, abbreviated as FDI, in the literature [7, 8].

1.3 Electromechanical Systems

Electromechanical systems are those consist of electrical and mechanical parts. These include electric motors and mechanical devices powered by them, such as switches, solenoids, relays, crossbar switches and stepping switches.

Every electric motor is an electromechanical energy converter, transforming electricity into a rotation due to the action of force between electric currents and magnetic fields [9] .The application of this report, which is an induction motor with a load attached to it, resembles a good example of an electromechanical drive system.

1.4 Induction Motors

Electrical motors, in general, can be defined as machines that transform electrical energy into mechanical energy. Electric motors account for 95% of all prime movers in industry and consume a large proportion of the generated power in the world [10]. Electric motors are also responsible for roughly 40% of electricity consumed worldwide [11] , and today they use two thirds of the total electricity consumed by industry [12]. Whether in mining, steel production, the pulp and paper industry, or in manufacturing. 20 million industrial motors worldwide consume 65 percent of the electricity for industrial usage [9]. Furthermore, induction ac motors resembled more that 90% all the motors employed in industry worldwide [13]. Prime movers

includes electrical movers, steam turbines, gas turbines, or reciprocating internal combustion engines.

There are several types of these motors used in industrial, commercial and residential applications. The AC induction motor is the dominant motor technology in use today and represents the majority of the installed motor capacity. With an efficiency that exceeds eighty percent, and low maintenance requirements, induction motors are considered highly reliable [10]. In an industrial country, IMs consume between 40-50% of all the generated power [14].

An induction motor is an electric machine in which alternating voltage is supplied to the stator directly, and to the rotor by induction due to the changing of magnetic field in the stator, hence the name induction motor.

An induction motor has, essentially, two main components, a stationary stator and a revolving rotor. These two components are separated from each other by a small air gap. Depending on the rotor construction, there are two different designs of induction motors which are: squirrel cage and wound rotor induction motors. Squirrel-cage rotor IM are the workhorses of industry, due to their simple and robust construction which is attributed to their rotor design. They are considered as the least expensive and the most versatile electrical machines. Hence they gained a wide spread into the daily life from domestic single-phase machines to the high voltage ones utilized in industry.

1.5 Machine Learning

Machine learning is a scientific discipline that is concerned with the design and development of algorithms that allow computers to evolve behaviours based on empirical data, such as from sensor data or databases [15]. Data can be seen as examples that illustrate relations between observed variables. A major focus of machine learning research is to automatically learn to recognize complex patterns and make intelligent decisions based on data; the difficulty lies in the fact that the set of all possible behaviours given all possible inputs is too large to be covered by the set of observed examples (training data). Hence the learner must generalize from the given examples, so as to be able to produce a useful output in new cases.

Due to the increased availability to computational resources and the vast algorithmic developments, the utilization of machine learning in the field of condition monitoring is becoming more dominant compared to conventional methods such as Fast Fourier Transforms [16].

There are several parallels between animal and machine learning. Certainly, many techniques in machine learning are derived from the efforts of psychologists to make more precise their theories of animal and human learning through computational models. It seems likely also that the concepts and techniques being explored by researchers in machine learning may imitate some features of biological learning in some creatures.

The application of machine learning for fault diagnosis is becoming more dominant compared to conventional methods and that is attributed to the increased availability to computational resources and the vast algorithmic developments [16].

Machine learning usually refers to the changes in systems that perform tasks associated with artificial intelligence (AI). Such tasks involve recognition, diagnosis, planning, robot control, prediction, etc. The “changes" might be either enhancements to already performing systems or ab initio synthesis of new systems.

Machine learning, a branch of artificial intelligence, is a scientific discipline concerned with the design and development of algorithms that allow computers to make intelligent decisions based on empirical data [15] .

1.6 Support Vector Machines

The support vector machine (SVM) is a relatively new and powerful technique for solving classification problems and is very useful due to its generalization ability [17].

In SVM machine learning method is used for fault detection and diagnosis where the algorithm is trained on example database of healthy states of sensor recordings and then used for detecting the faulty ones and determining the severity of the fault [18].

Support vector machines (SVMs) are a set of supervised learning methods used for classification and regression. When a set of data (training samples) is used as training examples, and each sample is labelled as belonging to one of two classes, the SVM has the capability to predict whether a new set of data examples (testing samples) falls into one class or the other [19].

1.7 Research Aims and Objectives

The objective laid for this work is to develop a condition monitoring system capable of detecting and diagnosing electrical faults commonly present in three-phase induction motors. The aim is then to investigate the utilization of machine learning techniques in the area of condition monitoring. As this application is an electromechanical system, the author's aim is to develop a condition monitoring system that's capable of detecting and diagnosing general faults commonly present in electrical and mechanical parts of the three-phase induction motors. To accomplish this aim the following objectives were set:

1. To study the effect of broken rotor bars, bearings faults, stator inter-turns and eccentric rotor faults on the performance of a three phase squirrel cage induction motor. This is achieved by reviewing the causes of these faults and their effects on the performance of squirrel cage induction motors.

2. To seed four known faults into four similar 7.5 KW motors using a test rig facility and to collect data for healthy and faulty motors

using signal conditioning and data acquisition (SCADA) methods.

3. To investigate the effect of stator shorted-turns, bearings, eccentricity, and broken rotor bar faults on the performance of a three-phase squirrel cage induction motor using motor current signature analysis (MCSA). This will be achieved by comparing the current spectrums of both healthy and faulty conditions in both time and frequency domains.

4. To conduct an experimental investigation into detection and diagnosis of squirrel cage motor electric faults under steady state condition at different load conditions, attempting the detection and diagnosis of the seeded faults through the designed system.

5. To develop a condition monitoring toolbox for induction motor faults using MCSA, statistical features extraction, and support vector machines diagnosis.

1.8 Report layout

The layout of this report is arranged according to the following sequence:

Chapters 2 through 4 present the background and literature review of predictive maintenance and condition monitoring of induction motors. **Chapter 2** introduces condition monitoring through model-based and model-free fault detection and diagnosis methods; as well as the signals that often monitored in the predictive maintenance processes. Four different types of induction motor electrical faults that are; bearings faults, stator shorted-turns,

eccentricity and broken rotor bar are illustrated in **Chapter 3**. **Chapter 4** presents a review of common aspects of faults detection and diagnosis using different up-to–date techniques.

Chapter 5 looks into the construction, basic principles and the operating theory of the three-phase squirrel cage induction motor. It also presents, in detail, a mathematical model for a 7.5 KW, 415V, 4 poles, and 50Hz squirrel cage induction motor using the dq representation.

Chapter 6 details the induction motor test rig on which the experimental investigations are carried out. A description of the faults that were seeded and how they were introduced into the test rig are also given in this chapter.

The motor outputs both in time and frequency domains are illustrated in **Chapter 7**. This chapter contains different plots of the signals that recorded during testing at several loading situations in time and frequency domains.

Chapter 8 illustrates the monitoring system methodology used for faults detection and diagnosis. The chapter presents how the features to be used for the FDD task are generated. It also discusses the fault detection principles of the machine learning technique used.

While **Chapter 9** discusses the detection and diagnosis results, **Chapter 10** outlines the conclusions, and the future plan of work.

Chapter 2. Condition Monitoring of IMs

A brief introduction to some generally used concepts and classifications in condition monitoring are reviewed in this chapter. Along these three serial chapters, literature reviews are presented on general methods of fault detection and diagnosis with special attention given to those related to induction electric motors, the application of this study.

Different signals that are fault features containers with significant faults ciphers are reviewed with an emphasis on the most practical used ones. The second part of this chapter is devoted to the signals usually used as a mean to read the condition of the machine while in operation.

Fault detection and diagnosis has been becoming more and more important for process monitoring because of the increasing demand for higher performance as well as for increased safety and consistency of dynamic systems. Early diagnosis of process faults while the system is still operating in a controllable region can help avoid development of abnormalities and the decrease of productivity losses.

Hence, fault diagnosis is a major research topic attracting considerable interest from industrial practitioners as well as academic researchers. The advancement of fault detecting and diagnosis methods has made condition based maintenance the most adopted procedure in many processes.

2.1 Predictive Maintenance of Induction Motors

Although the induction motor is reliable, it is possible to maintain its performance by using condition monitoring and diagnostics [20].

For instance, working in harsh environments, being switched on and off rapidly, driving fluctuating loads, besides human installation mistakes may all affect the performance of induction motors whose conditions may deteriorate due to such effects if not maintained at the right time.

Induction motors generally experience a number of mechanical problems, predominantly related to their stators, bearings and rotors [5, 14]. The inception of these faults can be detected traditionally by sensors attached to the casings of induction motors or preferably through nonintrusive means in order to schedule maintenance of such devices without unscheduled downtime i.e. employing an effective predictive maintenance.

2.2 Model-Free Condition Monitoring Approach

FDD is a very broad area of research and applications, and can be divided into two main branches, that is: model-free and mode-based condition monitoring techniques.

The hardware redundant method represents the traditional approach of model free fault detection and diagnosis. It is implemented through parallel sensors and actuators to measure and monitor certain variables. It is simple and easy to implement, but has a number of disadvantages of which being

costly and require an extra space for implementation which is not always available in all processes.

2.3 Model-Based Condition Monitoring Approaches

In order to monitor a system, information about it is obtained from primary data which then is processed using modern signal processing and analysis techniques. Through these techniques, the condition of the machine is assessed. Though this makes it is possible to diagnose faults, if any, before they could cause a severe damage, constant human interpretation is still required [21].

Traditional fault detection is associated with hardware redundancy which includes sensors and actuators. This could result in costly and cumbersome systems, where it might sometimes not be allowed. Meanwhile most of model based fault detection and diagnosis methods rely on the concept of analytical redundancy.

In contrast to physical redundancy, where measurements of parallel sensors are compared to each other, now sensory measurements are compared to analytically computed values of the respective variables. Such computations use present and/ or previous measurements of other variables and the mathematical plant model describing their nominal relationship to the measured variable. The idea can be extended to the comparison of two analytically generated quantities obtained from different sets of variables [8].

The main advantage of model based techniques is the replacement of hardware redundancy by analytical redundancy. While consistency is sought between identical components' outputs in hardware redundancy, it is checked against their computed counterparts obtained from the model, in the case of analytical redundancy. The presence of residuals, which are the differences between the measured and estimated values, is an indication of a system fault [7]. With the development of advanced modelling techniques, model based methods are becoming an attractive approach to FDD systems [22].

However, in practice it is almost impossible to obtain a model that exactly matches the process behaviour [23]. The mismatch between the behaviour of the model and the plant may lead to large error signals [24], which usually lead to false alarms. As most physical systems are nonlinear in nature, their mathematical description usually relies on linear approximations [7]. Furthermore, it can be impossible to describe some nonlinear systems by analytical equations [25].

When the system becomes nonlinear, the model is no more in use. Hence, nonlinear models with high accuracy are preferably representing systems with large dynamic ranges only. One of the most significant problems with nonlinear modelling is robustness to modelling errors. It is unrealistic to expect perfect modelling for complex systems [26]. These disadvantages increase the necessity to find alternative approaches such as neural network, and knowledge based approaches.

After the proper signal to monitor is decided on , FDD run though three main tasks; they are: generation of residuals (features), detection of changes when they occurred, and finally diagnosing the fault(s) in matter of size, place, and time of occurrence, if any.

Each of these three tasks is achieved through deferent techniques and methods of implementation. This chapter and the following two chapters look into some of these techniques. Figure 2.1 shows the main steps of a CM system.

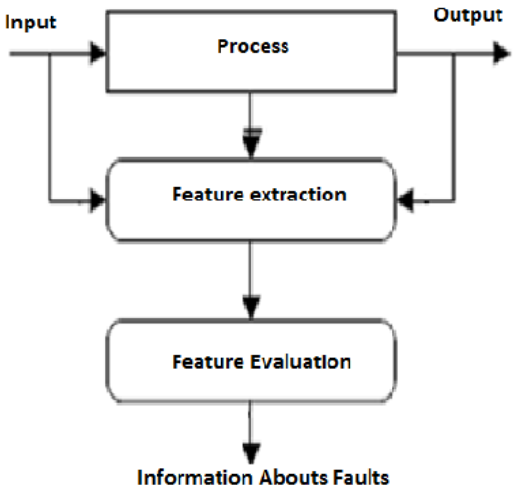

Figure 2.1 Simple CM System

2.4 Induction Motors Condition Monitoring

After deciding on the fault(s) to be monitored, CM process starts with sensing certain variables such as line current, voltage, vibration, motor speed, flux, and temperature. The feature generation or extraction, as referred to in some literature, is the following step of the CM process. The main aim of this step is to generate some features that are (preferably) unique, firmly tied to a

certain fault, and easily distinguishable from the others related to a healthy state or even other faults, if there is any. Then by examining these features, it would be possible to judge whether the system is healthy or not. This is what is called, in CM literature, fault diagnosis. The different components of a CM system are shown in Table 2.1, of which few blocks will be looked into in the next sections .It is worth noting that the last two steps, namely feature generation and fault detection and diagnosis (FDD), are inter related and it, sometimes, becomes difficult to say where each of them starts or ends.

Table 2.1 Online IM condition Monitoring Phases

IM Faults	Monitored Signals	Features Extraced	FDD
1. Stator	1. Current	1. FFT	1. Neural Networks
2. Rotor	2. Voltage	2. WT	2. SVM
3.Bearings	3. Vibration	3. Park Vector	3. Fuzzy Logic
4. Eccentricity	4. Temparure	4. RMS	4. Fault Trees
5. Imbalanced Voltage	5. Acoustic Monitoring	5. NSC	5.Genetic Algorithms
6. Misalingment	6. Speed	6. Statistical Metods	
	7. Torque	7.Parameter Estimation	
	8. Flux	8. State Observers	

The following section lights on the different signals that can be looked at for locating any faults related symptoms. Though it is possible to use a wide range of signals, the recent research trends are directed primarily towards using MCSA approach and vibration as sensed signals.

2.5 Human Sensing

Human sense-based monitoring is a conventional monitoring approach based on the basic human senses, that are touch, smell, sight and hearing,

which may provide an immediate detection of machine faults without additional analysis [27, 28]

Experienced engineers are often required to interpret measurement data that are normally inconclusive. Although the cost of human sense-based monitoring is low compared to modern condition monitoring techniques, it requires high inspection skills based on experiences and provides only qualitative results. The conclusions drawn by different inspectors are sometimes not the same, due to dissimilar individual experiences and personal skills [27].

2.6 Motor Current Signature Analysis (Current Monitoring)

Motor Current Signature Analysis (MCSA) is a powerful monitoring tool for electrical machine and motor-driven equipments that provides a nonintrusive mean for detecting the presence of mechanical and electrical abnormalities in the motor and the driven equipment, including distorted conditions in the process downstream of the motor-driven equipment [29].

MCSA is an electric machine monitoring technology developed in 1985 by Oak Ridge National Laboratory (ORNL) [30, 31] as a means for determining the effects of aging and service wear systems, but it is applicable to a broad range of machinery. It has been used as a condition monitoring method in electrical machines to detect and diagnose motor bearing wear, eccentricity problems, stator faults, as well as rotor broken bars for inaccessible motors

during plant operation [29, 32]. MCSA can be implemented using time or frequency domain analyses.

MCSA is based on the recognition that an electric motor driving a mechanical load acts as an efficient and permanently available transducer by sensing any variations in the motor components due to any faults, large and small, long-term and rapid, and converting them into variations in the induced current generated in the motor windings.

These current variations, though very small in relation to the average current drawn by the motor, can be extracted reliably and nonintrusively at a remote location from the equipment and processed to be used in studying the machine condition. Motor current signatures are obtained both in time and over time to alarm any early signs of deterioration of the motor condition.

MCSA has been successfully applied for condition monitoring to a wide range of technical areas which include not only electrical motors or motor-operated equipments but also pumps of various designs, blowers, and air conditioning systems. MCSA has been in the CM arena for so long, giving enough proof of utility at industrial environments [14]. The popularity of MCSA comes from being that the current consists of motor harmonics which every one shows some properties related to different situations like faulty conditions [32]. And for being a versatile, nonintrusive and inventive method, MCSA is chosen in this report as the main tool for condition monitoring.

2.7 Vibration Monitoring

Condition monitoring using vibration as the sensed signal is the most effective approach to detect and diagnose induction motor faults, particularly those that are mechanically related. So vibration monitoring finds wide application in CM of centrifugal pumps [33], and in CM of different defects in electrical motors as well [34, 35]. The technique uses vibration transducers, such as measuring accelerometers of piezo-resistive or seismic types with linear frequency spectrum [16, 36]. The transducers are often placed on the bearings in order to detect mechanical faults. However, by placing sensors on the stator, as well, it is also possible to detect problems such as irregular air gap, stator winding or rotor faults, asymmetrical power supply, and imbalances in the motor load [37].

The work in [38] proposes a method for sensorless on-line vibration monitoring of induction machines based on the relationship between the current harmonics and their associated vibration harmonics. Initially, two baseline measurements of current and vibration were recorded for healthy machine conditions. The baseline data is then evaluated to determine the critical frequencies to monitor on-line. Once these frequencies are determined, the baseline vibration measurement is simply used to scale the current harmonic signal to an estimated vibration level. Based on theoretical analysis, simulation results, and the experimental results a linear relationship between the current harmonics and vibration level can be initiated. The

results have shown the feasibility of this method for sensorless on-line vibration monitoring.

However, interpreting the vibration signal is a complex process that requires a specialized training and experience [4, 16]. The spectra from rotating machines are containing several sets of harmonics and also side bands as a result of various modulations [4] . Furthermore, there are few reasons that make the vibration technique is not the first choice normally looked at by the CM engineers. Of which it requires transducers to be carefully fixed around the system frame, often interrupting the motor operation.

Moreover, mounting vibration transducers is not always practically executable. An example for such situation is in the offshore petroleum industry, where the machines are positioned hundreds of meters of waters away from the data processing centre. The last but not least of these disadvantages is the cost which is an important factor in CM, as vibration transducers are more expensive if compared to other sensors.

2.8 Voltage Monitoring

Voltage signature analysis of line-neutral voltage preserves the advantage of being nonintrusive and of comparable simplicity to MCSA. The induced harmonics in the neutral voltage give reliable information on the motor condition.

A comparison study with the well known MCSA is underlined in [39, 40]. The authors of [39] have proposed an approach based on spectral analysis of

line-neutral voltage (voltage taking place between the supply and the stator neutrals) for the detection of rotor faults. It was shown development of diagnosis signatures using line-neutral voltage is more sensitive to the rotor defect and can be observed significantly at least near the 3rd, 9th, 15th and 21st harmonics. For that reason, the analysis of line-neutral voltage is more significant and so is suggested. The work also suggested the harmonic components detected were caused by rotor defects as constructional asymmetry or accidental faults like broken rotor bars. The fact is that a broken bars fault causes asymmetries in the mutual inductance of the machine, which give rise to harmonic components in the line-neutral voltage.

In [41], the effect of unbalance supplying voltage on the motor temperature rising has been investigated and showed that the increase of motor temperature depends on the positive, negative and zero sequence voltages which paves the way for using voltage monitoring as an indication of the motor temperature.

2.9 Induced Voltage Monitoring

Induced voltage is another method of IM monitoring. It is about studying the voltage induced in the stator winding after the motor being disconnected from the supply. At this point the stator currents rapidly draw down to zero, and hence the only source to induce voltages in the motor windings is the rotor current which is sinusoidal waves if the rotor is healthy. If any broken bar exists, it will then directly influence the voltages induced in the stator windings and the sinusoidal distribution of the voltage will be distorted.

For instance, the work in [42] involved the employment and evaluation of four different techniques for the detection of broken bars. The authors came to conclude that the two methods, involving the usage of both of internal and external search coil voltages appeared to provide the most useful, reliable, and cost effective diagnostic techniques.

The induced voltage approach is used predominantly for rotor condition monitoring. Milimonfared et al [43] have applied this practice to rotor defects and faults and they pinpointed the attractiveness of it because source faults like unbalance harmonics will not sway the detection. Also, more importantly, it is clear from the nature of the test that it can be performed even with an unloaded machine.

Additional researches have been concentrating to make improvements in the broken rotor bars detection procedure using induced voltage monitoring accompanied by advanced signal processing techniques [44, 45].

The main drawback of this monitoring method is that it has to be conducted during the motor rundown which is often not the preferred case for industry.

2.10 Monitoring of Acoustic Emissions

Acoustic-based condition monitoring has been widely used in industry because it is a renowned as a non-destructive technique [20]. i.e. does not permanently alter the article being inspected. Sensing the acoustic noise spectrum for IMs is one of the conventional condition monitoring methods.

Although this technique is very attractive in bearing faults detection, it has been applied for other faults detection as well [46].

The acoustic emissions technique has a wide usage in industry. For example; the authors of [47] have studied the usage acoustic emission for detecting incipient cavitation in a centrifugal pump, and for gearboxes [48]. On the IMs side, acoustic monitoring has been used for detecting different machine faults. Bearing faults and grease contaminants could be detected by many methods. However, acoustic emission monitoring proved to be the best method for the detection of both [49, 50]. The authors of [51] studied the effects of stator faults on the acoustic emission spectrum from an IM. They showed that the slot harmonics in the acoustic spectra of IM is a function of loose stator coils. The work in [52] focuses on the use of acoustic measurements for condition monitoring, and the feasibility of identifying static eccentricity by acoustic measurements is shown.

Microphones and other advanced devices are used as transducers in acoustic monitoring to acquire acoustic signals in many condition monitoring applications. Acoustic monitoring has clear shortcomings that are the accuracy of fault detection using acoustic measurement is reduced as it is usually contaminated by acoustic waveforms background from other machines operating within the surrounding area.

2.11 Instantaneous Angular Speed Monitoring

Instantaneous angular speed (IAS) refers to the variations of the angular speed that occur within a single shaft revolution [53]. IAS is another possible way for IM condition monitoring as it can provide information about the machine dynamics. Investigations show that IAS is useful for the condition monitoring of a wide variety of machines [54].

There are several types of sensors used to measure the angular speed of a shaft, such as encoders, capacitive sensors and potentiometers which are usually used in the contact method, while Hall-effect sensors are most commonly used in non-contact method. Encoders, which are often attached directly to the end of the rotary shafts of machinery and have their own power supplies, are the most commonly sensors employed in the contact method of IAS [54].

Compared with conventional structural vibration and acoustics monitoring, IAS has less noise contamination and is more directly related to machine dynamics. Therefore, it is easier to interpret IAS results and produce more accurate diagnoses [55].

The authors of [53, 55] have demonstrated the capability of IAS monitoring. It outperforms conventional vibration diagnosis of incipient faults of motor rotor bars and shaft misalignment. However, IAS monitoring technique is less known compared to the other existing conventional methods.

2.12 Electromagnetic Field Monitoring

Flux monitoring is one of the less common condition monitoring techniques. The magnetic field in the air gap will, during normal conditions, vary sinusoidally. Some stator and rotor faults cause deviations from the sinusoidal variations [36]. Rotor or stator faults can, thus, be detected by using a search coil that is fixed to the stator core to measure air gap flux**,** or by measuring the axial flux through a coil that placed around the motor shaft or by other sensing devices, such as Hall probes [36].

By monitoring the axial leakage flux, it is often possible to identify various asymmetries and fault conditions, such as a broken rotor bar, a stator winding inter-turn short circuit, an eccentricity, and so on [56]. However, practically speaking, these approaches are difficult to implement. The insertion of a series of search coils in the stator slots is not realistic for motors in use. In addition, the design of a conventional motor means that it is often not possible to install an axial sensing coil in the correct position for a reliable measurement. Hence flux monitoring finds less acceptance in the CM arena.

2.13 Thermal Monitoring

Thermal based condition monitoring is not a common technique among researchers and industrialists. Studies have shown that about half of motor failures are attributed to stator faults which are caused mainly by stator insulation breakdown [57].

Overheating is considered as one of major causes of the stator winding insulation degradation in small induction machines [58]. Motor stall, jam, overload, unbalanced operation, and warm environments are some causes of overheating in induction motors. It is stated that for every 10^{o}C increase over the motor rated ambient temperature, the winding insulation life is halved [58].

Temperature increase in the rotor and stator of induction motors play a key role in motor insulation degradation which may result in motor failures [59]. In most cases, it is necessary to monitor rotor bars and stator windings to make sure that their temperature remains within certain limits [60]. Hence, effective thermal monitoring not only protects the induction machines from overheating, but also enhances the performance of the overall drive system [61].

Thermal stress is monitored through two ways either with a direct means through embedded temperature sensors (as in Figure 2.2) or by utilizing nonintrusive techniques of which is modelling and temperature estimation. Each of these techniques has its own drawbacks. While sensors and their associated hardware are adding extra costs, simple thermal models are not greatly accurate in temperature estimation.

The authors of [61] have used an nonintrusive method by injecting a dc current into the stator windings of an induction motors fed by closed-loop inverter drives. The value of the injected DC voltage is accurately estimated and the stator winding temperature can hence be monitored based on the

estimated DC stator resistance. Temperature of rotor and stator can be estimated by rotor resistance identification [60, 62]

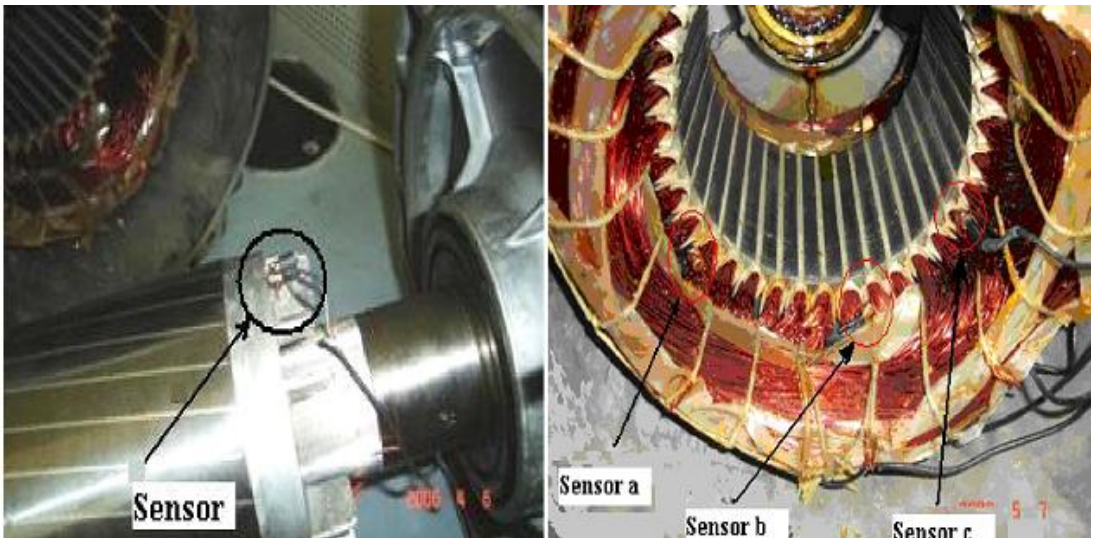

Figure 2.2 Rotor and Stator Thermal Sensors [59]

A different method of nonintrusive monitoring is using infra red thermography. Infrared thermography has been used for the detection and location of thermal hot-spots in large electrical machines. Salisbury [63] has used this technique for fault detection in cement plant in areas accessible to infrared inspection. This is done through a range of infrared lenses providing flexibility to view targets that are varying in size from an electrical panel, to conveyor bearings up to the kiln or pre-heater tower. It has proved to be a reliable and sensitive method to detect hot-spots in industrial situations [63]. This technique has been proved to be exceptionally useful especially where it is difficult to employ conventional surveillance equipment, or in hazardous atmospheres. Figure 2.3 shows an application for thermography in monitoring a motor bearing (Courtesy of FLIR Systems Ltd, UK).

Few processes that deal with the direct measurement of motor heating by means of temperature sensors seeded into stator windings and rotor parts are deployed in [41, 59, 64, 65]. In these methods, temperature monitoring of the stator is relatively easy, but the opposite for the rotary parts. Different techniques for data transmission from sensors including slip rings, optical facilities, wireless and infra red waves are employed [59, 64-66].

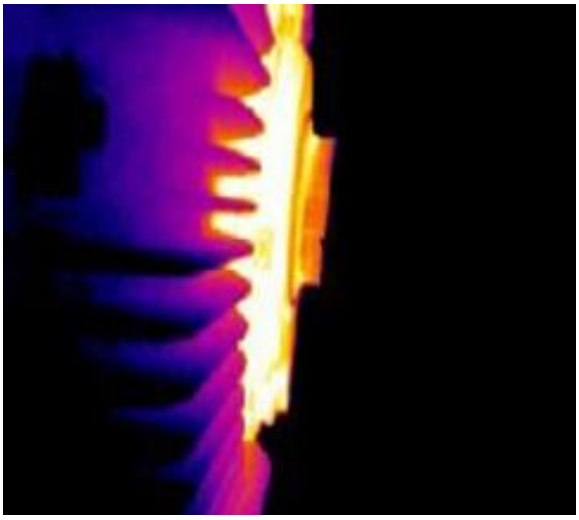

Figure 2.3 Thermo-Gram of Bearing with Insufficient Lubrication

In [64], in order to read the signal from the rotor sensors three slip rings were installed on the rotor shaft and the corresponding brushes were connected to the thermal stress monitoring system. A major drawback of this method is that the number of sensors is limited by the number of slip rings as one sensor is assigned for each ring.

The signal from the temperature sensors on the rotor can be digitized and transmitted via light through a coaxial optical fibre. The main advantage of

this kind of data transmission is immune to electromagnetic interference. However, construction of such a system is difficult and costly.

2.14 Instantaneous Input Power Monitoring

The instantaneous input power (IIP) can be measured as the so-called product power, i.e., a product of one line-to-line voltage and one line current, or as a total input power to the stator [67]. As the instantaneous power is the product of voltage and current, IIP monitoring relies on measuring and recording the instantaneous motor input voltage and current readings. Many researchers have used this approach in CM of induction motors. For instance, it has been used for rotor faults, for mixed faults of BRB and eccentricity, and mechanical defects of IMs [67-71].

Cruz and Cardoso [69] have demonstrated the effectiveness of the total instantaneous power spectral analysis in detecting the presence of rotor cage faults through both simulation and experimental work. Furthermore, the possibility of determining the severity factor, in order to evaluate the extension of the fault, is reported, and it is shown how the severity factor is almost independent of parameters such as the magnetizing current, motor rating and motor-load inertia.

The work presented in [70] utilizes the spectrum analysis of the IIP signal for the CM of rotor faults which are BRB and eccentricity. These two faults usually occur concurrently. Furthermore, their related pikes appear very close to that of the fundamental component in MCSA, especially those related to

the BRB which makes dealing with them is not always easy. The outstanding advantage of the proposed method is the ability to get rid of the interference from the fundamental component, and highlight fault characteristics.

Besides being nonintrusive, IP monitoring has the advantage of being a powerful technique in terms of separation of mixed faults [70] and the quantification of the fault extend compared to other signals like current or voltage [72]. Instantaneous power was observed to exhibit the highest values of the detection criterion in case of mechanical faults and for electrical faults at certain situations [67]. However, the cost of extra current and voltage cables and sensors is an additional burden. In addition to cost and the required signal processing, there will be cases where access for two cables may not be possible.

2.15 Summary

As mediums with significant ciphers of the fault, signals such as vibration, MCSA, and voltage, were each examined with different degrees of detail in order to realize the advantages and disadvantages of each scheme based on up to date researches in the field.

The consulted references show the wide usage of current, voltage and vibration in the condition monitoring arena of IMs. Besides being relatively cheap means, the different motor faults' signatures are easily detectable within these signals. Hence, it could be concluded that current, voltage, and vibration are the most viable signals for IMs condition monitoring.

Chapter 3. Faults of Induction Motors

Despite their robust construction, induction motors experience different faults due to wear and tear, transient conditions, the rotating nature of such machines, harsh working environments, and ageing.

This chapter symbolizes an introduction to induction motor faults. The common faults affecting the IMs performance are presented with a brief description of the main sources and causes of each fault.

Types and classifications of IM faults are discussed in detail especially those put up in the practical segment of this work.

3.1 Types and Classification of Faults

A fault is defined as an unpermitted deviation of at least one characteristic property of a variable from an acceptable behaviour. Therefore, the fault is a state that may lead to a malfunction or failure of the system [73]. i.e. a failure is the consequence of a fault, but a fault may not lead to a failure. In general, all failures are faults but not all faults are failures [74].

Faults can either be classified according to the way they behave or according to the way they interrupt the process. With regard to their time dependencies, faults are either abrupt (step wise), intermitted, or incipient as shown in Figure 3.1. Abrupt faults are fast occurring faults, meanwhile those with different active intervals are called intermittent.

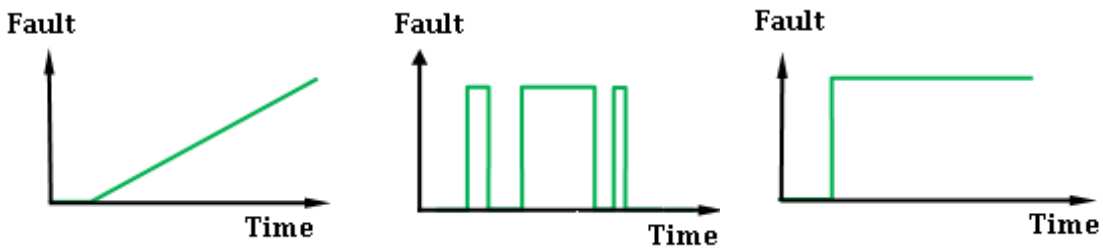

Figure 3.1 Left To Right; Incipient, Intermittent and Abrubt Faults [73]

The faults which are in the centre of CM concern are those known as incipient faults. Such faults happen due to aging of components, or due wear and tear. Besides being nonlinear in nature, they increase gradually [21]. Hence, such faults can be detected at early stages and the right maintenance activity is suggested prior to any more decline in the condition of the machine.

As in Figure 3.2, faults also may be classified according to which part of the system they influence or affect. This categorization which is linked to model based CM distinguishes between two classes of faults.

1. Additive process faults: they represent disturbances affecting the process and cause a shift in the outputs. Such faults represent leaks, loads, offsets of sensors etc.
2. Multiplicative process faults: they represent changes of the plant parameters whether they are incipient or abrupt faults. They might be caused by deterioration of equipments or loss of power [7].

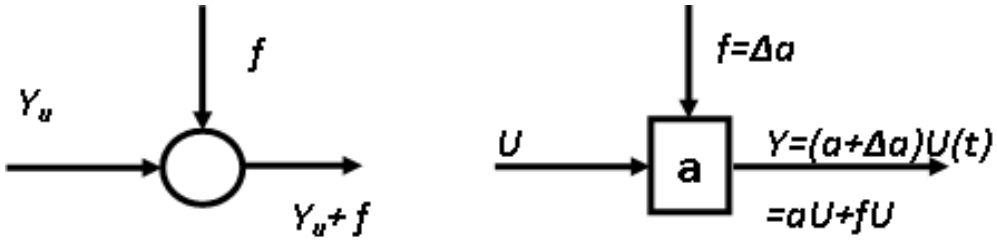

Figure 3.2 Faults Models, Additive on The Left and Multiplicative on The Right [73]

3.2 Faults of Induction Machines and Their Sources

Due to their structure, squirrel cage induction motors are considered as robust and fault tolerant machines in industry. However as rotating machines they still experience different faults due to a wide range of stresses, as it would be mentioned later in this chapter.

General machine faults can be classified as either mechanical or electrical faults. Mechanical faults mainly include eccentricity and bearings related defects. They may lead to faults such as rotor rubbing, excessive vibrations, and stator and rotor fatigue and so on. Electrical faults are those originated at the electrical system of the machine such as turn-turn or turn-earth faults. Faults in rotor may lead to bars or end ring cracks or weak connection of rotor parts.

In general, induction motors are subjected to primary types of faults and related secondary faults. The sources of motor faults may be internal, external or due to environmental causes, as presented in Figure 3.3. Internal faults can be classified with reference to their origin, i.e. electrical and mechanical [5].

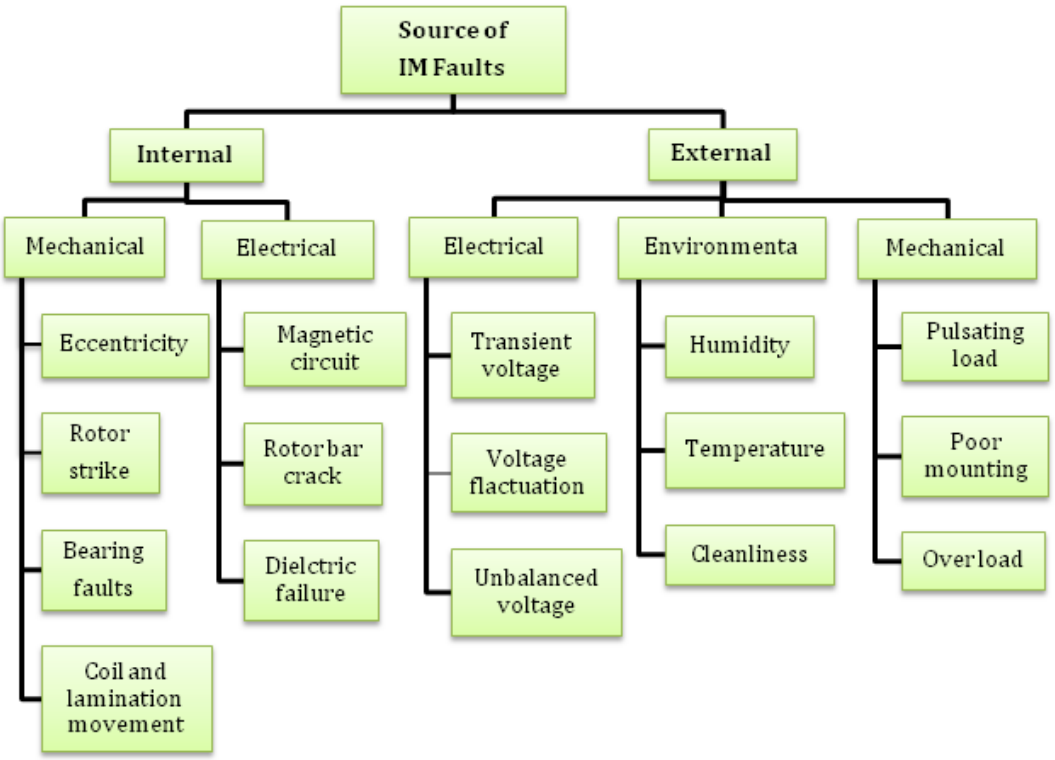

Figure 3.3 Sources of IM Faults [5]

Some induction machines failure surveys [5, 36] have categorized the faults according to the main components of the machine at which the fault was originated. They are classified as stator related, rotor related, or bearing related faults.

The authors of [5] have cited a study carried by and General Electric and General Applications - IEEE (IEEE-IGA), which both looked into the main sources of the IM faults. The study is carried out on the basis of opinion as reported by the motor manufacturer. The results of this study are presented in Table 3.1, where the failure is grouped according to major contributors.

An Industry Assessment Study (IAS) [75] , was conducted by General Electric Company- USA and Electric Power Research Institute- Canada, to evaluate the reliability of powerhouse motors. The statistics of this survey produced a very large body of data on motor failures on a sample of 4797 motors. There were 872 failed motors (a motor that failed one or more times) and 1227 total failures. Thus 335 of the 1227 were repeat failures.

The survey has found that the vast majority of failures, where a cause was indicated, was attributed to both bearings and stator windings (around 80%) while the rotor has contributed 10% towards such failures. The rest percentage was linked to different fault types.

Table 3.1 Distribution of Failures on Failed Components

	IAS		Thorsen		IEEE	Average Percent
Fault	No. of Failures	Percent	No. of Failures	Percent	Percent	
Bearings	409	41	129	51.6	41	44.5
Stator	372	37	62	24.8	28	29.9
Rotor	102	10	15	6	11	9
Other	122	12	44	17.6	20	16.5
Total	1005	100	250	100	100	100

Another section of the study was directed towards another angle of dealing with failures, where a significant number of machine failures were attributed by the equipment owners to design and workmanship. A considerable proportion of the failures were ascribed, by the equipment owners, to be the result of misapplication and disoperation (34.1 percent of reported cases).

The opportunity to improve reliability by reducing failures due to design, workmanship, misapplication, and disoperation appears to be significant.

In a different study, Thorsen and Dalva in [36] have accomplished comparable results for 250 high-voltage induction motors utilized in industry. The average results of these studies are shown in Figure 3.4.

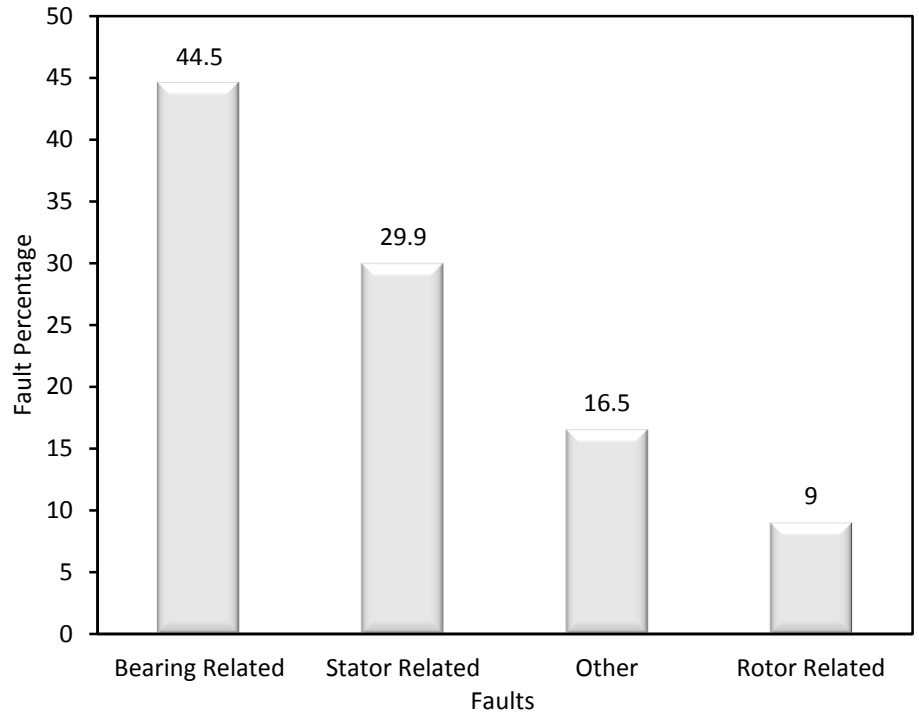

Figure 3.4 Average Results of Different IM Faults Surveys

According to the three studies, bearing faults are identified as the major type of faults in induction motors followed by the stator related ones. All of the studies came out with similar results. It was found that the vast majority of IM faults are attributed to both bearings and stator windings, as each of them is responsible for around 40 percent of the IM faults. While about 10 percent of the faults are rotor related, the rest of the faults are linked with other different

causes. Five faults will be studied in this section of which two are secondary (belong to faults called as other in Figure 3.4) faults.

3.2.1 Rotor Faults

As stated earlier rotor faults are, generally, not among various defects those frequently occur in induction machines as they only represent about 10% of the IM fault sources. But, the significant importance of rotor faults comes from the fact that they cause secondary failures which lead by succession to serious motor malfunctioning. Thus diagnosis of rotor failures has long been an important but an intricate task in the area of motor CM [46].

Statistical data of failures among utility-size motors indicate that at least 10% of the induction motor (>100 hp) failures are rotor related. Half of these defects were reported as "cage" faults. However, industry experience suggests that the rate of broken bars is much higher than reported [76].

Sometimes, induction motors are required to operate in highly corrosive and dusty environments. However, cage rotor design and manufacturing have undergone little change. As a result, rotor failures may account for a considerable percentage of total induction motor failures in such environments [76].

3.2.1.1 Rotor Faults Causes

Broken rotor bars can be caused by the following [77, 78]:

- Direct on-line starting duty cycles for which the rotor cage was not designed to withstand causes high thermal and mechanical stresses.
- Pulsating mechanical loads such as reciprocating compressors or coal crushers can subject the rotor cage to high mechanical stresses.
- Imperfections in the manufacturing process of the rotor cage.
- Thermal overload and unbalance, hot spots or excessive losses, sparking (mainly in fabricated rotors),
- Magnetic stresses caused by electromagnetic forces, unbalanced magnetic pull, electromagnetic noise and vibration.
- Residual stresses due to manufacturing problems,
- Dynamic stresses arising from shaft torques, centrifugal forces and cyclic stresses
- Environmental stresses caused by for example contamination and abrasion of rotor material due to chemicals or moisture,
- Mechanical stresses due to loose laminations.

Rotor stresses have been classified in [78] into different categories that is: thermal, mechanical, magnetic, dynamic and environmental stresses. These stresses are summarized in Table 3.2.

3.2.1.2 Broken Rotor Bars

Rotor related faults in three phase induction motors are predominantly attributed to broken bars and end rings [77]. The rotor bars can be partially cracked or even completely broken during the operation of induction machines, due to stresses or poor rotor geometry design. The bar cracking/ breakage is the major fault in the rotor of IM.

Table 3.2 Rotor Stresses [78]

1. Thermal Stresses	2. Evironmental Stresses	3. Magnetic Stresses
• Thermal Overlaod	• Contamination	• Rotor Pullover
• Thermal Unbalance	• Abrasion	• Noise
• Hot Spots	• Foriegn Particals	• Vibration
• Sparking (fabricated rotors)	• Restricted Vantelation	• Circulating Currents
• Excessive Rotor Lossess	• Ambient Temprature	• Laminations Saturation
4. Dynamic Stresses	**5. Mechanical Stressses**	**6. Other**
• Vibration	• Casting Variations	• Misapplications
• Rotor Rub	• Loose Laminations	• Poor Design Particles
• Overspeeding	• Incorrect Shaft/Core Fit	• Manufacturing Variations
• Cyclic Stresses	• Fatigue Or Part Breakage	• Loose Bar/Core
• Ceterfugal Force	• Material Deviations	• Transient Torques
	• Poor Rotor /Stator Geometry	• Wrong Rotation Direction

Once a bar breaks, the condition of the adjacent bars also deteriorates gradually due to the increased stresses resulting from the high rotational speed of the rotor. This reveals why the problem of broken rotor bars (BRB) should be detected in its early stages of happening when the bars are beginning to crack [77]. Besides that, broken rotor bars causes unbalanced currents and torque pulsation, and therefore decreases the average motor torque. Faults ascribed to broken bars cause excessive vibration, noise and sparking during motor starting [77].

BRB faults can be a serious problem, although they do not initially cause an induction motor to fail. Therefore, there can be serious secondary effects. The fault mechanism may result in broken parts of the bar hitting the end windings or stator core of high voltage motor at high speed. This can cause serious mechanical damage to the insulation and a consequential winding failure may follow, resulting in a costly repair and lost production.

3.2.1.3 Broken End-Rings

The conductive rotor bars are short-circuited on both sides by end-rings. Defective casting in the case of die-cast rotors, and/or poor end-ring joints in the case of fabricated rotor cages during manufacturing are the source of the end-ring faults. Once the initial defect occurs, local overheating may develop in the cage. Therefore, propagation of the fault is continued by multiple start-ups as well as load fluctuations, which produce high centrifugal forces. Harmonics injected in the stator current due to defective end rings are higher than those resulted from broken bars [79], consequently they are easier to detect.

3.2.1.4 Rotor Axial Distortion

Axial distortion of rotor is ascribed to an asymmetrical heating or cooling of the rotor, or to an axial symmetry thermal distribution of an asymmetrical rotor [80]. A rotor bow usually causes a pre load on the bearings, and can be classified into two types, local and extended [80]. Both rotor bow types produce an asymmetrical axial distortion on the cross-section of the shaft.

The local bow happens when asymmetrical heating is localised in a part with a small length. A typical example is rotor-to-stator rub. The extended bow, which is the actual shaft bow, is an asymmetrical heating that extends to a certain length of the rotor, ending in the rotor part limited by two bearings [81].

3.2.2 Stator Faults

The stator, as the name implies, is a stationary and an essential part in any electric motor that encloses the winding coils which is the producer of the magnetic field.

It is known that approximately 30-40% of induction motor failures are ascribed to failure of the stator winding, and it is believed that these faults start as undetected turn-to-turn faults within a coil, then lead to catastrophic phase-to-phase or phase-to-ground short circuit faults which result in the burn out of the stator winding [5, 36, 82].

3.2.2.1 Types of Stator Faults and Their Sources

Stator windings faults are categorized into five classes [78, 83, 84] and shown in Figure 3.5. These classes include:

1. Turn to turn fault within a coil.
2. Short between coils of the same phase.
3. Phase to phase short circuit.
4. Phase to earth short circuit.

5. Open circuit in one phase (single phasing).

On-line monitoring to diagnose the faults stated in (1) and (2) above is the key to avoid the occurrence of the faults in (3) and (4) for induction motors i.e. diagnosing the turn to turn fault is a precaution of the successive faults.

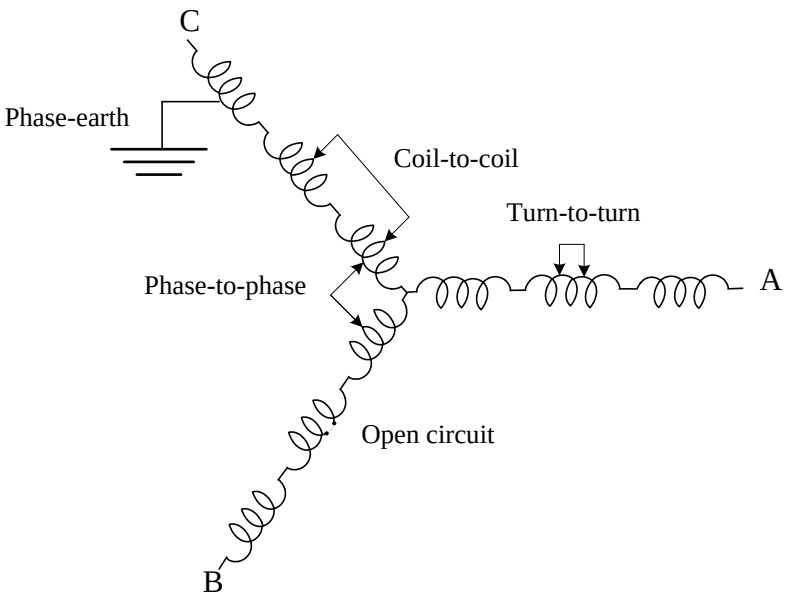

Figure 3.5 Y-Connected Stator Showing Possible Failure Modes [58]

The stator faults are the product of some stresses. If a combination of a number of these stresses acting upon the motor component, they would predominantly lead to a motor failure. When these stresses are kept within the rated values of the system, premature failure should not occur.

However, if any combination of them exceeds certain limits, then the motor life time may be significantly shortened and a failure could occur [58]. Bonnett and Soukup [58] have classified the stator stresses that effect its functioning into four groups that is: thermal, electrical, mechanical and environmental causes. Table 3.3 shows these groups and the causes behind each of them.

Table 3.3 Stator Stresses [78]

1. Thermal Stresses	2. Mechanical Stressses
• Thermal Ageing	• Coil Movement
• Voltage Variations	• Rotor Strikes
• Cycling	• Defective Rotor
• Loading	• Flying Objects
• Ventilation	• Lugging of Leads
3. Electrical Stresses	**4. Evironmental Stresses**
• Dielectric Ageing	• Chemicals
• Tracking	• Abrasion
• Corona	• Damaged Parts
• Transients	• Moisture
	• Restricted Ventilation

The following figures illustrate different coil faults. The two photos in Figure 3.6 are for turn to turn within the same phase and coil to coil shot circuits, respectively.

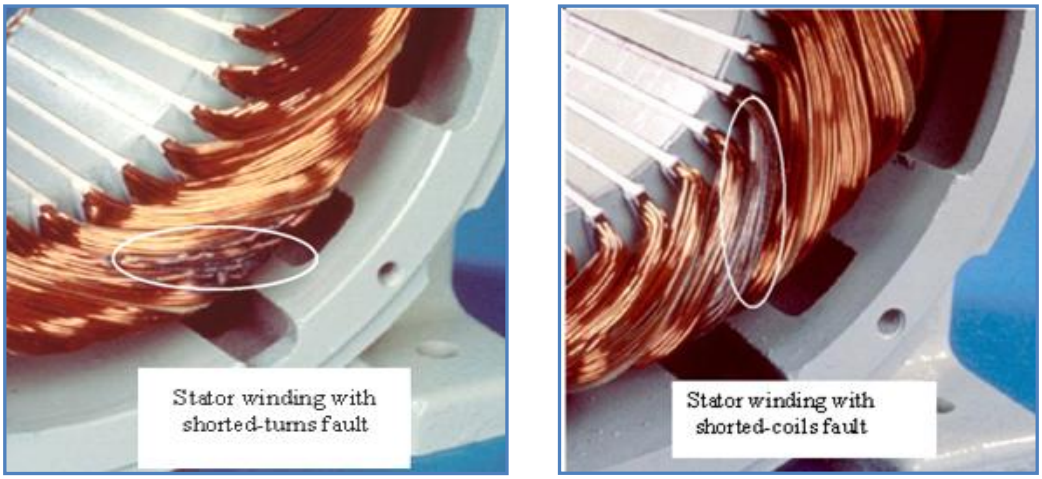

Figure 3.6 Faults Within The Same Phase (Courtesy of Baldor)

Faults (3) and (4) can be seen Figure 3.7. These two faults exceed the phase boundaries to reach an advanced stage of fault which will definitely lead to a failure. This usually happens when the monitoring system fails to detect the prior stages of defect.

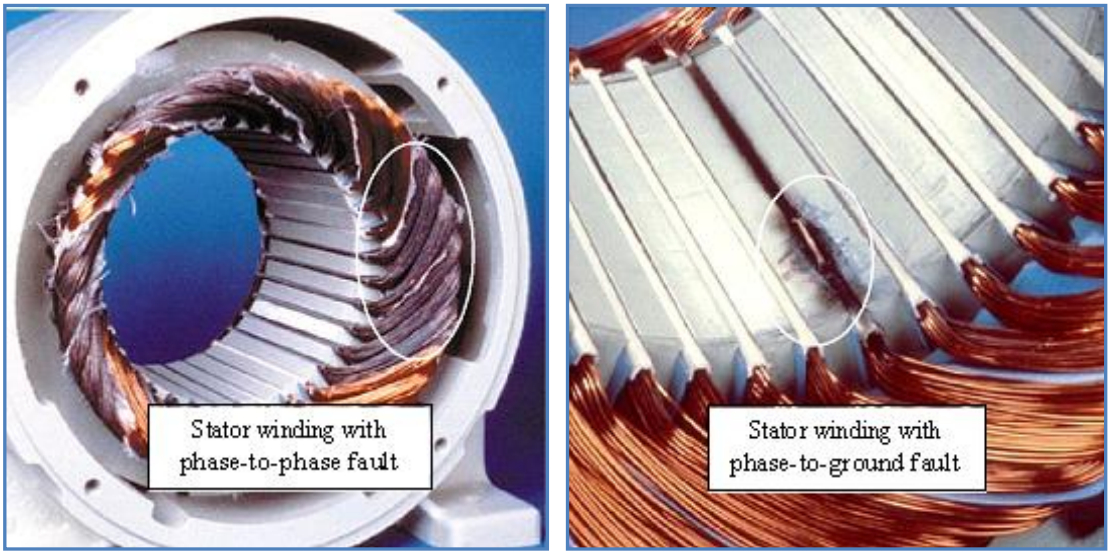

Figure 3.7 Out-Boundary Phase Faults (Courtesy of Baldor)

3.2.3 Bearings Faults

Bearings are used in the vast majority of electrical machines, and surveys showed that around 40% of all motor failures are bearing related [5, 36]. As shown in Figure 3.8, a bearing consists of two rings: inner and outer. A set of balls or rolling elements placed in raceways rotates inside these rings [2].

Bearing defects are categorized into two groups, the single point faults and the generalized roughness defects [85, 86]. The first where local damage is on one of the four bearing elements which include: inner raceway; outer raceway; balls; and the cage. In the second group of bearing defects the whole surface of a bearing element deteriorates considerably.

Roughness usually happens due to corrosion or lack of lubricant. Even under normal operating conditions with balanced load and good alignment, fatigue

failures may take place. These faults may lead to increased vibration and noise levels [87].

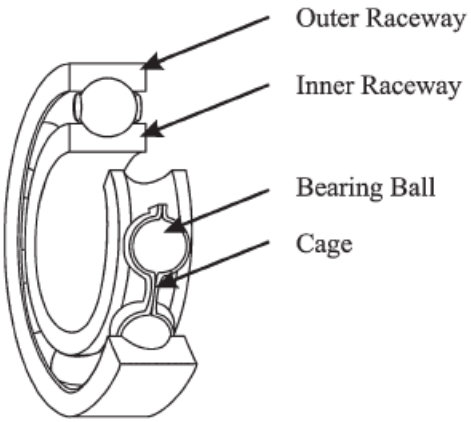

Figure 3.8 Bearing Main Component [85, 86]

3.2.3.1 Causes of Bearing Failures

The following list contains the most common causes of bearing failures [88].

- Thermal Overloads
- Inadequate Lubrication
- Contamination
- Improper Shaft and Housing Fits
- Misalignment
- Vibration
- Excessive Loading (Axial/Radial Combined)
- Machinery Defects
- Shaft to Ground Currents
- Incorrect Mounting
- Load, Life and Fatigue Factors
- Improper Application
- Machinery Defects
- Damaged During Transportation or Storage

Bearings stresses have been arranged into different groups of which are: thermal, electrical, mechanical and environmental causes. Table 3.4 shows these groups and the causes behind each of them.

Table 3.4 Bearing Stresses [78, 88]

1. Thermal Stresses	2. Evironmental Stresses	3. Vibration Stresses
• Friction	• Condensation	• Rotor
• Lubricant	• Restricted Vantelation	• System
• Ambient	• Foriegn Particals	• Driven Equipment
	• Excessive Temprature	
4. Dynamic Stresses	**5. Mechanical Stressses**	**6. Electrical Currents**
• Radial	• Loss of Clearances	• Rotor Assymetry
• Axial	• Missalingment	• Static Charges
• Preload	• Shaft/ Housing Fits	• Electrostatic Coupling

Early detection of defects allows replacement of the bearings, rather than replacement of the motor. If we knew that for a 100 hp three-phase ac motor, a bearing costs approximately one thirtieth of the motor cost [89], it can be imagined how a fault bearing detection could save money.

Bearings faults can be detected using different techniques. The most widely studied methods in bearing condition monitoring are based on measurements of vibration, acoustic noise, or temperature. Vibration and stator current based methods seem are of the most popular.

When monitoring bearing damage in induction motors, the characteristic frequencies of bearing damage are often used to monitor certain frequency components in either vibration or stator current signals [90]. Bearing defects are capable of injecting additional components into the stator current, so MCSA is used for such application as in [90-93]. The main disadvantage of using MCSA in this application is that the effects of a bearing fault are often subtle and difficult to predict [93]. A part of the work done in this project tries

to improve the detection and diagnosis of bearing defects using current monitoring.

3.2.4 Eccentricity

In electrical machines, when the air gap between the stator and rotor is non-uniform, it is said that the rotor is eccentric. Eccentricity can exist in the form of static or dynamic eccentricity or both, in which case it is called a mixed eccentricity fault.

Eccentricity occurs when the rotor is not centred within the stator. The eccentricity can be either static (the offset is in a fixed direction) or dynamic (the offset rotates with the rotor). Eccentricity distorts the uniformity of the machine air-gap between rotor and stator and this in turn leads to changes in the induction process that happens between the stator and rotor.

Due to some design and manufacturing imperfections, eccentricity may have an inherent nature. References have indicated that up to 10% eccentricity is allowable [94, 95], but when eccentricity becomes larger, the resulting unbalanced radial forces (also known as unbalanced magnetic pull or UMP) can cause stator to rotor rub, and this can result in damage of the stator and rotor [87, 95-97].

3.2.4.1 Causes of Eccentricity

Static and dynamic eccentricities can be caused by:

1. Manufacturing imperfection that lead to an oval stator core

2. Misalignment due to bearing misassembles
3. Bearing wear and tear
4. Misalignment of mechanical couplings
5. Mechanical resonance at critical speeds can result in dynamic eccentricity.

3.2.4.2 Static Eccentricity

Referring to Figure 3.9, in an ideal healthy symmetrical motor, the rotor symmetry point, C_r, and the stator symmetry point, C_s, coincide with the centre of rotation for the rotor (at the axis cross point).

The incidence of eccentricity means the separation of one of the three points from the other two, or the separation of all of them. When point C_s separates from the other two, static eccentricity occurs. In other words, static eccentricity can occur when a rotor has emigrated from a bore centre, but it is still turning about its bore centre [98, 99].

Eccentricity results in a non-uniform air gap over the stator inner circumference, which results in regions with the air gap length shorter or longer than that of the healthy motor. In this case, the position of minimum (and maximum) air gap versus stator is static.

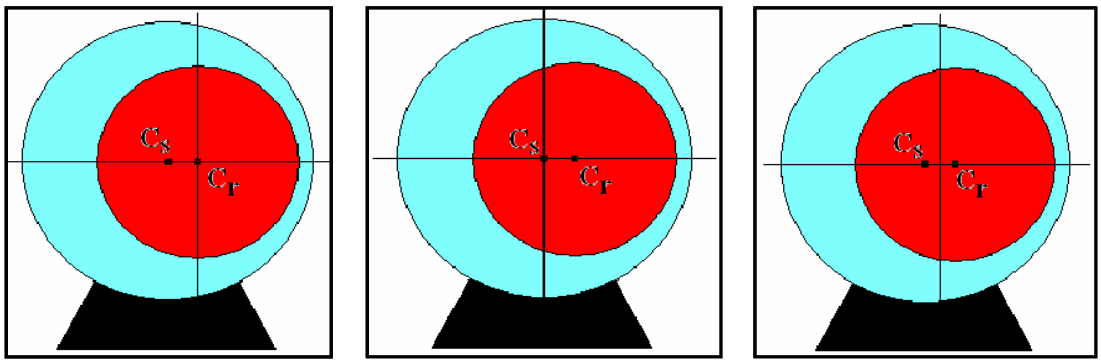

1.Static **2. Dynamic** **2. Mixed**

Figure 3.9 Eccentricity Types [100]

The position of a minimum radial air gap is fixed in space. It causes a steady unbalanced magnetic pull (UMP) in one direction. This can lead to a bent rotor shaft or bearing wear and tear. It can also lead to some degree of dynamic eccentricity.

3.2.4.3 Dynamic Eccentricity

Dynamic eccentricity occurs when a rotor turns upon a stator bore centre but not its own centre. It causes a minimum air gap that is always moving over the stator inner circumference. When the rotor centre rotates upon the motor centre with the rotational speed, the motor is said to experience a dynamic eccentricity [98, 99].

It is obvious in Figure 3.9, when centre, C_r, separates from the other points; the position of minimum (and maximum) air gap versus stator rotates with the rotor and is therefore called dynamic eccentricity.

3.2.4.4 Mixed Eccentricity

Both static and dynamic eccentricities have a tendency to co-exist in induction motors. With this condition, a rotor turns around neither its bore centre nor a stator bore centre, but around a point between the stator and rotor centres. Figure 3.9 shows that the rotational centre or the motor centre can be anywhere between the stator and rotor centres [98]. i.e. the commencement of mixed eccentricity is marked by the separation of all of the above mentioned three points from each other. Finally, when all three centres are separate from each other, the eccentricity is called mixed eccentricity. In mixed eccentricity, not only the position of minimum (and maximum) air gap versus the stator, but also the length of it varies with the rotation of the rotor [96].

During the last few decades, eccentricity faults in induction motors were one of the most popular topics among researchers [101]. The importance of studying eccentricity faults comes from the fact that they often are associated with large induction machines, where the repair or replacement costs arising out of such a scenario may easily run into tens of thousands of dollars [94].

Eccentricity faults could be diagnosed by monitoring some signals like motor current and air gap flux in induction motors. In [56], Internal and external search coils are placed in the stator and the spectral constituents of their induced voltage were observed for diagnosing. Long, W. et al [102, 103] have employed the MCSA technique along with artificial intelligence to detect and diagnose motor eccentricity.

It is worth noting that eccentricity is, in general, looked at as a secondary effect of other faults like rotor or bearing, thus it normally doesn't appear as one of the main IM faults statistics.

3.2.5 Shaft Misalignment

Shaft misalignment is defined as the deviation of the shaft position relative to the centreline of a coupled shaft-rotor system. Misalignment is one of the common faults in mechanical arrangements which produces another fault in the system [104].

The correct alignment of industrial motors to their driven units (pumps, gearboxes etc) is of vital importance in order to maintain plant reliability. If the motor is not correctly aligned, the stress placed on the motor shaft will cause premature wear and successive failure of the motor bearings leading to plant breakdowns and loss of production. This explains the importance of misalignment being monitored.

Misaligned motors, in addition, are a major source of wasted energy. When a motor is misaligned, there is friction increment on the shaft, making it harder to turn. Therefore, a motor will draw more current in order to turn its misaligned shaft which means an increase in energy consumption. Statistics show that, more than 60% of rotor faults are initiated as a misalignment fault before it aggregated [105]. Table 3.5 shows the IM components affected by various faults sources.

Table 3.5 Stresses Vs Motor Components [78]

Types of Stress	*Stator*	*Rotor*	*Bearings*	*Shaft*
Thermal	√	√	√	√
Electrical / Dielectric	√	√	√	
Mechanical	√	√	√	√
Dynamic		√	√	√
Shear				√
Vibration / Shock	√	√	√	√
Residual		√		√
Electro-Magnetic	√	√	√	√
Environmental	√	√	√	√

Misalignment generally manifests itself through vibration. Shaft misalignment is a major cause of vibration in machines [106]; hence vibration monitoring is one of the most commonly used approaches applied in misalignment CM. Vibration measurement is a good qualitative indicator for detecting the degree of misalignment in machinery while it is running [106]. MCSA also can be used for alignment detection as well. Obaid et al [107] have developed a method to detect shaft misalignment by only using the RMS value of the line current as a fault feature.

3.2.5.1 Causes and Types of Misalignment

There are few causes to which the occurrence of shaft misalignments is attributed; of which [106, 108, 109]:

- Temperature changes due to friction in the bearings.

- Improper mounting of the motor and the equipment being driven.
- Distortion forces due to motor starting up.
- Soft foot of the motor or load.

So far, only a few researchers have paid attention to shaft misalignment, due to the complexity in modelling the phenomenon [106].

There are two basic types of shaft misalignment: parallel misalignment and angular misalignment. Parallel misalignment occurs where the centrelines of the shafts are parallel but not co-linear. When the extended centrelines are cross not parallel, this is called angular misalignment.

In practice, misalignments in industry usually involve a combination of the two types, where the shafts suffer both parallel and angular misalignment [106]. This phenomenon is called combination misalignment which is obviously more damaging to the coupling and equipment than either of the two individual misalignments types.

Misalignment is also classified according to the source where the problem is initiated. From this definition, rotor misalignment can be classified into: coupling misalignment and bearing misalignment [110].

3.2.6 Oscillating Loads

Oscillating loads have unfavourable effects on the detection process of other faults and generally they mask the characteristic features of other faults.

Efforts are normally spent, as in [102, 103]; to get rid of such effects and reach the exact diagnosis of the root fault of the motor.

Influences from oscillating loads on stator currents have been presented in [71]. Such influences may lead to the wrong conclusions. Therefore, this point should be considered when one makes a diagnosis. With the assumptions that induction motors are lossless and are fed by the perfect sinusoidal supply voltages, it is possible to consider the effects of the oscillating loads in stator currents.

3.2.7 Secondary Faults

About 10-20% of the fault types statistics in Figure 3.4 and Table 3.1 are categorized as Other faults which don't fall under any of the main three classes of faults. Eccentricity, oscillating loads, and shaft misalignment, which are discussed in previous sections, are members of this group.

There are also few faults involving movement of conductors in the stator and failure of electrical connections in the motor. These are usually secondary effects due to one of the primary faults causing shock or excessive vibration [5]. Some faults cause others to progress as they happen. Misalignment belongs to this category. Table 3.6 shows how faults can affect the performance of IMs.

Table 3.6 IM Faults and Their Major Effects [111]

Fault / Effects	Unbalanced air-gap and line current	Increased torque pulsations	Decreased average torque	losses and efficiency reduction	Excessive heating
Stator Faults	√	√	√	√	√
Abnormal Connection of The Stator Windings			√	√	
Broken Rotor Bar or Cracked Rotor End-Rings			√	√	
Static and/or Dynamic Air-Gap Eccentricity	√	√		√	
Bent Shaft	√	√		√	√
Shorted Rotor Field Winding			√		
Bearing And Gearbox Failures				√	√

3.3 Summary

An introduction to induction motor faults was presented. The chapter arguments were consolidated by the relevant statistics when possible. The common and main sources and causes behind each fault were included and mentioned in brief, compared to the huge material available concerning that. Besides the main IM faults, examples of non-main or secondary faults were touched on, as well.

Chapter 4. Features Generation and Faults Diagnosis

Signal processing and spectral analysis methods are applied in industry for the monitoring of rotating machines such as motors and generators [73]. Besides other processing techniques, spectral analysis usually utilizes Fast Fourier Transform (FFT), Wavelet Transforms (WT), RMS calculations, and Park Vector Approach, to name few. A certain degree of expertise is needed in order to distinguish between a faulty system and a healthy one. This is because the monitored spectral components can result from a number of sources, including those related to healthy conditions [112].

The chapter looks into some fault detection and diagnosis techniques that detect the occurrence of the fault and decide on the condition of the induction machine and the incipient fault and its severity, if any.

4.1 Feature Generation

Feature is synonymous of attribute or characteristics, and feature generation or extraction means finding a good data representation. In the present context, it cab defined as finding the most relevant data that indicates the presence of a motor fault. This section present few techniques used for extracting the useful features representing the induction motor faults.

4.1.1 Park Vector Approach

The Park's transform (discussed in 5.9) allows the representation of the variables of a three phases machine through a co-ordinates system with two

perpendicular axes; direct (d) and quadrature (q) [113]. Hence, it allows the differentiation between the healthy and faulty machines through its locus as in Figure 4.1.

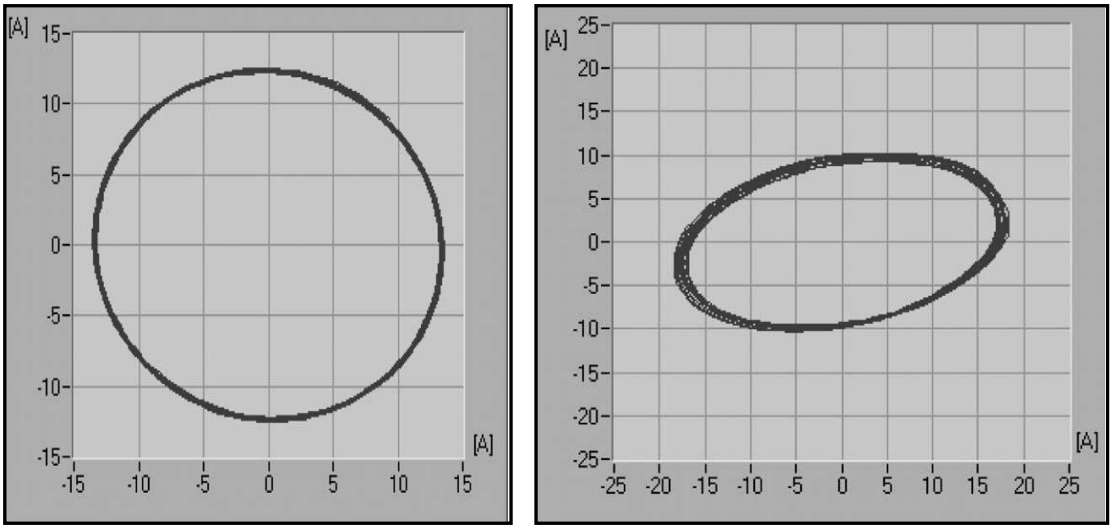

Figure 4.1 Geometric Locus For The Park's Currents Vector For A Healthy And With Inter-Turn Stator Fault Motor [113]

Park Vector Approach (PVA) has been successfully applied in the diagnosis of several faults in three-phase induction motors. In [29, 96, 114, 115], this diagnostic technique has been used to detect and locate phase and inter-stator faults, stator voltage unbalance, static eccentricity, and bearings faults, respectively.

This technique is based on identifying the appearance of an elliptical pattern, corresponding to the motor current Park's Vector representation, whose ellipticity increases with the severity of the fault and whose major axis orientation is associated with the faulty phase [116].

A new diagnostic technique, called Extended Park's Vector Approach (EPVA), was first introduced in order to improve the diagnosis of rotor cage

faults [117]. EPVA was also successfully applied in the diagnosis of stator windings faults as in [113, 114] , and bearings faults as in [118, 119]. The drawback of this approach is that it is not effective for static and dynamic eccentricities either [100].

4.1.2 Fast Fourier Transform

The essence of Fast Fourier Transform of a waveform is to decompose it into a sum of sinusoids of different frequencies. i.e. if these sinusoids are added together, the sum is the original waveform. FFT has the ability to allow one to look to a function in both time and frequency domains.

FFT has been utilized for generating the fault related features of different signals as current and vibration. Benbouzid et al [120] and Cabal-Yepez et al [121] have indicated MCSA-FFT analysis, is a reliable tool for multiple induction motor faults detection.

Durocher and Feldmeier [122] have designed an algorithm that uses MCSA and FFT signature to diagnose faults, including pump cavitations and misalignment leading to bearing failure. Other faults such as rotor [123], bearings [124], and monitored signals like speed [125, 126] were addressed.

FFT is a fundamental problem-solving tool in the educational and industrial sectors. And with the fast developments in computer technology, it has become one of the major tools utilized in the signal processing technology [127]. It is considered as one of the simplest methods that can be used for fault detection, and FFT analysis has been proved to be a very effective

method for stationary systems and has been widely used in the monitoring, fault detection and diagnosis in the industry [128]. FFT has been used as a feature generation tool in the field of IMCM.

4.1.3 Wavelet Transform

The FFT is suited to the analysis of stationary signals as it contains no information on how the frequency content varies over time. A popular approach to obtaining this time-frequency information is to use the Wavelet Transform [127].

Wavelets are mathematical tools that have recently emerged for applications such as waveform representations and segmentations, time-frequency analysis, detection of irregularities, and feature extractions [129].

One application is the fault detection and diagnosis during start-up for lightly loaded machines. However, the FFT method is incapable for such transient signals. The wavelet-based method can be used in these cases [129, 130].

Many researchers [131-135] have used WT as features extracted for several IM faults. Eren and Devaney [131] have shown how bearing faults are detected by analysing the motor current with wavelet transforms. The work presented in [105] has proved the success of WT in the detection of IM rotor faults.

In [133] Wavelet and Fourier transformations were applied to extract fault characteristics from the motor current for broken rotor bars, bowed rotor,

bearings, and eccentricity in an IM. The work has pointed out that FFT was insufficient to determine some faults. In the case of BRB and eccentricity, WT has the advantage of extracting more information to decide on the faulted situation. The two transformations were exploited as complementary to each other.

Another common fault among IMs was studied in [135]. Stator inter-turn short circuit fault with less than 5% of turns short circuited in stator winding have been presented. Wavelet transform was employed to obtain the characteristic features of the fault.

4.1.4 Negative Sequence Current

Stator fault detection is largely based on the principal that the negative sequence current (NSC) of healthy (ideally symmetrical) motors powered by symmetrical multiphase voltage is null. When turn-to-turn fault pops up, it breaks that symmetry and gives rise to negative sequence current which in return provides an indication of fault presence and can be used as fault severity measure. The theoretical basis for this approach is presented in [136].

Unbalanced supply voltages and inherent machine asymmetry also give rise to negative sequence current. However, neglecting inherent asymmetries can lead to misdetection, and catastrophic consequences [137]. For electrical machines, the negative-sequence current is the fundamental fault signature

for a winding fault [138]. NSC has been also used for the detection of eccentricity symptoms in the motor current as in [103].

It has been said that during unbalanced conditions, the produced negative sequence current component rotates in the opposite direction from the rotor. But, in reality, positive, negative and zero sequence currents are linear combinations of phase currents; thus, the vector of each sequence current rotates in the same direction as the phase current [139].

It is very well known that negative sequence current could cause rotor damage, and that damage is highly unfavourable to rotating machines such as motors and generators [139].

The work developed in [140] shows a reliable detection mechanism of turn fault using NSC and Neural networks. The detection of one shorted turn, out of 648 turns per phase, (0.15%) was demonstrated with the fault indicator becoming fully matured in just two cycles of line frequency after commencement of the fault. In addition, the effects of unbalanced supply voltages or load have been overcome.

The authors of [141] have utilized the performance of the angle and the amplitude of the negative sequence component of the stator current as a fault indicator. It has been shown, by modelling and experimentally, a direct correlation between the amplitude of the NSC component of the stator current and the severity of the fault.

Inter-turn winding fault detection based on various monitoring techniques are presented in the literature, however, the sequence component approach superimposes them in the sense it provides a better signal-to-noise ratio, is easier to measure, and it only requires current sensors, no other instrumentation [138].

4.1.5 Motor Current Root Mean Squared Value

In MCSA monitoring, one of the direct methods to look for fault characteristic features is by utilizing the Root Mean Squared (RMS) value of the motor current signal as in [142]. The basic idea of the used approach is to diagnose the fault from the FFT analysis of the RMS value of the input current. Since the RMS value of the stator current is constant, varying only with motor load, its spectrum only has a dc component. The presence of a fault is flagged through the detection of abnormal frequencies in the FFT analysis of RMS oscillatory component. RMS magnitude reflects the fault severity. The assumptions of this study were consolidated by simulation and experimental results.

RMS value of current or voltage can be used as a feature for simple as well as advanced detection systems. Obaid et al [107] have developed a method to detect eccentricity and shaft misalignment by only using the RMS of the

line current technique over a certain frequency. After being recorded, the line current was filtered to eliminate the line frequency component. The harmonics associated with faults are sufficiently large in practical applications that undesirable operating conditions can be detected without the need of excessive analysis of the current frequency components.

4.1.6 State or Output Observers

Model based condition monitoring is built mainly on the idea of utilizing analytical redundancy and modelling. The following are some of the techniques used for features extracting for this type of monitoring.

State observers are state estimators that reconstruct the state of the system using a linear model of the system, measured inputs, and outputs of the system. It is possible to design an observer-based FDD from the input-output relationship of the system. State observers are used in control systems to curb inconsistency between modelled and measured systems caused by noise or model errors. They can be used for FDD, if the process parameters are known and faults can be modelled as state variable changes of monitored system (e.g. actuator or sensor faults) [143].

When the constant parameters are unaffected by possible faults and only the state of the system, is affected by the faults; in this case the model acts as a state observer [21, 80]. The system state is represented by a set of generally immeasurable state variables (which is function of time).

For measured states, a residual is the difference between the measured and estimated states. But, for immeasurable states, a residual is the difference between the estimated and the measured system output.

4.1.7 Parameter Estimation

When the characteristic constant parameters of the process or of the components are affected by the fault, parameter estimation is used [21, 80]. Figure 4.2 illustrates a parameter estimation processes.

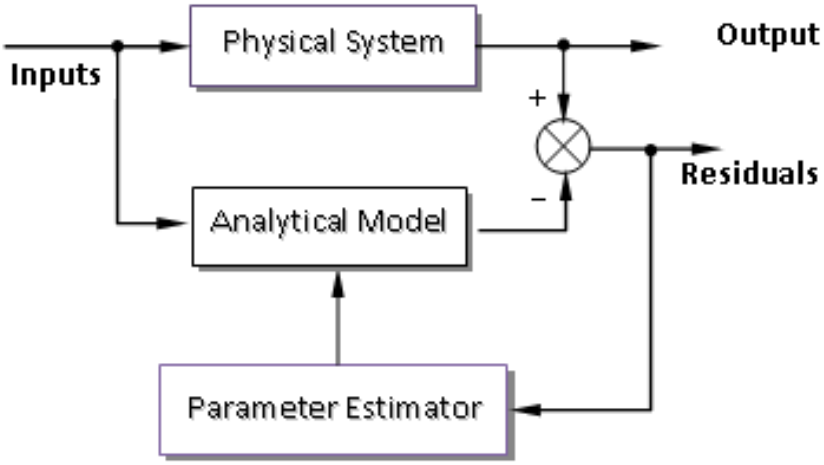

Figure 4.2 Parameter Estimation Diagram [111]

For most practical applications, the process parameters are not known. So they are determined by parameter estimation methods, as long as the inputs and outputs of the process are available. Models are used in parameter estimation algorithms. Since the parameter changes reflect the faults that occurred, they represent good features for condition monitoring.

4.2 Fault Diagnosis

After detecting the presence of fault characteristic features, the last stage of any CM process is attributing this feature, preferably to a certain fault, and then deciding on the severity of it. This often is called fault diagnosis.

In some situations, the diagnostic engine is fairly simple as in [14, 107, 113, 142], but for efficient online CM, more advanced techniques are exploited.

The diagnosis process becomes more complex if multiple faults of different degrees exist at the same time. To overcome such problems, a good interpreter is needed. Humans can perform this task, but an alternative solution is the usage of artificial intelligent (AI) techniques [5].

Artificial intelligence tries to emulate the mental capabilities of the human being and other creatures by using computational models. Beside others, AI techniques include Fuzzy Logic, Expert (Knowledge-Based) Systems, Genetic Algorithms (GA), Particle Swarm Techniques, and Artificial Neural Networks [135]. These techniques are the most used for FDD [144]. Such techniques are used for fault classifications.

The goal of classification is to categorize faulty and normal modes and determine the severity of the fault. A great deal of work has been reported in the literature on AI-based fault detection and diagnostic systems. Recent developments towards online IM fault diagnosis include artificial intelligence based techniques such as expert systems [120, 145], fuzzy logic [146, 147],

artificial neural networks (ANN) [148], and Neural-Fuzzy systems [149] are presented.

4.2.1 Fault Thresholds

Fault Threshold is a simple way of fault detection. It uses the threshold of a certain parameter. For example, in the spectrum of the current signal of a motor with rotor broken bars; it is possible to report the degree of the defect through looking at the amplitude difference between the main supply and side bands. The lesser the difference is the more bars are broken [14, 113].

4.2.2 Support Vector Machines

Support vector machines (SVMs) are a set of related supervised learning methods used for classification. If a set of data (training data) is used as training examples, each marked as belonging to one of two categories, SVM training algorithm has the capability to generate a model that can predict whether a new set of data example (testing data) falls into one category or the other.

The support vector machine (SVM) is a relatively new and powerful technique for solving supervised classification problems and is very useful due to its generalization ability [150].

SVMs are used as a classifier for the diagnosis engines. In [151-154] SVM was used for the monitoring process of gear box, and bearings. Rojas and Nandi [151] have attained at least 95% of successful classification, in the

study they carried out. They pinpointed that filtering of the signals is not always required, and there may be no need to introduce further complexity in the design of the classification systems. Therefore, the biggest advantage of the anticipated scheme is that it is extremely practical. Besides being very effective, the adequate software is available, allowing the implementation of the classifier very simple even for those users with little or no previous knowledge of SVMs [151].

In [155], different cases were examined using empirical data sets of vibration and stator current signals, and the results were compared in order find the best performance of classification process which was attained by using kernel functions (similarity measures). SVM has proved to be outstanding.

SVM was used for BRB detection and an accuracy of 97% was achieved which reveals that it is a powerful method for fault detection in rotor fault mentoring [156]. Using SVM with six features, 100% classification success was achieved in all testing cases. In all the cases considered, the training time of SVMs was substantially less compared to ANNs [152].

4.2.3 Artificial Neural Networks

The neural networks (NN), shown in Figure 4.3, emulate the neutrals of the human brain. It is widely used for fault diagnosis within induction motors like in [113] or in other applications as in [157]. ANNs consists, in general, from input, output and hidden layers of neurons.

The training of the NN involves feeding input and output data of the system to be used as a reference (training data); hence the NN would have the capability to diagnose the data associated with other conditions (tested data). In [133] The neural network system is constructed for fault classification and detection with the assistance of FFT and WT . The authors have validated the convenience of the neural network in a way that if the motor is changed, all that is needed is revisiting the transformations for the target motor to have the relevant features for the new machine updated. A reliable output could be obtained if other measurements such as vibration, or sound is used.

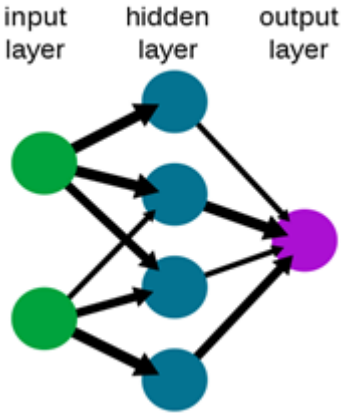

Figure 4.3 Simple NN Construction

4.2.4 Fault Trees

Fault trees (FT) are initiated and developed in the area of safety engineering. However, due to its ability of providing a thorough logical structure relating causes and effects, it has gained an acceptance into the field of fault diagnosis. In order to describe the relationship between the events of FT starting from the basic till the top event, FTs are made of logic gates, mainly AND and OR gates. The interactions between these gates are governed by Boolean algebra. Figure 4.4 illustrates FT example.

Preferably, the data to be used for FD is collected from practical runs of the system under consideration. However, it is possible to attain diagnosis by using models of the system of study where the faults can be modelled. Utilizing system models facilitate the running of an enormous number of experiments with a lot of saving of money and time. FT would be most useful when no analytical model exists, or after some ad hoc modifications to the system made it very different from that originally designed.

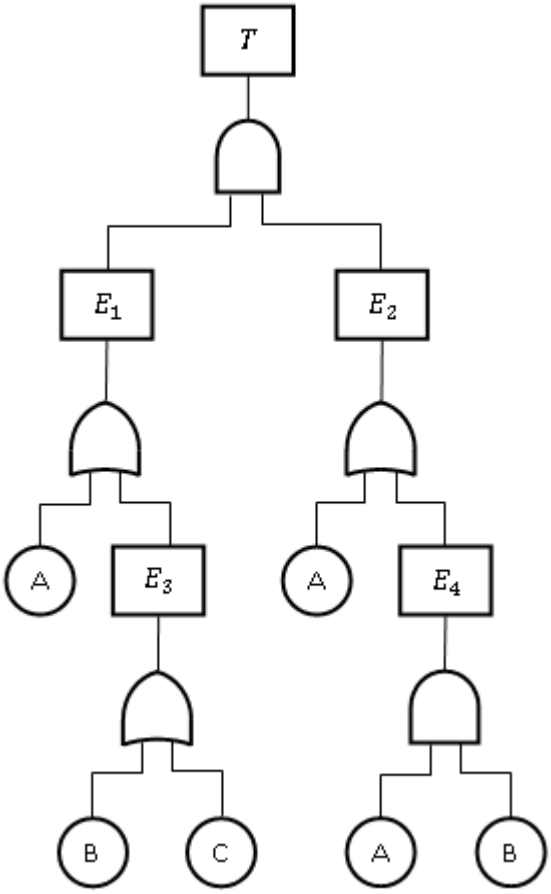

Figure 4.4 Fault Tree Example

Even though FTA is mainly used for safety and reliability studies, it has been used in the field of FD [158]. The authors of [159] have pointed out the possibility of using FT approach for the fault detection of electromechanical systems and the authors of [160] have indicated the well performance of fault trees in monitoring and diagnosis of incipient faults of a real electromechanical machine. From the literature, it has been shown that FTs have the capability of diagnosing faults in electromechanical systems, but little use has been made of them in the condition monitoring arena.

4.2.5 Fuzzy Logic

Fuzzy systems rely on a set of rules. These rules, while apparently are similar, allow the input to be fuzzy, i.e. more like the natural way that humans convey ideas. Therefore, the natural format greatly eases the interface between the user and the domain expert [161].

Fuzzy Logic has surfaced as an instrument for the controlling of different systems from simple applications to the most complex ones, from subway and industrial processes, to household, entertainment appliances, and fault detection and condition monitoring methods and application. Fuzzy logic approach facilitates the diagnosis of induction motor faults. It is reminiscent and evocative of human thinking processes enabling decisions to be made based on fuzzy information [162].

Fuzzy logic basically allows intermediate values to be defined between conventional evaluations like yes/no, true/false, etc. It makes notions, like “faulty” or “healthy”, can be formulated mathematically and processed by computers. In this way an attempt is made to apply a more human-like way of thinking in the programming of computers.

In [163] current, speed , and torque were used as mediums for the detection of few simulated IM faults. The fuzzy decision system achieved high diagnosis accuracy

Pereira and Gazzana [164] have examined the operation of a rotor using MCSA monitoring and fuzzy logic as a failure diagnosis technique. The

results were in good agreement with practice and the effort put was able to detect the correct number of rotor broken bars.

In condition monitoring of induction motors, Fuzzy logic was utilized mainly for the purpose of diagnosis. It was used for monitoring of bearings [146], broken rotor bars [164], stator winding inter-turns [162, 165], in the estimation process of some machine parameters [166] , as examples. The presented results, in general, found good acceptance by the authors and achieved high diagnosis accuracy.

Finally, it worth noting that in order to improve the performance of the detection and diagnosis process, some researchers have opted to combine two or more of the above mentioned techniques. For instance, the author of [152] has acquired a classification accuracy of 100% by combining NN, SVM and GA.

A thorough review of related works revealed that, hitherto, Neuro–fuzzy and NN based fault detection schemes are performed well for large machines; however, they are expensive and complex in application [167]. Appendix I presents detection of broken rotor bars fault using fuzzy logic analysis.

4.3 Summary

Chapter 4 has presented an overview of the different techniques and methods are in use to detect and diagnose faults in electric motors with special attention given to induction machines.

Fault detection was exposed through describing few methods for extracting the characteristic features related to each fault in both model-based and model-free CM techniques. The chapter is sealed with examining some diagnosis methods through the applications of mainly artificial intelligence.

This chapter and the preceding two chapters indicate the widespread nature of condition monitoring techniques which has been reflected in the huge literature concerning the condition monitoring of induction motors topic and this was presented by the number of references used; revealing the importance of such machines in the different aspects of life as mentioned. However, some approaches discussed here are more applicable to one project than the others.

From the above chapters, the importance and need for comprehensive non-intrusive monitoring systems is revealed, and that is the aim of this project. The system monitors different faults which are the main causes of more than 90 percent of induction motor faults.

Chapter 5. System Theoretical Analysis

This chapter will be confined to an electrical induction motor. It looks into the construction of the induction motors and their principles of operation. The chapter also introduces the development of a dq model that could be used for model based condition monitoring, which is beyond the scope of this project, in a later stage through modelling different faults of the IM. The model is verified against the real data collected during the testing stages from the test rig.

The equations that represent the induction motor are derived in order to build the Matlab-Simulink model of the IM. The a-b-c phase winding quantities are converted into equivalent dq quantities to get rid of the effect of mutual inductances between the stator and the rotor windings.

5.1 Induction Motors

Induction machines are widely used in industry as well as in home appliances. In industry, induction motors are used to drive various machines, such as pumps, fans, compressors, to just name a few. IMs with squirrel cage rotors are the most preferred due to their simple rugged construction and low running cost [168, 169]. So, condition monitoring of the performance of electric drives has received a substantial attention in recent years [21, 170], and as one of the tools for accomplishing that, modelling has attracted a wide attention.

As they are the most used type of movers in industry, squirrel cage rotor IMs has drawn the attention of engineers as well as industrialists. One of the fields that got a considerable attention is the fault detection and diagnosis (FDD) of such motors [5] as fault detection can prevent catastrophic failures and save huge losses that could be incurred.

IM can be classified according to their power ratings. Single phase motors which are used in low power ratings (fractions of KW or few KW) in applications where their speed doesn't have to be continuously controlled. Wound rotor induction generators are used in large power ratings (300 KW and higher) as in wind-electric generation [171].

An induction motor is an electric machine in which alternating voltage is induced into its revolving rotor due to the changing magnetic field in the stator. While the stator is fed with current directly, the rotor has its current because of induction, and hence the name comes, i.e. the current in the rotor is induced by that of the stator [169, 172-174].

In a simple way of description, an induction motor is, essentially, two main components, a stationary stator and a rotating rotor that are separated from each other by a small air gap that ranges from 0.4 mm to 4mm depending on the motor power [169]. According to the structure of its rotor, IMs are either Squirrel cage (SCIM) or Wound-Rotor induction motors.

5.2 Types of AC Electrical Motors

Since power companies generate alternating current exclusively, ac motors are the most extensively used type of machines. In addition to that, ac motors are cheaper compared to their dc counterparts. There are two classes of ac motors: Synchronous motors, and asynchronous (Induction) motors. The induction motor is the most common type of ac motors.

Single-phase induction motors are used for residential and commercial applications, but industry relies on the three-phase machines with a capacity of several kilowatts to thousands of kilowatts for their smoother operation and higher efficiency. Their characteristic features include [168, 169]:

- Simple, low-priced and rugged construction due to their rotor structure.
- Low cost and minimum operational costs with high reliability and efficiency.
- Need no extra starting motor and need not be synchronized.
- Run at constant speed from zero to full-load.

5.3 Structure of Induction Machines

An asynchronous motor is a type of motor where the speed of the rotor is less than that of the rotating magnetic field. Figure 5.1 shows a view of the different parts of SCIM. Both types of asynchronous motors operate on the same principle of induction and have the same stator arrangements but differ in rotor construction.

More than 90% of the induction motors utilize squirrel cage rotors because of their simple and robust construction [168]. The rotor is constructed of a laminated core with conductors placed in parallel to the shaft. The conductors are made of copper or aluminium bars. Each end of the rotor is short circuited by continuous end rings of similar material to that of the conductors. The rotor conductors and their end rings form a complete closed circuit and the rotor resembles a squirrel cage.

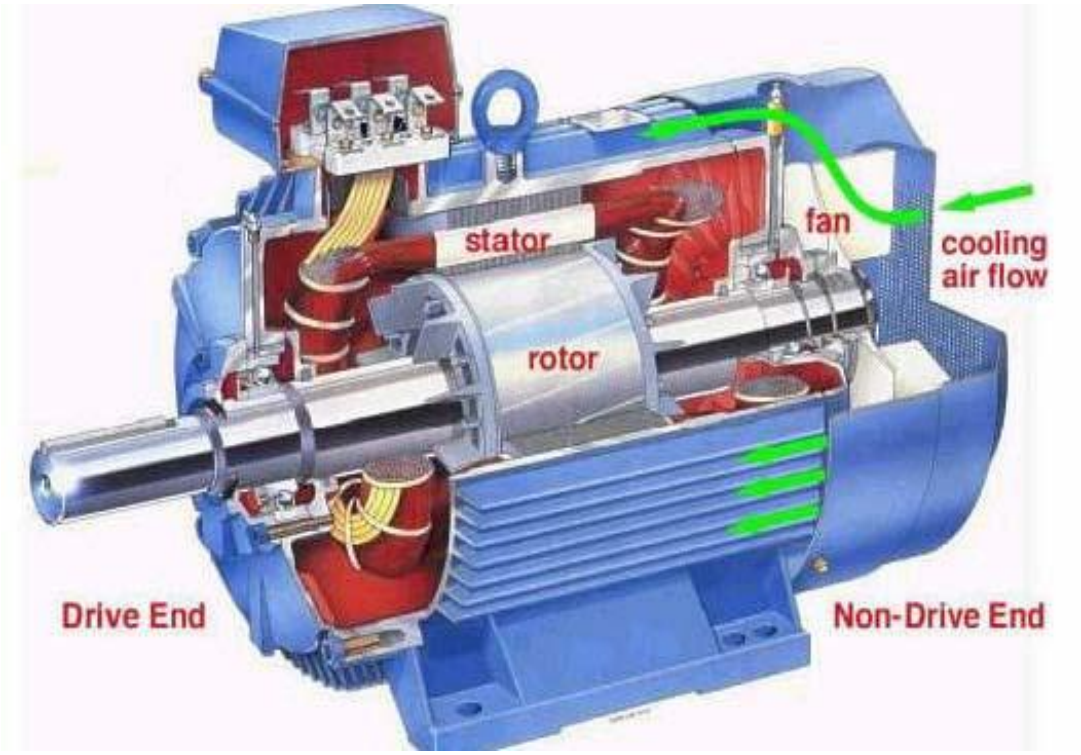

Figure 5.1 View of 3-phase SCIM

5.3.1 Cage Rotors

Cage rotors are of two types: cast and fabricated. They are mainly made of cooper or aluminium. Previously, cast rotors were only used in small machines. Advances in technology allowed casted rotors to be used even in

high power rated motors of thousands of KWs. Cast rotors though are more rugged than the fabricated type, but have the disadvantage of being almost unrepairable once faults develop in them [77]. Fabricated rotors are generally found in larger or special application machines. Figure 5.2 shows a die-cast aluminium squirrel cage rotor.

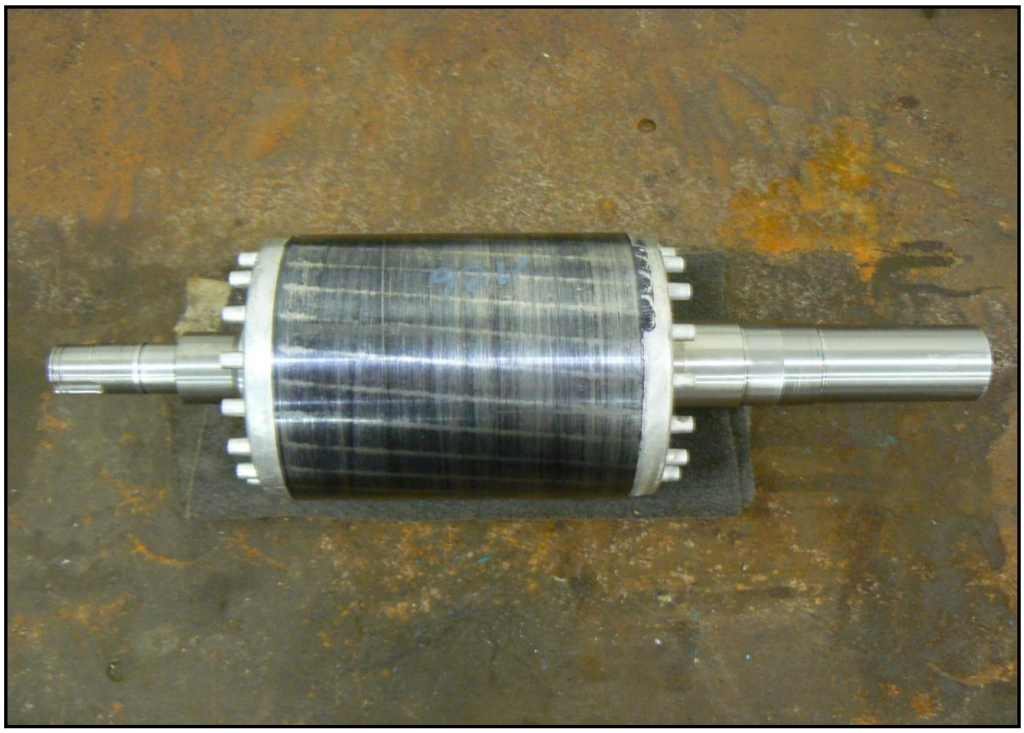

Figure 5.2 Squirrel Cage Aluminum Rotor

Wound rotors has a 3-phase winding similar to that of a stator. The winding is uniformly distributed in the slots and usually connected in wye. Wound rotor machines are equipped with slip rings to which the rotor windings are connected. The rotor slips turn with the rotor. Such rings provide the connections of the motor to external resistors through stationary brushes. The limiting resistors are normally engaged during the staring up of the motor. For normal running of the motor the three brushes are short circuited.

Wound rotor motors are known to have higher operational costs due to its maintenance cost to upkeep the slip rings, carbon brushes and also rotor windings [173].

5.3.2 Stator

Stator, for squirrel cage or wound rotor machines, is made up of a number of steel laminations stacked together forming a hollow cylinder. Coils of an insulated wire are inserted into slots of the stator core to form the stator core. Figure 5.3 shows a stator of a 3 phase induction motor.

Figure 5.3 Stator of an IM

The terminals of the three-phase windings can be connected in either a star or delta arrangement dependent on the motor application. When a high torque is required it is recommended to connect the stator winding in a delta arrangement. For these reasons it is common to find a direct-on-line motor

with an electric starter-unit which switches to star for start-up and then switches to delta for normal operation [175]. For three-phase motor the stator windings are geometrically placed at 120^{o} degrees.

The stator is wound for a definite number of poles as per speed requirements. The number of poles of the motor and consequently the motor speed depends on the way the coils are wound. To reduce eddy currents in the stator core, it is assembled of high grade, low electrical loss silicon steel laminations.

5.4 Basic Principles of Induction Motor Operation

The operating principles of induction motors are based on [171]:

1. An electromagnetic force (emf) is induced in a conductor moving in a magnetic field.

2. Force is produced on a current-carrying conductor when it is subjected to an external-established magnetic field.

In general, it could be said that the operation of 3-phase induction motors is based upon the application of Faraday's Law and the Lorentz Force on a conductor principle.

Consider a series of conductors of length (l) in the form of a ladder (Figure 5.4) whose ends are shorted by bars A and B. A permanent magnet moves at a speed (V), so that its magnetic field sweeps across the conductors.

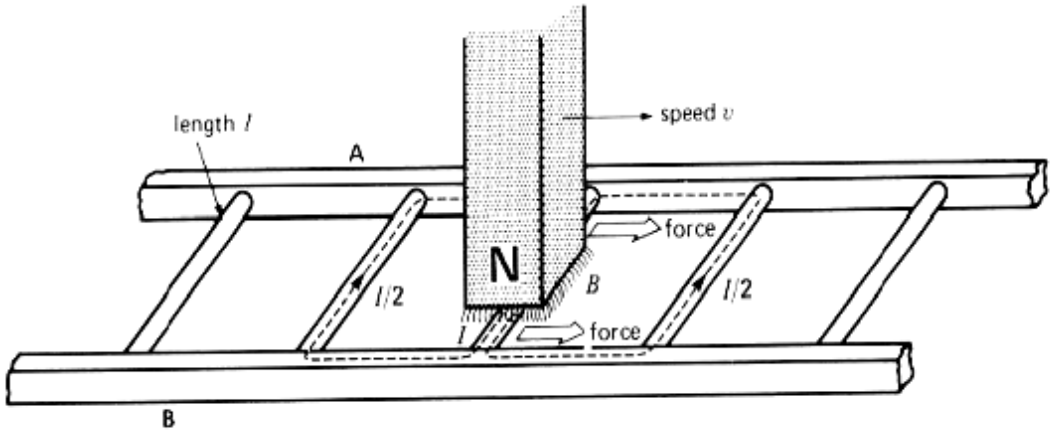

Figure 5.4 Magnet Moving Over Shorted Conductors [169]

A relation would initiate between the direction of the magnetic field and the direction of current flow. The left-hand rule for conductors would be applicable. The rule states; If a current carrying conductor is grasped with the left hand with the thumb pointing in the direction of electron flow, the fingers will point in the direction of the magnetic lines of flux.

Due to this observable fact, a force is generated according to Fleming's left-hand rule (for motors). That is when an electric current flows in a wire, and an external magnetic field is applied across that flow, the wire experiences a force perpendicular both to that field and to the direction of the current flow.

As the conductors are short-circuited, Faraday's law is applicable to a closed circuit made of thin wire and states that: The induced electromotive force (emf) in any closed circuit is equal to the time rate of change of the magnetic flux through the circuit.

Since there is a magnet producing an essentially constant and uniform magnetic field is placed above the first shorted conductor. If the

magnet is then moved to the right at a constant speed, the magnetic field of intensity *B* (Tesla) would sweep across the conducting rods.

As each conductor is cut by the flux, a voltage is induced in it. This induced voltage depends on the magnetic field intensity, conductor length and speed of the magnet. The voltage induced in a single bar and electromagnetic force are given by [169, 171]:

$$B = \Phi / A \quad \textbf{5.1}$$

$$E = B*l*v \quad \textbf{5.2}$$

$$Fem = B*l*i \quad \textbf{5.3}$$

Where:

E : the induced voltage (V),

V: the velocity of the bars (m/s),

L : the length of conductor (m),

B: the magnetic flux density (T),

Φ : the flux imposed on the conductor (Wb),

I: the current through the conductor (A),

*A:*s the conductor's cross sectional area (m^2),

Fem: electromagnetic force produced (N.m).

The voltage is induced in each conductor while it is being cut by the flux (Faraday's Law). The induced voltage produces currents which circulate in a loop around the conductors (through the bars). Since the current-carrying conductors lie in a magnetic field, they experience a mechanical force (Lorentz force). The force always acts in a direction to drag the conductor along with the magnetic field.

Now if the ladder is closed upon itself to form a squirrel cage, and placed in a rotating magnetic field – you have an induction motor! The movement of the ladder (rotor) will be circular which resembles the movement of the rotor.

5.5 Permanent Magnet Approach

To see how a rotor works, a magnet mounted on a shaft can be substituted for the squirrel cage rotor as in Figure 5.5 (Figures 5.5 through 5.8 are courtesy of Siemens). When the stator windings are energized, a rotating magnetic field is established. The magnet has its own magnetic field that interacts with the rotating magnetic field of the stator. Both of the stator and rotor resemble two magnets.

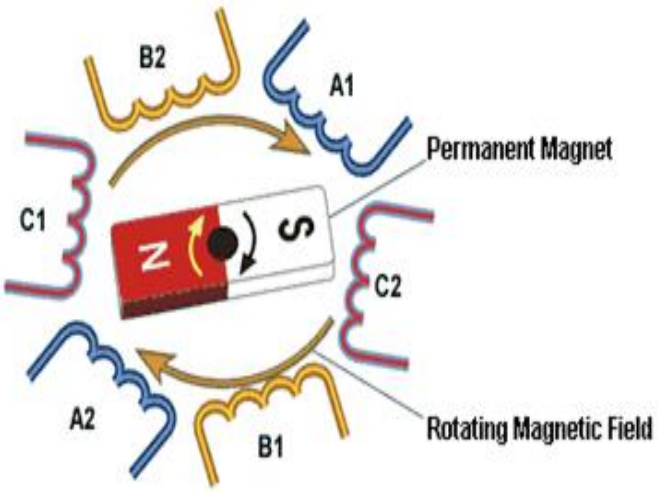

Figure 5.5 Permanent Magnet Concept

The north pole of the rotating magnetic field attracts the south pole of the magnet, and the south pole of the rotating magnetic field attracts the north pole of the magnet. As the rotating magnetic field rotates, it pulls the magnet

along causing it to rotate. When used for motors, this design is referred to as a permanent magnet synchronous motor.

The squirrel cage rotor acts essentially the same as the magnet. When power is applied to the stator, current flows through the winding, causing an expanding electromagnetic field which cuts across the rotor bars.

5.6 Electromagnetic Force Mechanism

When a conductor, such as a rotor bar, passes through a magnetic field a voltage (emf) is induced in the conductor. The induced voltage causes a current flow in the conductor. Current flows through the rotor bars and around the end ring. The current flow in the conductor bars produces magnetic fields around each rotor bar. Remembering that in an ac circuit, current continuously changes direction and amplitude.

The resultant magnetic field of the stator and rotor continuously change. The squirrel cage rotor becomes an electromagnet with alternating north and south poles.

For more illustration, Figure 5.6 shows a simple stator with 6 salient poles is considered. The windings are mechanically spaced at 120° from each other. The windings are connected to a 3-phase source. AC currents I_a, I_b and I_c will flow in the windings. Each winding produces its own mmf, which creates a flux across the hollow heart of the stator. The 3 fluxes combine to produce a magnetic field that rotates at the same supply frequency.

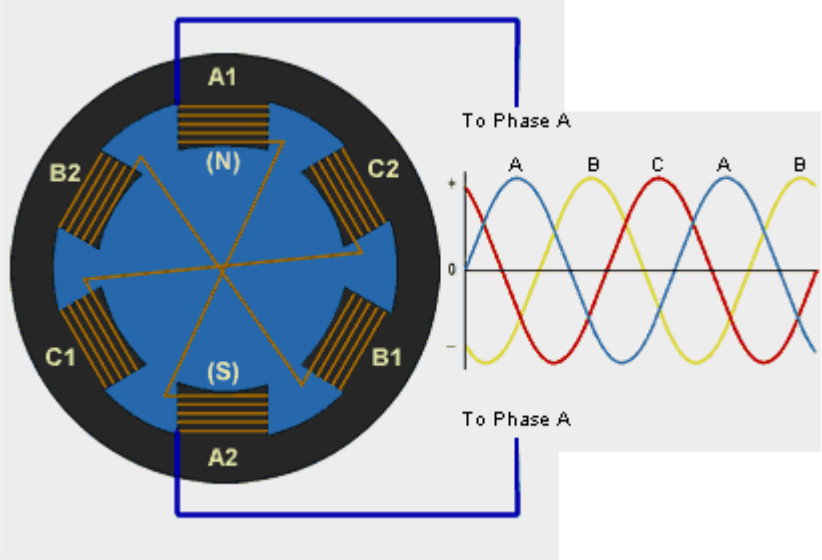

Figure 5.6 Six-Salient Pole Stator

Out of the six coils, two are used for each of the three phases. The coils operate in pairs. The coils are wound around the core material of the stator. These coils represent the motor windings. Each motor winding becomes a separate electromagnet. The coils are wound in such a way that when current flows in them one coil is a north pole and its pair is a south pole. For example, if A1 were a north pole then A2 would be a south pole. When current reverses direction the polarity of the poles would also reverse.

The number of poles is determined by how many times a phase winding appears. Here each phase winding appears two times. This is a two-pole stator. If each phase winding appeared four times it would be a four-pole stator. When AC voltage is applied to the stator, current flows through the windings.

The magnetic field developed in a phase winding depends on the direction of current flow through that winding. The chart in Figure 5.7 is used here for

explanation. It will be used in the next few illustrations to demonstrate how a rotating magnetic field is developed. It assumes that a positive current flow in the A1, B1 and C1 windings result in a north pole.

Timing	Winding	Current Flow Direction	
		Positive	Negative
0^0	A1	North	South
60^0	A2	South	North
120^0	B1	North	South
180^0	B2	South	North
240^0	C1	North	South
300^0	C2	South	North

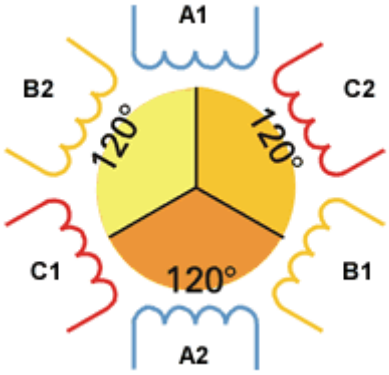

Figure 5.7 Stator Windings Current Flow and Distribution

It worth noting that when both of the stator and rotor are completely circular, the inner gap between them is uniform and the magnetic reluctance as well and the machine is called a non-salient pole motor [171].

5.6.1 Start (0 degrees)

The step by step operation of the motor can be explained with the help of Figure 5.8. As the motor is a 2-pole, 3-phase, the full rotation of the rotor would be looked at as intervals of 60 degrees each. It is easier to visualize a magnetic field in the following illustration, for example, a start time has been selected arbitrary during which phase A has no current flow. Phase B has current flow in a negative direction. Phase C has current flow in a positive direction. Based on the above chart, B1 and C2 are south poles and B2 and

C1 are north poles. Magnetic lines of flux leave the B2 north pole and enter the nearest south pole, C2. Magnetic lines of flux also leave the C1 north pole and enter the nearest south pole, B1. A magnetic field results, as indicated by the arrow.

5.6.2 Time Slots 1 and 2 (60 and 180 degrees)

If the field is evaluated at 60° intervals from the starting point, at Time 1, it can be seen that the field will rotate 60°. At Time 1 phase C has no current flow, phase A has current flow in a positive direction and phase B has current flow in a negative direction. Following the same logic as used for the starting point, windings A1 and B2 are north poles and windings A2 and B1 are south poles.

At Time 2 the magnetic field has rotated 60° (120° from start). Phase B has no current flow. Although current is decreasing in phase A it is still flowing in a positive direction. Phase C is now flowing in a negative direction. At start it was flowing in a positive direction. Current flow has changed directions in the phase C windings and the magnetic poles have reversed polarity. B is at the edge of changing polarity.

5.6.3 Time Slot 6 (full cycle)

At the end of six such time intervals the magnetic field, as well as the rotor, will have rotated one full revolution or 360°. This process will repeat every 20 msec on a 50 Hz stator supply.

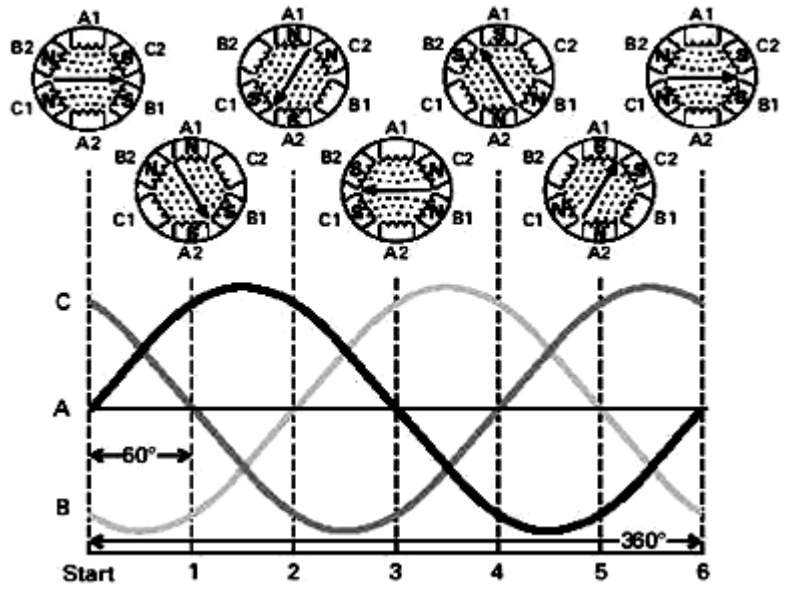

Figure 5.8 Stator Electromagnetic Field

5.7 Synchronous Speed and Slip

The speed of the rotating magnetic field is referred to as synchronous speed (ω_S). Synchronous speed depends on supply the frequency (f) and the number of poles (P). Synchronous speed is directly proportional to the supply frequency and inversely proportional to the number of poles according to the following relation:

$$\omega_S = 120 * f / P \qquad 5.4$$

There must be a relative difference in speed between the rotor (ω_r) and the rotating magnetic field (ω_S). If the rotor and the rotating magnetic field were turning at the same speed no relative motion would exist between the two, therefore no lines of flux would be cut, and no voltage would be induced in

the rotor. The difference in speed is called slip (S). Slip is necessary to produce torque. Slip is dependent on load. An increase in load will cause the rotor to slow down or increases slip. A decrease in load will cause the rotor to speed up or decreases slip. Slip is expressed as a percentage and can be determined with the following formula. Where: ω_S, ω_S are the synchronous and rotor speeds in (rpm) respectively.

$$\text{Slip (s)\%} = (\omega_s - \omega_r) * 100 / \omega_s \quad \textbf{5.5}$$

The slip of fully loaded, large induction machines (of 1000 KW and more) seldom exceeds the limit of 0.5%, and for small motors (10 KW or less), it seldom exceeds 5%. Under normal loads, the gap is very narrow between the rotor and synchronous speed [169]. Where f_r is frequency of voltage and current in the rotor, the frequency induced in the rotor depends on the slip and is:

$$f_r = s*f \quad \textbf{5.6}$$

5.8 Simulation of Induction Motor

Simulation is the imitation of a real system or process through equations that represent its physical behaviour in the form of a computer algorithm. Such algorithm constitutes a model of the system. The main advantage of simulation is allowing investigation of the behaviour of simulated system under different circumstances and studying the consequences of changing system parameters, or exploring a new system operating strategy, in a

quicker and cheaper way than by conducting a series of experimental studies on an actual system, which means saving time and money. Simulation is also used when the real system cannot be utilized. The real system may not be engaged because it may not be accessible, it may be dangerous or unacceptable to engage, or it may simply does not exist [176]. Even though models and simulations can never replace observations and experiments, but they constitute an important and useful component [177].

5.9 dq Representation of The Motor

It is known that the mutual inductances between the stator and the rotor windings are dependent on the rotor angle θ_m and that affects the rotor and stator flux linkages λ_r and λ_S.The stator and rotor phase currents i_a, i_b, i_c, i_A, i_B, and i_C, respectively can be represented by the following equations:

$$\overrightarrow{\imath_s^a}(t) = i_a(t) + i_b(t)e^{j2\pi/3} + i_c(t)e^{j4\pi/3} \quad \textbf{5.7}$$

$$\overrightarrow{\imath_r^A}(t) = i_A(t) + i_B(t)e^{j2\pi/3} + i_C(t)e^{j4\pi/3} \quad \textbf{5.8}$$

And hence the magneto motive force (mmf) produced is:

$$\overrightarrow{F_r^A}(t) = \frac{Ns}{P}\,\overrightarrow{\imath_r^A}(t) \quad \textbf{5.9}$$

$$\overrightarrow{F_s^a}(t) = \frac{Ns}{P}\,\overrightarrow{\imath_s^a}(t) \quad \textbf{5.10}$$

Where:

Ns: number of stator windings

P: number of poles.

$\overrightarrow{i_s^a}(t), \overrightarrow{i_r^A}(t)$: The resultant stator(rotor) current space vector with respect to a (A) axis.

In Park transformation (Figure 5.9), two virtual orthogonal axes are used and the equivalent stator and rotor windings are placed along these two axis. As the mmf produced by the dq windings currents is the same as that by the three phase winding currents.

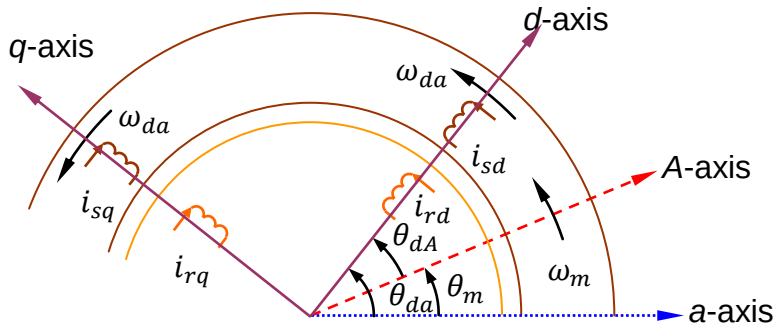

Figure 5.9 dq Representation of Stator and Rotor windings [168]

The mmfs $\overrightarrow{F_s}(t)\ and\ \overrightarrow{F_r}(t)$ and the currents $i_s(t)$ and $i_r(t)$ can be produced by the components $i_{sd}(t)$,$i_{sq}(t)$, $i_{rd}(t)$, and $i_{rq}(t)$ respectively flowing through their respective windings as each of stator (rotor) windings has a resistance R_s (R_r) and leakage inductance $L_{ls}(L_{lr})$.

While the mutual inductance between these two orothogonal windings is zero, the mutual inductance between the d-axis windings on the stator and the rotor equals L_m due to the magnetizing flux crossing the air gap. Also the

mutual inductance between the stator and the rotor q-axis windings equals L_m. The mutual inductance between any d-axis windings with any q-axis windings is zero because of their orthogonal orientation which results in zero mutual magnetic coupling of flux. Both rotor and stator 3-windings are assumed to be sinusoidally-distributed. The rotor windings are , of course, hypothetical. In order to produce the same mmf distribution in the air gap, the number of the two sinusoidally-distributed orthogonal windings are chosen to be $\sqrt{3/2}Ns$ turns. Choosing this number of turns for each winding results in their magnetizing inductance to be L_m (same as the per-phase magnetizing inductance for the normal windings). The first winding is positioned at the Direct (d) axis, while the other at the Quadra (q) axis. The angle between d and the stator axis a is chosen arbitrary at θ_{da} with respect to phase-a axis. With these two orthogonal windings, the torque and the flux within the machine can be controlled independently [168].

$$\frac{\sqrt{3/2}}{P} Ns \left(i_{sd} + j i_{sq}\right) = \frac{Ns}{P} \overrightarrow{\imath_s^d}(t) \qquad \textbf{5.11}$$

Equation 5.11 simplifies to:

$$\left(i_{sd} + j i_{sq}\right) = \sqrt{2/3}\, \overrightarrow{\imath_s^d} \qquad \textbf{5.12}$$

As d-axis is displaced by angles θ_{da} and θ_{dA} from the a- and A-axes respectively, therefore:

$$\overrightarrow{\imath_s}(t) = \overrightarrow{\imath_s^a}\, e^{-j\theta_{da}} \qquad \textbf{5.13}$$

$$\overrightarrow{\iota_r}(t) = \overrightarrow{\iota_r^A}\, e^{-j\theta_{dA}} \quad \textbf{5.14}$$

Substituting $\overrightarrow{\iota_s^a}$ and $\overrightarrow{\iota_r^A}$ from 5.7 and 5.8 into 5.13 and 5.14 respectively leads to:

$$\overrightarrow{\iota_s}(t) = i_a(t)e^{-j\theta_{da}} + i_b(t)e^{-j(\theta_{da}-\frac{2\pi}{3})} + i_c(t)e^{-j(\theta_{da}-\frac{4\pi}{3})} \quad \textbf{5.15}$$

$$\overrightarrow{\iota_r}(t) = i_A(t)e^{-j\theta_{dA}} + i_B(t)e^{-j(\theta_{dA}-\frac{2\pi}{3})} + i_C(t)e^{-j(\theta_{dA}-\frac{4\pi}{3})} \quad \textbf{5.16}$$

Where:

i_{sd}, i_{sq}: Stator current in d and q windings respectively.

$\overrightarrow{\iota_s^d}$: The current space vector with respect to d axis.

Since the imaginary and real parts of equations 3.5 and 3.8 can be equated, from which it could be derived that:

$$\begin{bmatrix} i_{sd} \\ i_{sq} \end{bmatrix} = \underbrace{\sqrt{\frac{2}{3}}\begin{bmatrix} \cos(\theta_{da}) & \cos(\theta_{da}-2\pi/3) & \cos(\theta_{da}-4\pi/3) \\ -\sin(\theta_{da}) & -\sin(\theta_{da}-2\pi/3) & -\sin(\theta_{da}-4\pi/3) \end{bmatrix}}_{[T_S]_{abc\to dq}} \begin{bmatrix} i_a \\ i_b \\ i_c \end{bmatrix} \quad \textbf{5.17}$$

Where: $[T_S]_{abc\to dq}$ is the stator transformation matrix to transform the a-b-c phase winding currents to their corresponding dq winding currents, and

$$\begin{bmatrix} i_{rd} \\ i_{rq} \end{bmatrix} = \underbrace{\sqrt{\frac{2}{3}}\begin{bmatrix} \cos(\theta_{dA}) & \cos(\theta_{dA}-2\pi/3) & \cos(\theta_{dA}-4\pi/3) \\ -\sin(\theta_{dA}) & -\sin(\theta_{dA}-2\pi/3) & -\sin(\theta_{dA}-4\pi/3) \end{bmatrix}}_{[T_r]_{ABC\to dq}} \begin{bmatrix} i_A \\ i_B \\ i_C \end{bmatrix} \quad \textbf{5.18}$$

Where: $[T_r]_{ABC\rightarrow dq}$ is the rotor transformation matrix to transform the equivalent A-B-C phase winding currents to their corresponding dq winding currents.

The same matrix relates the stator (rotor) flux linkages and the stator (rotor) voltages in phase (the equivalent A-B-C) windings to those in the corresponding stator (rotor) dq windings [168].

5.10 Flux linkages, voltages, and currents of dq windings

As there is no mutual coupling between the windings of d axis with those of q axis, the flux of each winding is only due to the currents passes through it and the presence of the other winding located on the same axis. Therefore:

$$\boldsymbol{\lambda}_{sd=}\boldsymbol{L}_s i_{sd} + \boldsymbol{L}_m i_{rd} \quad \textbf{5.19}$$

$$\boldsymbol{\lambda}_{sq=}\boldsymbol{L}_s i_{sq} + \boldsymbol{L}_m i_{rq} \quad \textbf{5.20}$$

$$\boldsymbol{\lambda}_{rd=}\boldsymbol{L}_r i_{rd} + \boldsymbol{L}_m i_{sd} \quad \textbf{5.21}$$

$$\boldsymbol{\lambda}_{rq=}\boldsymbol{L}_r i_{rq} + \boldsymbol{L}_m i_{sq} \quad \textbf{5.22}$$

Where: $L_s = L_{\ell s} + L_m$ and $L_r = L_{\ell r} + L_m$

Equations 5.19 through 5.22 can be written in a vector form which yields to:

$$\begin{bmatrix}\lambda_{sd}\\ \lambda_{sq}\\ \lambda_{rd}\\ \lambda_{rq}\end{bmatrix} = \underbrace{\begin{bmatrix}L_s & 0 & L_m & 0\\ 0 & L_s & 0 & L_m\\ L_m & 0 & L_r & 0\\ 0 & L_m & 0 & L_r\end{bmatrix}}_{\boldsymbol{M}_L}\begin{bmatrix}i_{sd}\\ i_{sq}\\ i_{rd}\\ i_{rq}\end{bmatrix} \quad \textbf{5.23}$$

The voltages of d and q windings for both the stator and rotor are represented by the following equations:

Where $\omega_d$is the instantaneous speed of the dq winding in the air gap (electrical rad /sec) and $\frac{d\theta_{da}}{dt} = \omega_{da}$. The last two equations can be put in a vector form where the rotate matrix $\boldsymbol{M}_R$= $\begin{bmatrix} 0 & -1 \\ 1 & 0 \end{bmatrix}$ corresponds to the (j) operator which has the role of rotating the space vectors $\boldsymbol{\lambda}_{s\_dq}$ and $\boldsymbol{\lambda}_{r\_dq}$ by an angle of 90 degrees.

$$\frac{d}{dt}\begin{bmatrix}\lambda_{sd}\\ \lambda_{sq}\end{bmatrix} = \begin{bmatrix}V_{sd}\\ V_{sq}\end{bmatrix} - \boldsymbol{R}_s\begin{bmatrix}i_{sd}\\ i_{sq}\end{bmatrix} - \omega_{da}\begin{bmatrix}0 & -1\\ 1 & 0\end{bmatrix}\begin{bmatrix}\lambda_{sd}\\ \lambda_{sq}\end{bmatrix} \quad \textbf{5.24}$$

$$\frac{d}{dt}\begin{bmatrix}\lambda_{rd}\\ \lambda_{rq}\end{bmatrix} = \begin{bmatrix}V_{rd}\\ V_{rq}\end{bmatrix} - \boldsymbol{R}_r\begin{bmatrix}i_{rd}\\ i_{rq}\end{bmatrix} - \omega_{dA}\begin{bmatrix}0 & -1\\ 1 & 0\end{bmatrix}\begin{bmatrix}\lambda_{rd}\\ \lambda_{rq}\end{bmatrix} \quad \textbf{5.25}$$

For the steady state operation, the left sides of the last two equations will be zeroes as all the dq winding variables are dc quantities and both of V_{rd} and V_{rq} as well. By substituting all of the flux linkages in the last two equation from equations 5.19 through 5.22 and by letting ω_d=ω_{syn} (knowing that: $\omega_{syn} = 2\pi f$) will result in the voltage- current relation with regard to the stator and rotor inductances as in 5.26.

$$\begin{bmatrix}V_{sd}\\ V_{sq}\\ 0\\ 0\end{bmatrix} = \underbrace{\begin{bmatrix} R_s & -\omega_{syn}L_s & 0 & -\omega_{syn}L_m \\ \omega_{syn}L_s & R_s & \omega_{syn}L_m & 0 \\ 0 & -s\omega_{syn}L_m & R_r & -s\omega_{syn}L_r \\ s\omega_{syn}L_m & 0 & s\omega_{syn}L_r & R_r \end{bmatrix}}_{A}\begin{bmatrix}i_{sd}\\ i_{sq}\\ i_{rd}\\ i_{rq}\end{bmatrix} \quad \textbf{5.26}$$

The mechanical torque, load, electrical and mechanical speeds are related according to the following equations:

$$T_{em} = \frac{P}{2}\left(\lambda_{rq} i_{rd} - \lambda_{rd} i_{rq}\right) \quad \textbf{5.27}$$

$$\frac{d}{dt}(\omega_{mech}) = \frac{T_{em} - T_L}{J_{eq}} \quad \textbf{5.28}$$

$$\omega_{mech} = \frac{2}{P}\omega_m \quad \textbf{5.29}$$

Where: T_m is the elect mechanical torque produced by the motor,

T_L is the load torque, J_{eq} is the combined inertia of the load, motor and

ω_{mech} and ω_m are the mechanical and electrical speed of the rotor respectively.

5.11 Simulink Model

The Simulink block diagram of AC motor is shown in Figure 5.10. The input and output signals from each block are labelled for convenience.

Three phase input voltage $\boldsymbol{v}_{s\_abc}$ is transformed to $\boldsymbol{v}_{s\_dq}$ through park transformation block. The stator and rotor fluxes state equations are continuously calculated using the dq parameters of currents and voltages through two blocks named stator and rotor. The voltage vector for the rotor is zero as the rotor bars are short circuited.

Next the flux vector is used to obtain the stator and rotor currents using transformation of Equation 5.23. Both torque and mechanical rotor speed were calculated using the stator and rotor currents as in Equations 5.27-5.29.

5.12 Model Validation

The model will be validated using data collected using the test rig. The validation process is limited to the healthy motor only. The motor parameters used for the simulation model can be found in Appendix II.

Figure 5.11 shows both the simulated and actual line currents, it is noted that the model takes longer to reach its steady state as some friction and other losses due to eddy currents were not taken in account. Furthermore the motor parameter values used for the model calculations could add some more errors as those concerns the used motor could probably differ from that supplied by the manufacturer.

Another point to be mentioned here is that the measured transient current values are limited to a maximum of 124 A by the DAQ system starting from the sensor box which is designed to for steady state current signals. Whereas, for steady state, Figure 5.12 and Figure 5.13 demonstrate a good agreement with less than 10% difference between the model and actual system at full and no load which coincide with the results in Chapter 7.

The motor shaft torque plot is illustrated in Figure 5.14. It has shown poor agreement between the measured and simulated graphs especially during the transient period which took longer time than that of the currents.

The lack of full agreement could be attributed to few factors of which are supply unbalance, friction, and eddy currents losses. The supply unbalance is responsible for negative torques affecting the motor resultant torque.

Friction and eddy current losses also add to the previous effect. A third factor is that the dq model representation of the load is not optimum and hence the overall result is affected. The agreement is clear after the motor reaches steady state and both of the simulated and actual signals are fluctuating around the target full load.

.

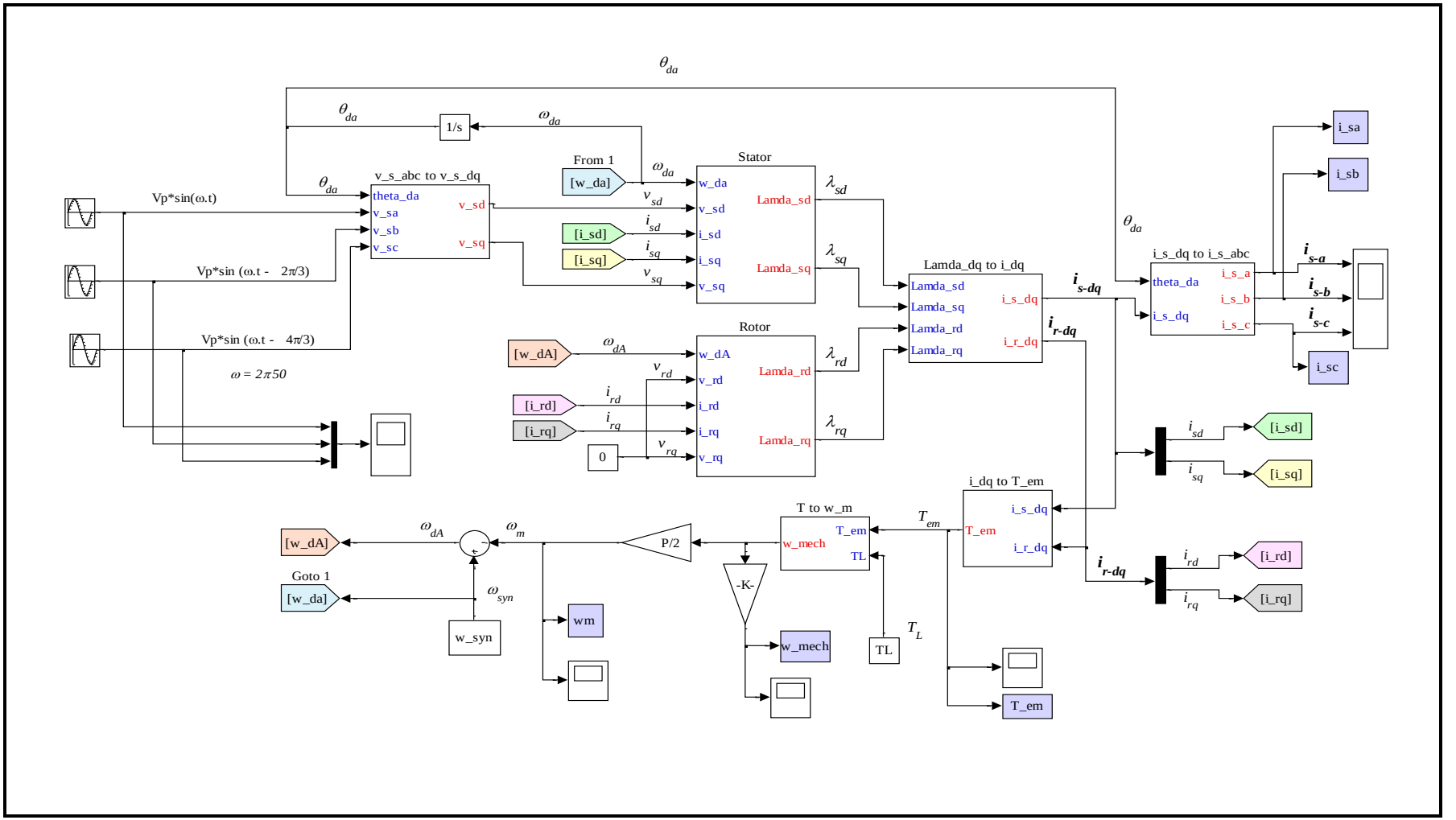

Figure 5.10 Simulink dq-Model of The IM

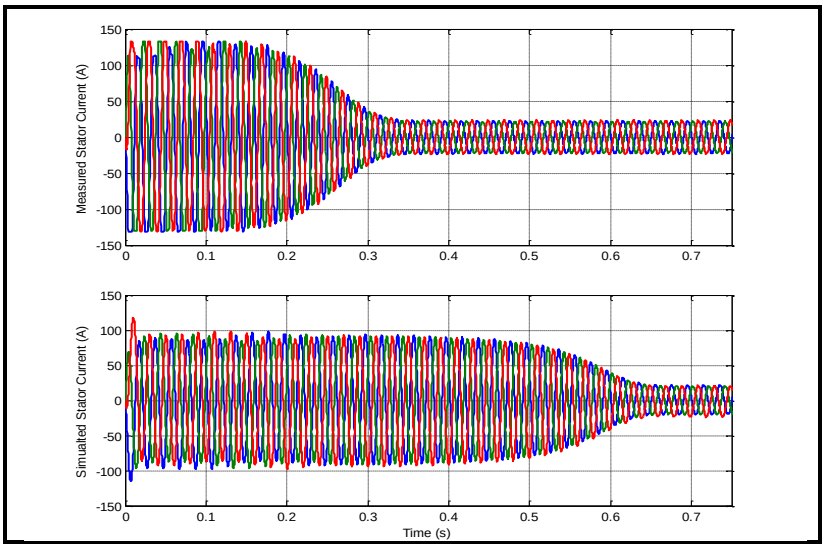

Figure 5.11 Measured and Simulated Motor Currents

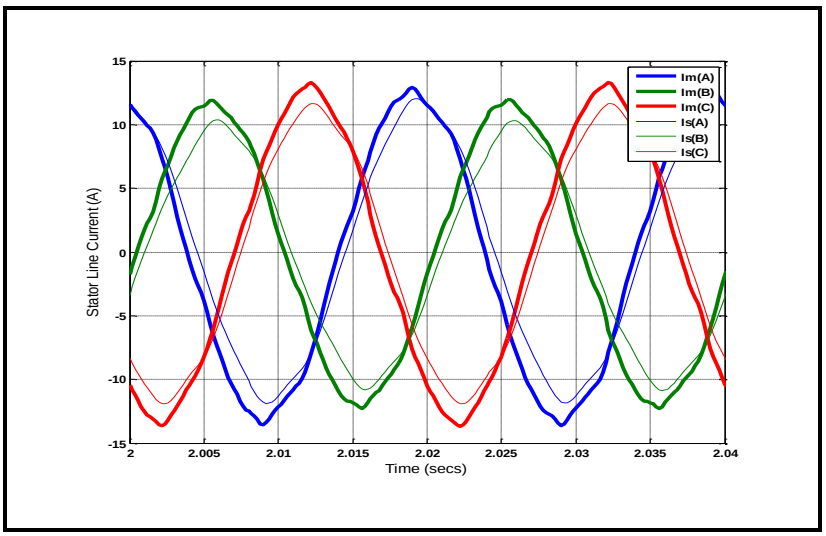

Figure 5.12 Simulated and Actual Motor Currents at Full Load

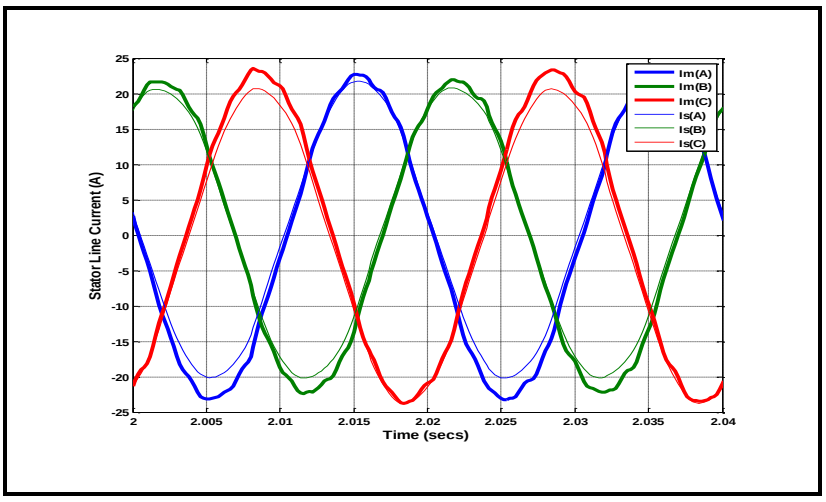

Figure 5.13 Simulated and Actual Motor Currents at No Load

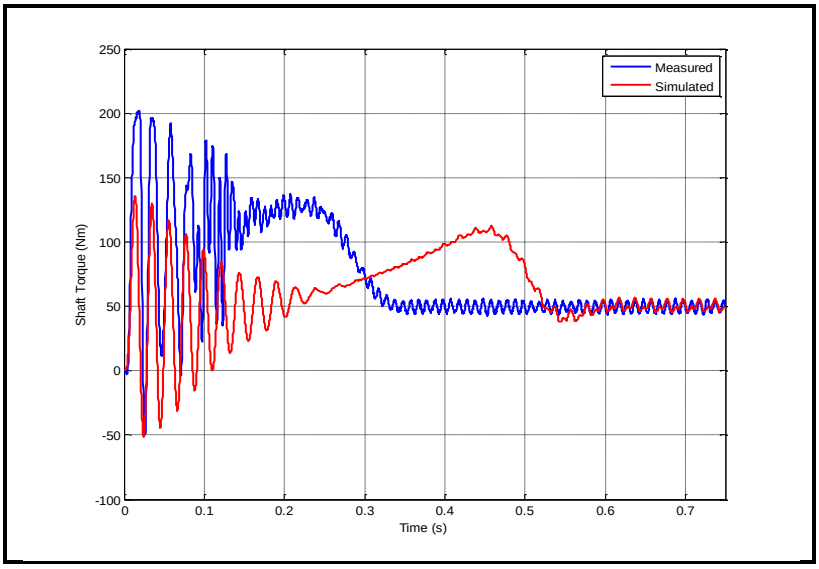

Figure 5.14 Measured and Simulated Motor Shaft Torque

5.13 Summary

In this chapter the types, construction, and basic principles of induction motors are presented. A simple method of analysing induction motors, two axes dq model, is considered and the results for the benchmark motor are illustrated and validated. For being fairly uncomplicated and able to simulate the overall and time-varying performance of the induction machines, this method is used in engineering practices where applications do not require highly accurate results.

Chapter 6. Test Facility and Faults Seeding

This chapter provides a general description of the test rig that has been allocated within the HyperC laboratory in the School of Engineering, Design and Technology, University of Bradford. The components of the test rig are described in detail then a number of the tests done are mentioned.

This test rig, shown in Figure 6.1, is designed to run different tests through collecting different sensed signals of the motor under test while it has been exposed to different levels of loading using a regenerative motor drive. The tested motor can be in a healthy or faulty condition. The sensed signals are current, voltage, vibration, speed and torque.

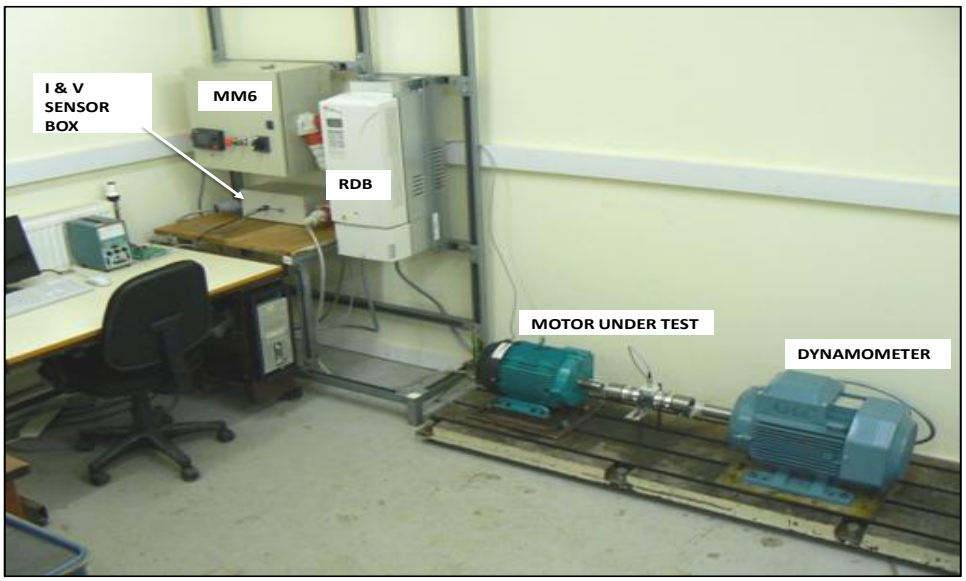

Figure 6.1 Genral View of The Test Rig

6.1 Main Rig Components

Besides the motor under test, the components of the rig include: Motor Manager 6 (MM6) Box, ABB Regenerative Variable Speed Drive Box, and AC Load Motor (Dynamometer).

6.1.1 Motor Manager Unit

The Motor Manager Unit (MM6) is produced by switchgear and Instruments (S&I) Ltd. It is an intelligent relay used to monitor a three-phase motor and provide control, protection and fast communications. The device provides motor data (measured and calculated) in text message format on a colour Liquid Crystal Display [178]. A view of the unit is shown in Figure 6.2.

A. Outside View **B. MM6 From Inside**

Figure 6.2 Motor Manager 6

The unit is operated through different modules, which are display and control (DCM), starter and control (SCM), and protection and metering modules (PMM). The modules are interconnected via Controller Area Network, which provides a high-speed link for exchanging information between the different modules. All

modules are designed to operate in an ambient air temperature of –5 Deg C to +75 Deg C, and relative humidity of 95% non-condensing.

The SCM is the data concentrator providing sufficient digital I/O for starter control. The SCM provides also two-speed; star, delta connections.

The DCM is based around a colour LCD graphical user interface that allows the user to monitor, control and configure the MM6. The PMM is a standalone measurement and control module that samples current/ voltage transformer inputs and uses thermal modelling techniques to provide accurate motor protection. The SCM and DCM have inbuilt sensors for monitoring the starter and switch room temperatures. In short, for control and protection purposes, the motor is supplied through the MM6 unit.

6.1.2 Loading Motor

The load motor (dynamometer) is a 22kW, 3 phase motor from Asea Brown Boveri (ABB) Ltd. It has the ability to work as a motor (driving) or as a generator (driven). It is connected through couplings to the (driving) motor under test.

During the beginning of the testing, the motor torque is less than that of the load motor when the dynamometer is still in the motoring region. With the increase of the driving motor (under test) torque, the load motor transfers from the motoring to the generating region and starts to behave as a generator where its electrical output is retransferred to the general grid through the regenerative variable speed drive, which is discussed in the following paragraph.

6.1.3 ABB Regenerative Drive Unit

The ACS800 Regenerative Drive Box (RDB) is a four-quadrant, where the machine can operate as a motor or generator (regenerative braking), wall mountable drive for controlling AC motors. The main circuit consists of two converters, a line-side converter and a motor-side converter, integrated into the same frame [179].

The line-side converter is a converter that is connected to the supply network and is capable of transferring energy from the network to the DC link or from the DC link to the network. The motor-side converter is a converter that is connected to the motor and controls the motor operation.

The ACS800 is a variable speed drive that is designed and produced by ABB. It facilitates the speed and direction control of the load motor at different loads that set by the operator. Besides providing the safety measures, it is capable of transforming the generated power during the regenerative braking operation to a 50 Hz signal to be fed back to the main grid.

6.1.4 Motor under Test

Four 3-phases, 7.5 KW, 4-poles AC motors are used for the purpose of creating faults on them and studying the signatures of such faults on the different signals. The motors are made by Brook-Crompton. The data sheet of these motors is attached in Table 6.1.

The four motors were numbered as M1 through M4 so that each is assigned for a specific fault creation. The different faults were seeded into these motors during the various stages of work. The faults created on the motors were: rotor, bearings, stator, and eccentricity faults into Motor 1, Motor 2, Motor 3, and Motor 4 respectively.

Table 6.1 Specifications of The Testing Motors

PARAMETER	VALUE	PARAMETER	VALUE
Number of Phases	3	Number of Poles	4
Voltage - Delta (V)	380 – 415 (V)	No. of Rotor Bars	28
Current (A)	15.1 -15.9	Power Factor	0.82
Rated Load (Nm)	49.6	Speed (Rpm)	1445
Make	Brook Crompton		

6.2 Auxiliary Components

The test rig utilizes five different sensors and transducers, which are looked at in this section.

6.2.1 Current and Voltage Sensors

The current and voltage sensors are housed in a box (Figure 6.3). They are provided by Powell Electrical Group. The sensor board is in the form of a pass through box for direct connection to the existing 415V supply and gives a signal output equivalent to the voltage and current of each phase. The unit is built

around two main transformers that are current and voltage transformers. The main advantages of these sensors are being nonintrusive as they are connected ahead of the motor under test. The outputs of the MM6 flows though this box to the motor.

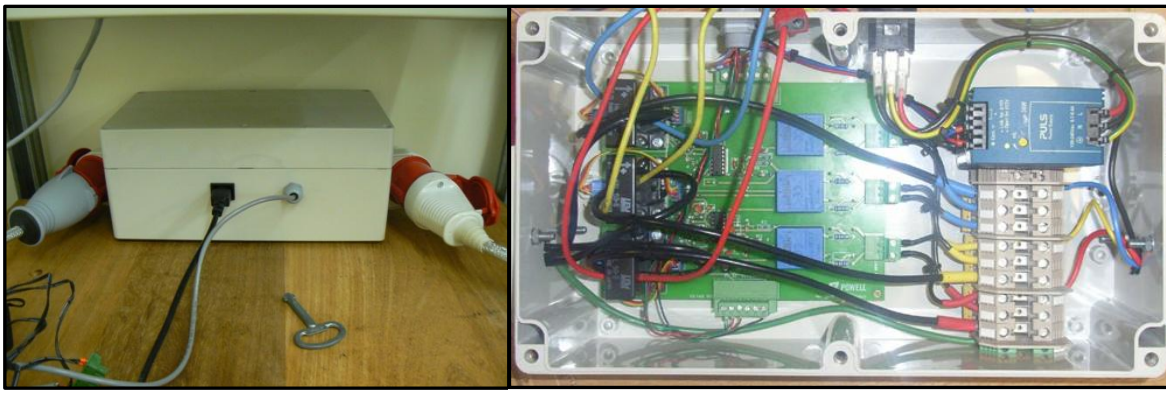

A. Outside View **B. The Box Inside**

Figure 6.3 Current and Voltage Sensors' Box

For the current sensor, the ratio of I_{in}(rms) to V_{out}(rms) is 1 A: 80 mV approximately. This gives a maximum input Current based on a maximum peak signal value of 5V (3.5V(rms)) of 44A(rms). While for the voltage sensor The ratio of V_{in}(rms) to V_{out}(rms) is 1V: 6.9 mV approximately [180].

6.2.2 Vibration Transducer

The vibration transducer that is used (Figure 6.4) is a piezo-electric accelerometer A/ 23-3 from DJB Instruments with a frequency range of 1- 10 KHz. It can measure acceleration up to 5000 m/squared second. It is a lightweight (4.5g) vibration transducer with flat base adhesive attachment, and side mounted connector. Being adhesive mounted allows abrasive cleaning of the attachment face resulting in reduced base thickness over time, but sparing

use of adhesive will aid longevity. Its welded construction maximises temperature range, reliability, and sensitivity.

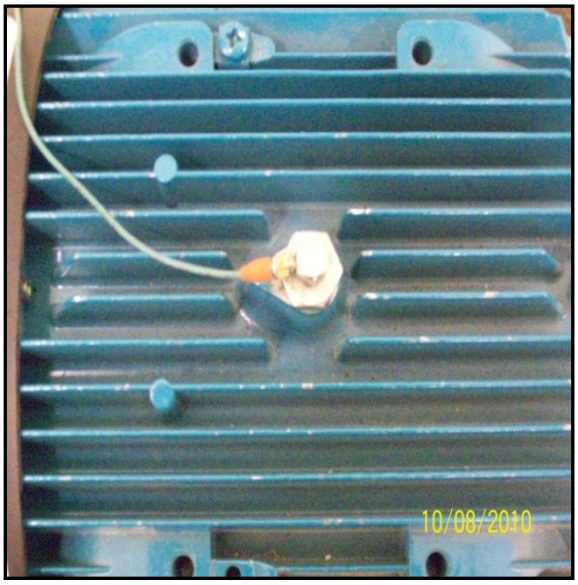

A. Accelerometer

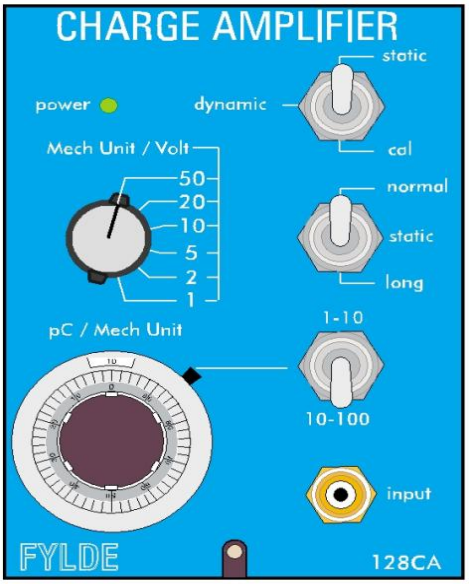

B. Charge Amplifier Front view

Figure 6.4 Vibration Transducer and Amplifier

The output of the transducer is fed to a charge amplifier which converts the transducer output to an equivalent dc voltage. The output is in the range of ±10V and is suitable for data acquisition systems, tape recorders, oscilloscopes and other indicating and storage instruments. A low pass filter is incorporated; this may be internally set for cut off frequency by means of a removable resistor network.

6.2.3 Speed Encoder

The speed encoder (755 HS), shown in Figure 6.5, is attached to the non-drive end of the load motor. Its function is to provide the speed of the motor under test. It is produced by the British Encoder Products Company. The Model 755HS Size is ideal for applications requiring a small, high precision, high performance encoder. It fits where many encoders cannot. All metal construction and shielded ball bearings provides years of trouble-free use. A variety of blind hollow bore sizes are available, for shafts up to 10mm. Attaching the encoder directly to a motor is quick and simple with an innovative flexible mount. This industry standard mount eliminates couplings, increases reliability, while reducing overall length and cost. Where critical alignment is required, a Slotted Flex is available. It resembles a perfect replacement encoder where high reliability is required. The output signals are 0 to 20 mA. While 0 mA corresponds to 0 rpm, the 20 mA represents the motor's nominal speed of 1500 rpm.

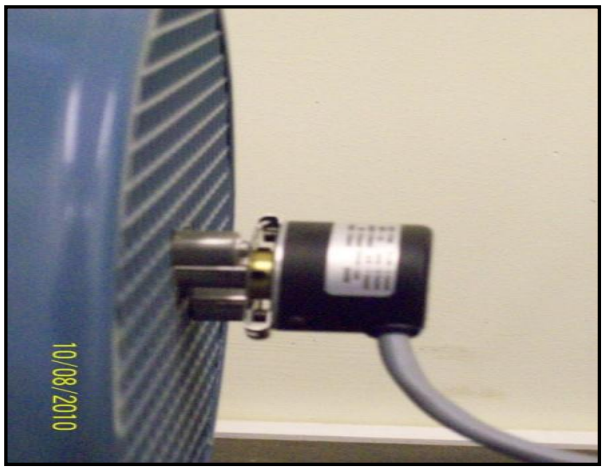

Figure 6.5 Speed Encoder

6.2.4 Torque Transducer

The motor and the load are connected through two adaptors and two mechanical couplings. In between these, the torque transducer (T22) is

mounted as in Figure 6.6. It is rated for torques up to 200 Nm. It is from the HBM Company. The transducer already comes with an integrated electronics; this saves time and costs as no additional, external amplifiers are required for upgrading the measurement chain.

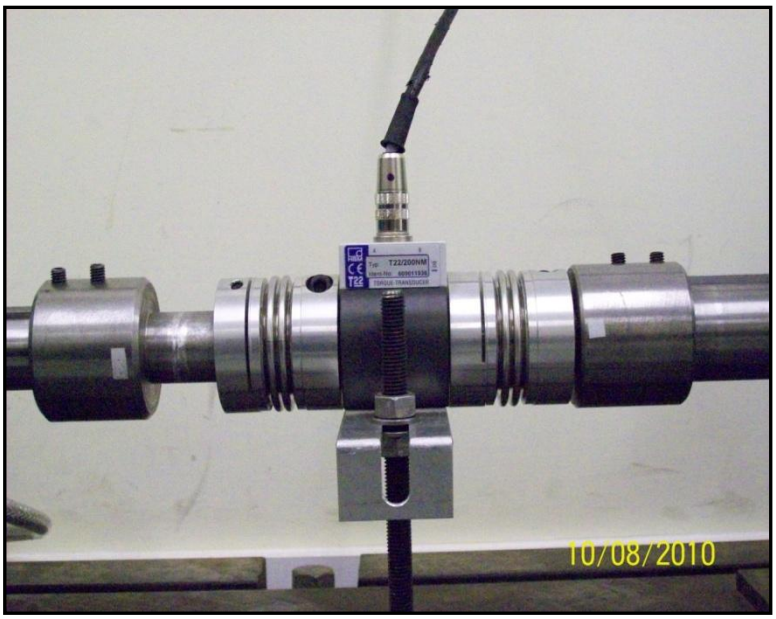

Figure 6.6 Torque Transducer

The bellows couplings are designed to be used specifically with the torque transducer and are rated for torque up to 200Nm and therefore suitable for motors up to 30kW (running at rated load). They are of a flexible corrugated metal design and are tightened onto the torque transducer shaft using screws (40 Nm in this application). The other end of the bellows couplings are attached to the adaptors which are then in turn attached to each of the motor shafts. The adaptors are manufactured with a keyway to fit the specific motor shafts and are held in place with tightening screws.

6.3 Data Acquisition System

The hardware components used to create the Data Acquisition (DAQ) set-up is composed of few sensors as detailed in 6.2, National Instruments DAQ card, and a computer. A schematic diagram of the data acquisition systems is shown in Figure 6.7.

During the experimental work all the collected data was acquired using the National Instruments PXI cards. The PXI 6251 is a multifunction data acquisition card; it accepts 68 pin cables with up to 24 digital inputs and 16 analogue inputs and is housed within the PXI 1031.

During the data acquiring process the number of data points and the sampling frequency were 20 KHz. 100,000 sample s were recorded for each run. Which means for such setting the required time to collect this length of data is 5 Sec.

During each run, nine parameters were recorded. That includes time, three line currents, three phase to phase voltages, speed, vibration, and torque. All of these signals are available for visual inspection of the operator on computer screen.

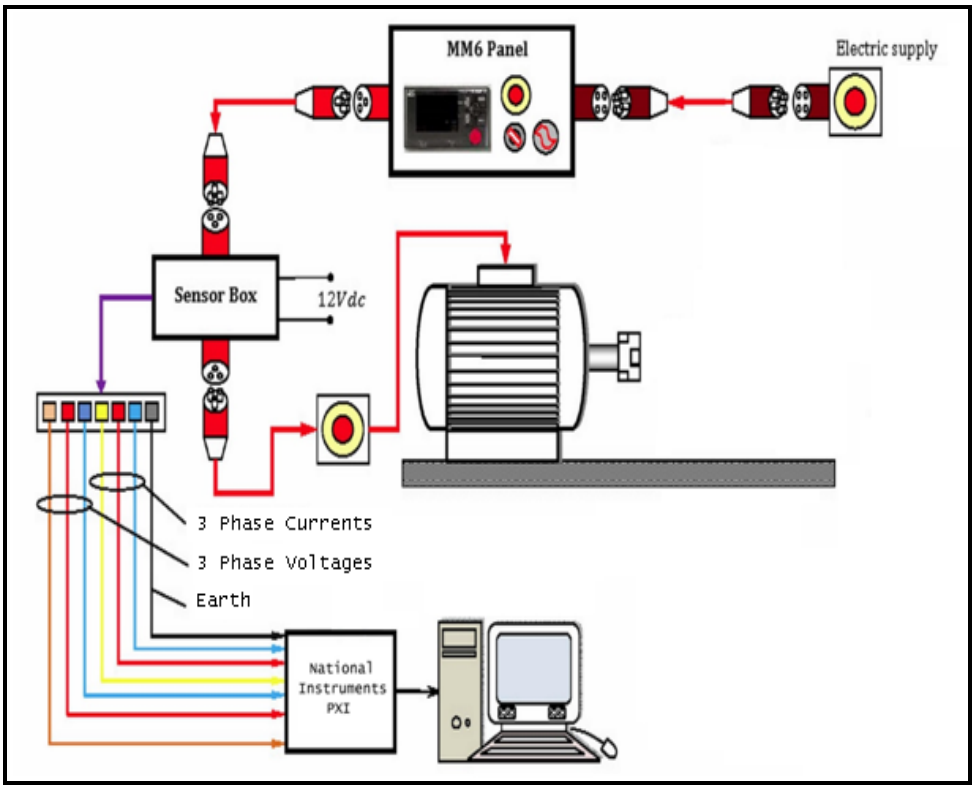

Figure 6.7 Data Acquisition System for Current and Voltage

6.3.1 Labview programming Environment

Labview (short for Laboratory Virtual Instrumentation Engineering Workbench) is a program development application, which uses a graphical programming language to create programmes in block diagram form. Labview is a proprietary product of National Instruments (NI) Company.

The programming language used, also referred to as G, is a dataflow programming. Labview uses expressions, icons, and notes familiar to researchers and relies on graphical symbols rather than textual language to describe programming actions.

Labview has extensive libraries of functions and subroutines for most programming tasks and also contains some libraries that specified for certain

applications such as data acquisition, analysis, presentation, and storage. Labview programmes are called virtual instruments because they imitate actual instruments in their appearance and functioning. Virtual instruments have both friendly user interface and a source code equivalent. Furthermore they accept parameters from higher level virtual instruments. The version used is Labview7. Labview was only used for data acquisition and recording. Other signal processing techniques were carried out using MATLAB. Figure 6.8 shows how the Labview screen looks during the data acquisition process.

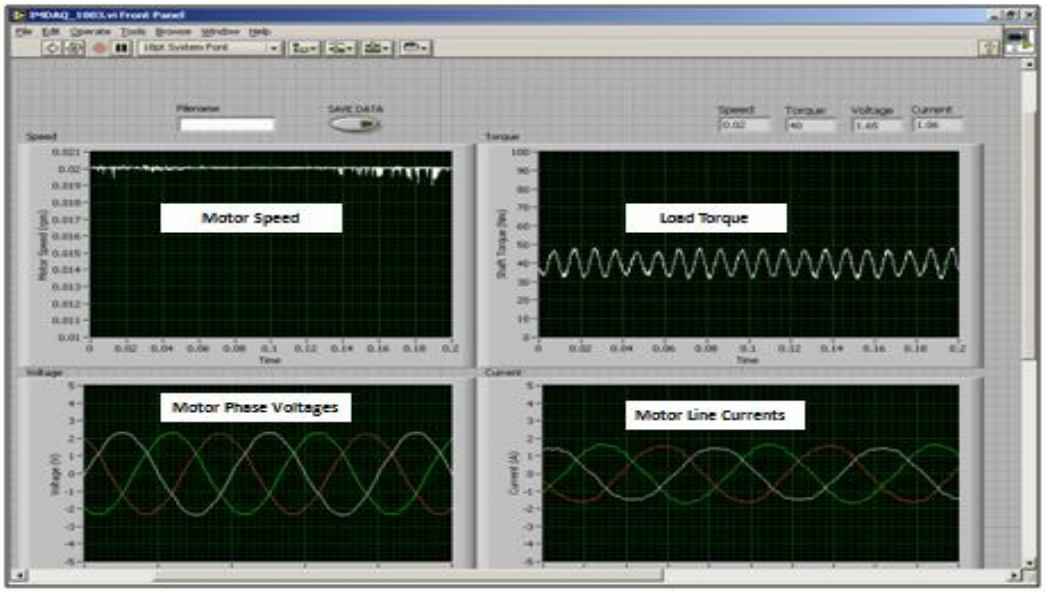

Figure 6.8 A Snap Shot of The Labview Screen

6.4 Voltage Supplies

The test rig is supplied through two points. The first is for the motor under test which passes through the MM6 unit. The second supplies the dynamometer though the regenerative drive unit and it accepts the regenerated power from

the dynamometer to be fed to the grid. Rated at 63A, both out points are fitted with circuit breakers of 32A.

6.5 Seeded Faults and Tests

For each of the tests, the motor under test is run for one hour under a load of 40 Nm (80% of the motor load) to make the test as similar as possible to the practical environment. After that, the different readings of few signals such as current, voltage, vibration, load, and motor speed are recorded at different loading conditions.

6.5.1 Broken Rotor Bar Fault

The first motor (M1), of the four used for creating the different faults to be studied for this project, is assigned for the broken rotor bar fault .The one broken bar fault (as in Figure 6.9) was created by drilling one of the bars by making a hole of 2.5, 3.5, 4.5 and 6 mm diameter throughout one of the bars .The fault was created by drilling a hole of with a depth that allows the full height of the bar is taken and making sure that one of the rotor bars is partially or completely broken. The spectrum diagram of the motor current with one broken bar is illustrated in the next

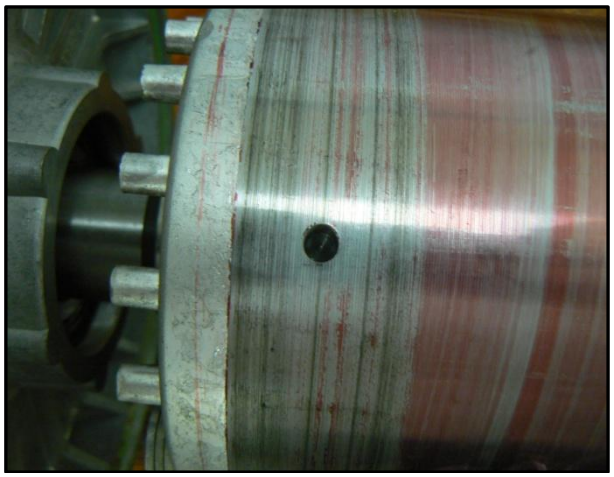

Figure 6.9 Rotor with One Broken Bar

chapter. The last stage of this test was by breaking two adjacent bars of the rotor through two holes of 6 mm diameter each.

6.5.2 Bearings Faults

The second motor (M2) has been assigned for studying the bearing faults. The first of them is a hole in the outer race. A hole of 1 mm diameter was drilled into the outer race way of the bearing. Due to the bearing was ungreased; the bearing balls have crumpled after running the motor for half an hour at a load of 40 NM. Figure 6.10 shows both the outer race hole and the state of bearings after testing.

Figure 6.10 Faulted Bearing Before and After Test

The test was redone with a bearing point fault. In this test the hole is made with a rectangular shape of 0.5 mm width and 30 mm length for the first time before the same test is repeated with 1.5 mm width as in Figure 6.11.

The faulted bearing, was re-greased, by the same amount was used by the manufacturer, after creating the fault on the outer race way. This led to a successful testing even after running the motor for 90 minutes with 80% of its nominal load of 50 Nm.

Figure 6.11 Re-greased Faulted Bearing

The abrasive test was done by clearing off the grease of the bearing test and replacing it with Carborundum powder to emulate the state of a bearing employed in a harsh environment.

Carborundum wich is Silicon carbide (SiC), is a compound of silicon and carbon with chemical formula SiC. It occurs in nature as the extremely rare mineral moissanite. Silicon carbide powder has been mass-produced since 1893 for use as an abrasive.

6.5.3 Turn-To-Turn Stator Fault

The stator of each of the motors under test is made of 3 phases. Each phase is consisted of 210 turns where each 105 turns form a pole pair. Each phase winding appears four times. That is a four-pole stator. The third motor (M3) was for studying the stator fault.

In order to create shorts for certain number of turns, the impedance of each turn should be known. The total impedance of each phase is calculated through injecting current at different values into the phase, and measuring the voltages corresponding to those readings. The next step was to solder few wires at the points corresponding to 1, 2, 3... 14 shorted turns as shown in Figure 6.12.

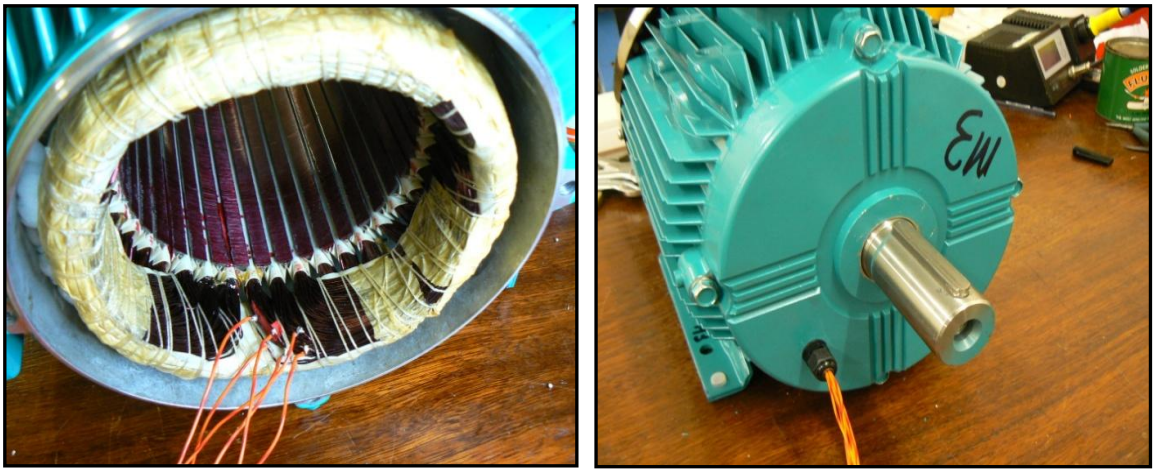

Figure 6.12 Stator Fault Seeding at Different Stages

Due to the high current at starting of the motor and inadequate soldering, unfortunately this test ended into a fail resulting in the burn out of the stator windings. This constitutes that for such tests the turn shortening should be executed through proper winding which is normally done by professional

experts and that what was done in the repeated test. The new arrangement is shown in Figure 6.13.

In order to practically introduce a shorted-turns fault in the test rig, M3 was sent to Bradford Armature Winding Co Ltd for re-winding and having proper and safe taping for 0 to 14 turns in the stator U-phase winding.

To ensure that the stator is close to its original condition, the phase's impedances were calculated by injecting a current in each phase separately. The results shown in Table 6.2 suggest that the three phases are balanced even after the rewinding has taken place.

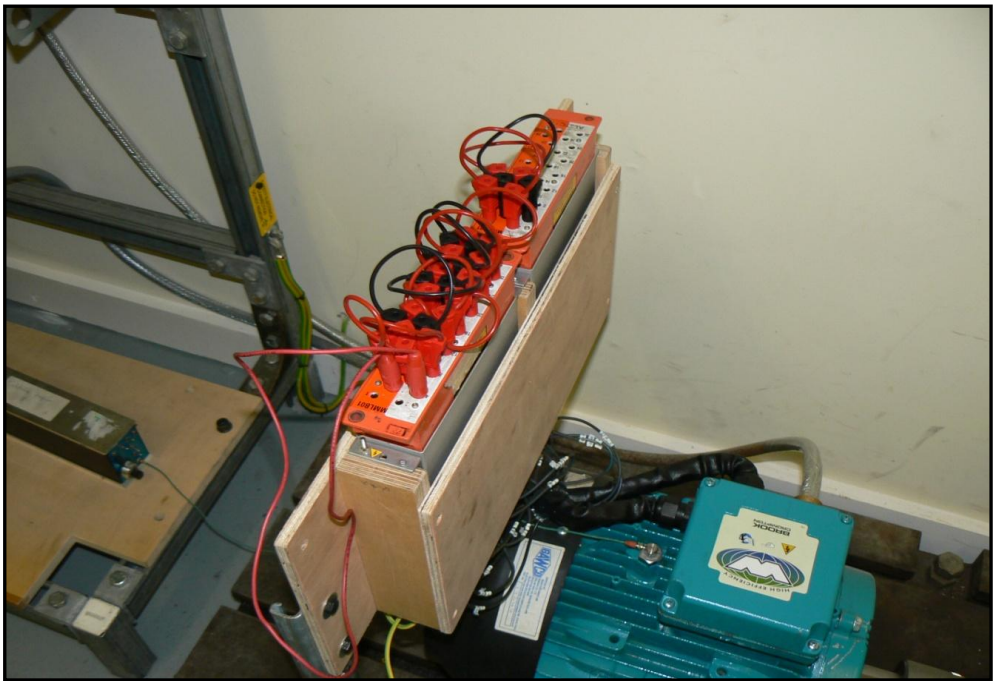

Figure 6.13 Stator Fault Test Arrangement

For connection purpose the taps were connected to the motor terminal box and for safer usage and easier introduction of the required shorted-turns an ABB connection box is utilized. Every caution was taken during the testing as it was

a direct dealing with currents in amperes scale of which was earthening the connection box and putting on gloves.

Table 6.2 Phases Impedance Measurements After Modification

Test	1		2		3		Av. Z
	V (V)	I (A)	V (V)	I (A)	V (V)	I (A)	(Ohm)
Phase U	19.940	1.104	19.940	1.104	19.960	1.105	18.06
Phase V	19.900	1.097	19.900	1.095	19.920	1.098	18.15
Phase W	19.940	1.097	19.960	1.098	19.980	1.100	18.17

The linear relation, in Figure 6.14, between the number of shorted turns and phase impedance is noticeable. This linearity is attributed to the exact shorting of turns and the perfect work done by Bradford Armature Winding Co Ltd.

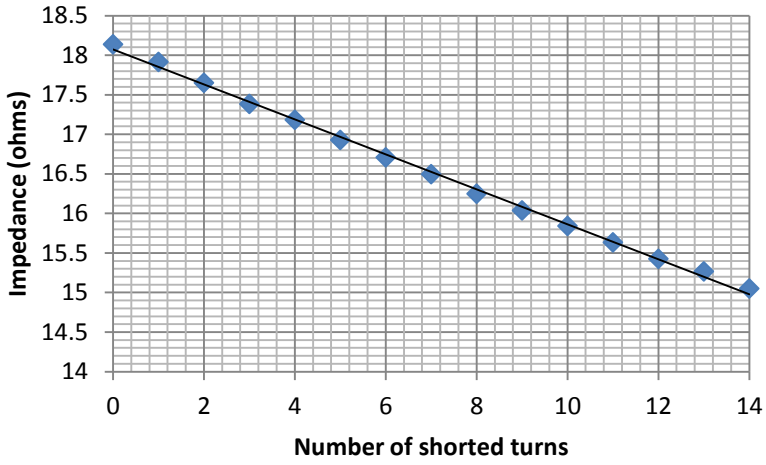

Figure 6.14 Stator Shorted Turns Against Phase Impedance

6.5.4 Eccentricity Fault

This fault is seeded into the forth motor (M4). The test was carried out in two stages namely: static and dynamic eccentricities. The static eccentricity is implemented by using two rings of unequal circumferential widths, one for each

rotor end. The rings used for eccentricity fault realization are shown in Figure 6.15. These rings are used as extra outer covers of two healthy bearings. Through this method, the rotor was made eccentric by approximately 40% of the motor air gap (0.4x0.45=0.18 mm).

Figure 6.15 Eccentricity Rings

The dynamic eccentricity was realized by the same way. The main difference is that the added rings were used as extra layers to the inner race ways of the healthy bearings. The new dynamic eccentricity of the rotor resembles another 0.18 mm of the air gap too.

Two more rings were used in each test to get the right size of the modified bearings. There were two inner rings during the static eccentricity stage and two as outer rings for the dynamic eccentric rotor.

In order to employ the mixed eccentricity, it is needed to use both of the above mentioned eccentric rings for each rotor end at the same time, but the

technology used was not advanced enough to get the accurate modifications. This led to a rub occurring between the rotor and stator, as in Figure 6.16. It is worth noting that it is more practical for such faults to be realised in bigger motors (of 30 KW for example).

Figure 6.16 Stator Damage Due to Rubbing and Burnout

6.6 Belt Coupling

The way the load (dynamometer) is coupled to the motor was changed from direct to a belt coupling as it is in most practical situations. Figure 6.17 shows the new arrangement of the test rig. The same four fault tests were redone under the new test rig arrangement.

6.7 Summary

The test facility located at the University of Bradford was described. It has been used to carry out the experimental tests for this thesis with the cooperation of Switchgear and Instrumentation Ltd, Bradford.

The chapter has given an overview of the test rig and described the components as well as the work that carried out during the experimental and data collection phase of this project.

In order to achieve the best results, every care was taken during the preparations and testing processes. For the safety of staff and visitors, all moving parts were covered with grid besides using eye glasses and gloves.

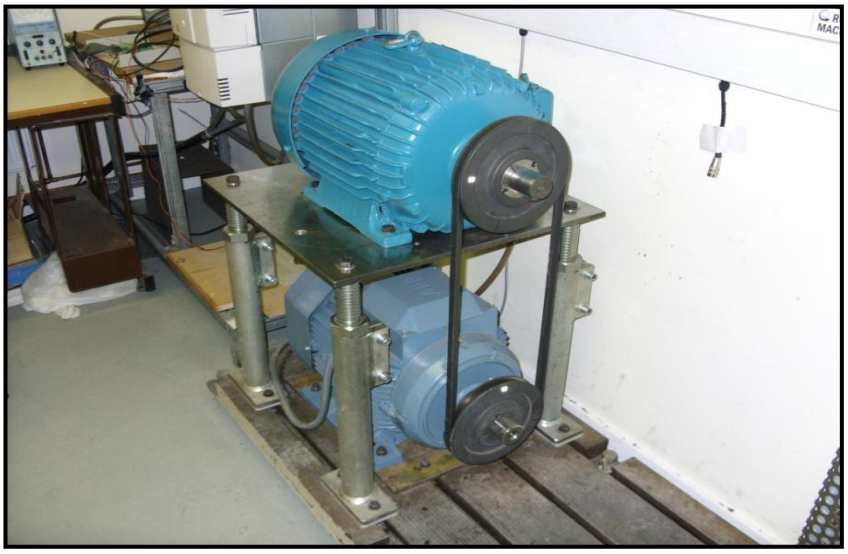

Figure 6.17 Motor-Load Belt Coupled Arrangement

For the security of data and to get accurate recordings as possible all cables were insulated and kept away from each other to eliminate any unwanted signals are picked up. To have readings that are near to practical environment, the motor under test was allowed running for more than one hour when that is allowable.

All the data files and folders were given unique labels that contain the date of the experiments, the fault type, the sampling rate, to name few. In addition all sensors were calibrated before usage.

From the results obtained, it could be said that the test facility is well equipped and it could be run for accurate and sophisticated tests with confidence and assured good results.

Chapter 7. System Responses and Tests Results

It is commonly difficult or even impossible to interpret the information contained in a raw signal to meaningful information by just looking at it. In addition, raw signals obtained from an instrument measuring a physical process always contain noise that hampers the useful information contained.

This chapter is allocated to the data collected from the four motors with different faults. The motors were tested and different signals were saved. Then the motors were failed and retested again. The work was done through collecting different sensed signals of the motor under test while it has been exposed to different levels of loading through an induction motor run by a motor drive. The tested motors can be in a healthy or faulty condition. The sensed signals are current, voltage, accelerometer signal, and speed.

Plots of the recorded motor output signals both in time and frequency domains are illustrated and discussed. The first section covers the measured signals from the healthy motors. It includes current, voltage speed, and vibration. The tests were carried out at 0, 25, 30, 35, 40, and 50 Nm which is the rated motor load. In the last section, few figures illustrating the location of the faults harmonics are presented using Fast Fourier Transformation.

It is worth noting that apart from the current, other signals are not scaled as the interest is to observe the differences, if any, between the healthy and faulty signals.

7.1 Rotor Fault

In this section, the effect of the broken rotor bars fault on the motor under test's signals is illustrated. Figures plotted are for healthy and different degrees of fault severity at the same level of loadings and for the same degree of fault at different load conditions.

7.1.1 Current Signals

From the figures to come, it has been noted the direct effect of loading on the line current of the motor drastically, the more load applied to the motor, the more current drawn as shown in Figure 7.1. The current is minimally affected by the severity of the rotor fault.

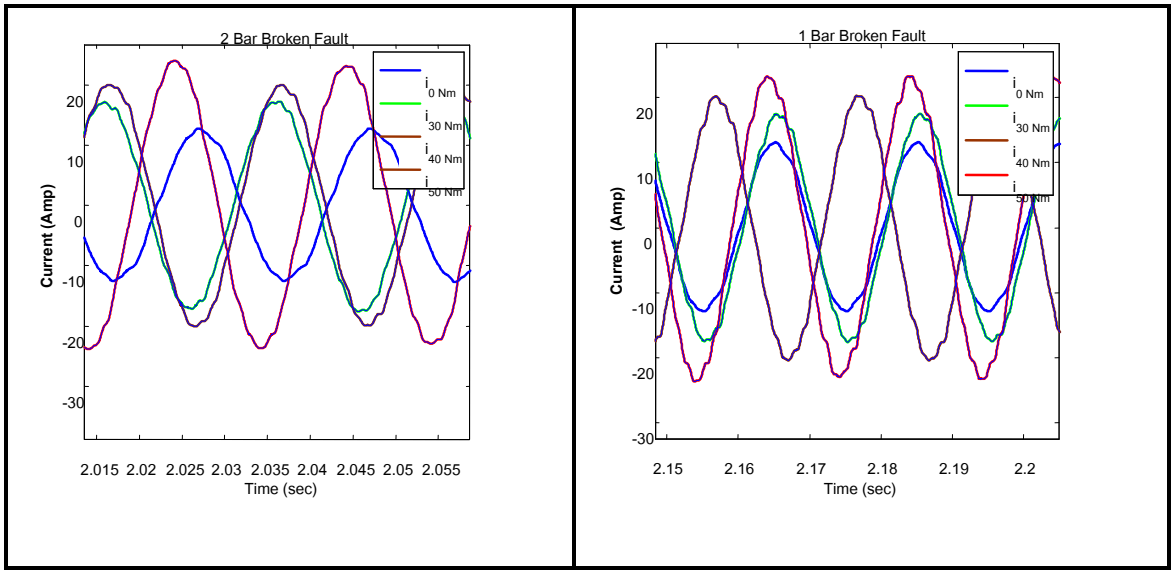

Figure 7.1 Line Current at Different Loads and Fault Severities

Some signal distortion could be noticed, but the proper way to see the effect of the fault upon the current and other signals in general is through signal processing methods.

Figure 7.2 shows that the severity of broken rotor bars has a direct effect on the motor currents. All the plots were at the same loading, but due to the rotor breakage, the line currents have been noticeably affected.

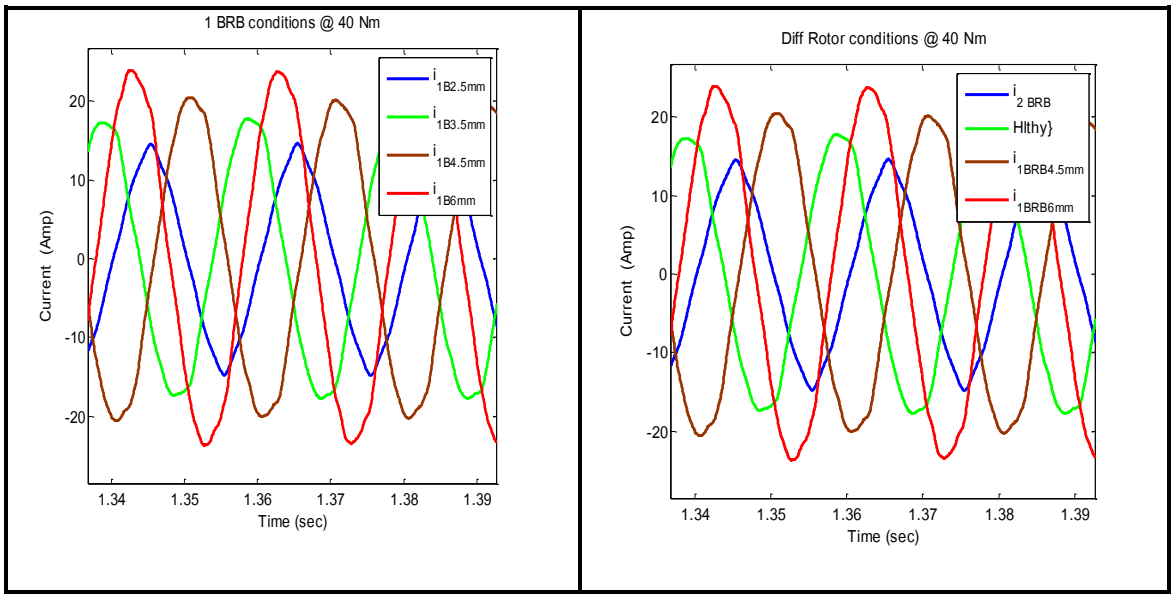

Figure 7.2 Effect of Broken Rotor Bars on Motor Line Current

The more severe the fault, the lower the line current is. This could be linked to the current deformation happens within the rotor circuit due to the broken bars. The increment of the rotor broken bars decreases the induced rotor voltage and current.

7.1.2 Voltage Signals

The broken rotor bar fault has no apparent effect that can be noticed by scanning the voltage figures. Figure 7.3 illustrates the motor phase voltages for a faulty rotor at different loadings where no change can be seen by the eye alone. Also voltages don't change for fixed load for healthy or faulted rotor motor with different severities.

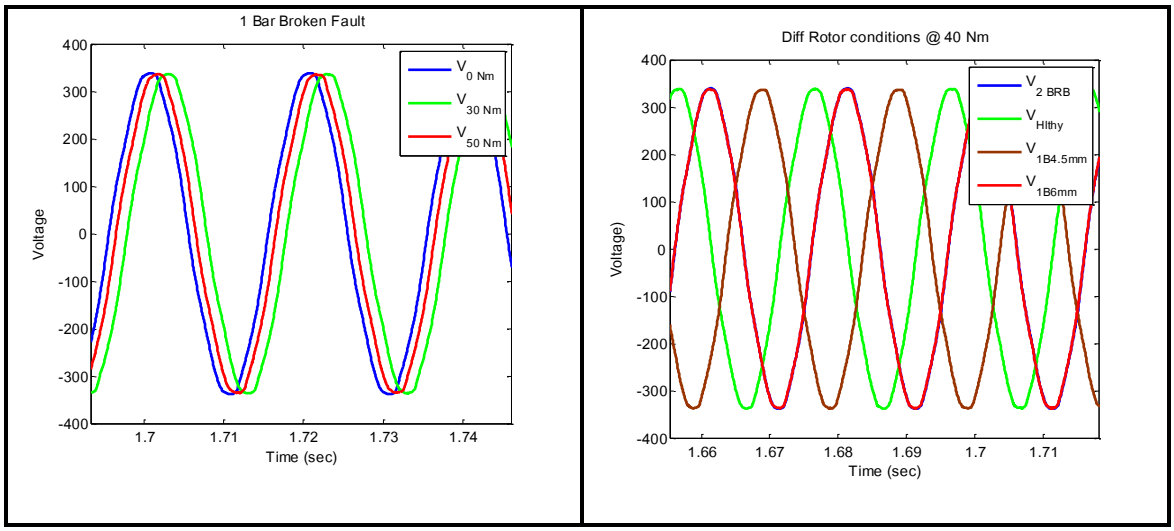

Figure 7.3 Effects of Broken Bars on Motor Voltages

In general, for the normal viewer it could be said that while the motor voltage is noticeably unaffected by rotor faults and loading, such effects are reflected in the current signal. The same principle applies to healthy motors as in Figure 7.4

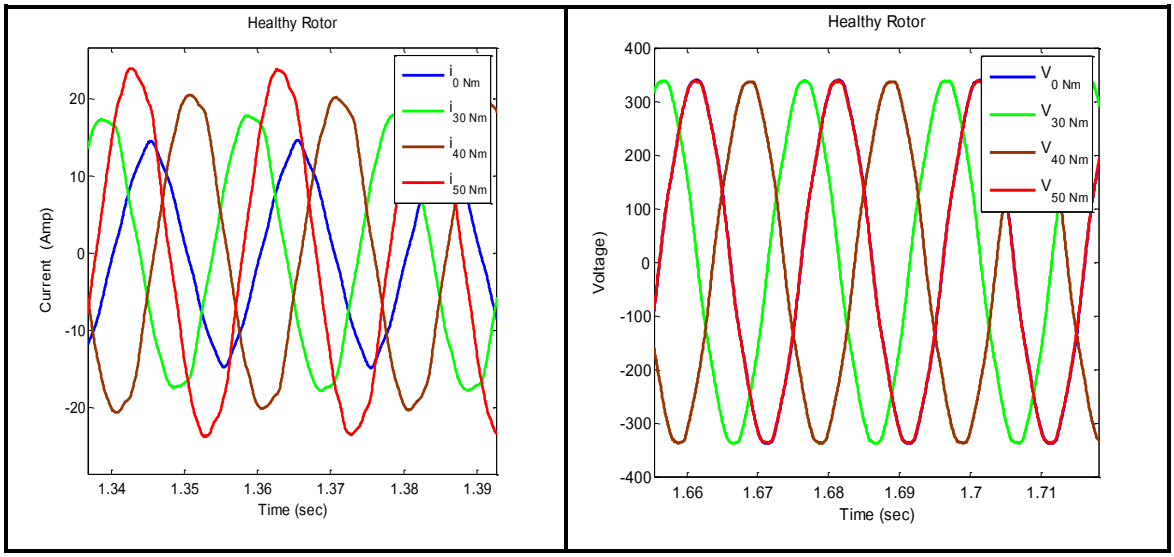

Figure 7.4 Healthy Motor Currents and Voltages at Different Loadings

In practice, rotor faults have an effect on the line voltage and it can be seen through signal treatments and processing.

7.1.3 Speed Signals

The motor rotor speed is proportional to the load. As the load increases, the line current follows and that leads to the increase in speed. Figure 7.5 illustrates the motor speed signal for different loads and state conditions.

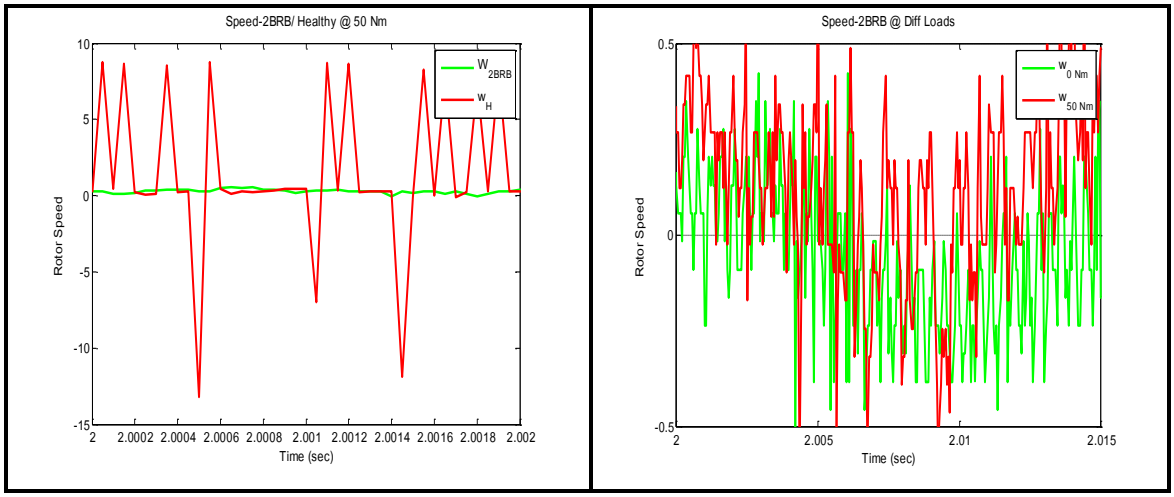

Figure 7.5 Effect of Rotor Fault on Motor Speed

As shown in the left hand part of Figure 7.5, it should be noted that for the same load, the speed of a healthy rotor is much higher than that of a defected one because the rotor induced voltage is linked to the density of the magnetic field which has been lowered by the leakage occurring due to the rotor bar breakage.

7.1.4 Vibration Signals

The accelerometer output signal increases in amplitude with an increase in both load (for the same type of fault) and fault severity when compared to the healthy state at the same loading as in Figure 7.6.

A rotor with broken bars causes the vibration signal amplitude to increase compared to a healthy rotor at the same load.

The vibration increases with the increase of the load for the faulty motor.

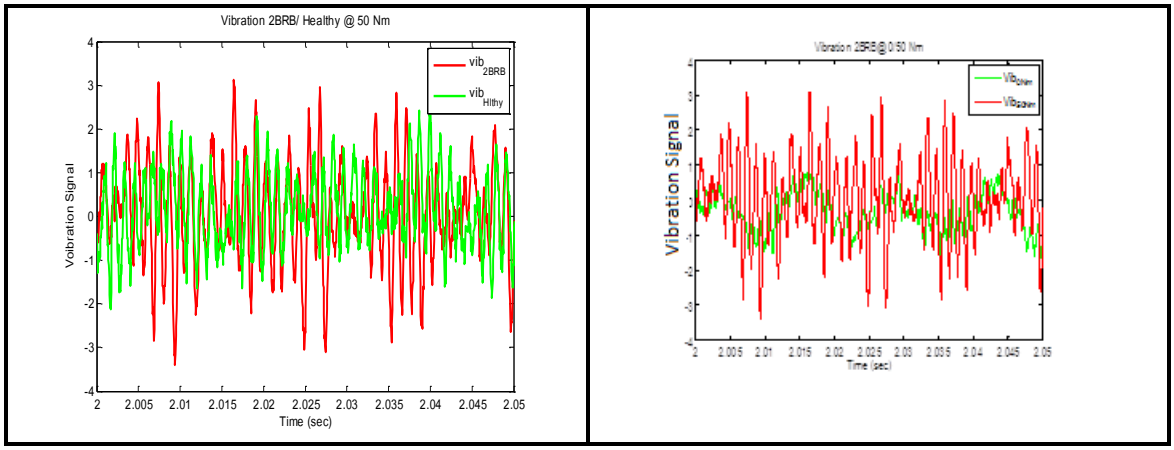

Figure 7.6 Vibration Signals at Various Health Conditions and Loads

7.2 Bearing Fault

The bearing test is done in three phases, a healthy and two faulty situations. The faults seeded and tested are abrasive or generalized roughness, and outer race defects. In the outer race, a test hole is made with a rectangular shape of 1.5 mm width and 30 mm length.

7.2.1 Current Signals

For the healthy motor at no load the current is of around 13 A peak. But when the motor is loaded the current withdrawal has increased, as expected, and it reached around 20 A peak value for full load, as shown in Figures 7.7 and 7.8.

The values of line currents are comparable regardless of the bearing state being healthy or not, for the same load magnitudes. Also, for the same load, line current is preserved for both outer race and cage faults as in Figure 7.7 where the proportioned relation of the load and line current is the norm.

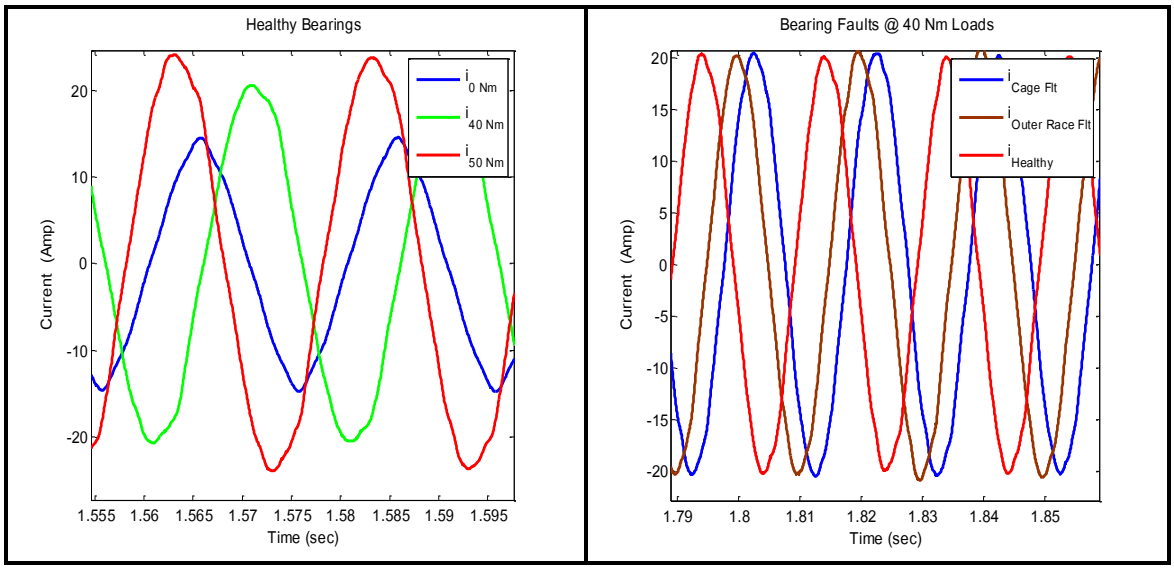

Figure 7.7 Motor Currents For Different Bearing Conditions

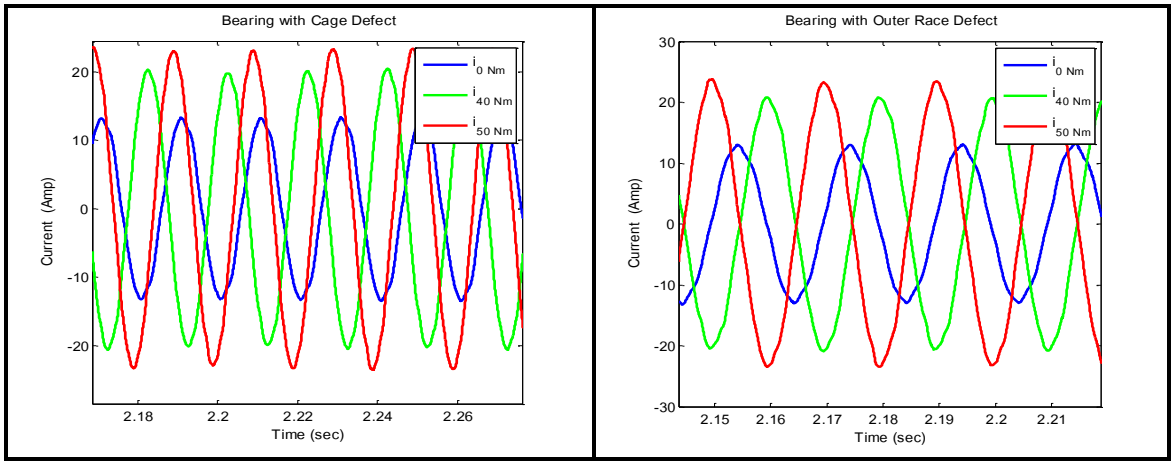

Figure 7.8 Motor Current with Bearing Defects at Different Loads

7.2.2 Vibration Signals

While studying bearing fault it worth looking at the vibration signal. The amplitude of the recorded signal increases significantly when the motor is loaded as in Figures 7.9 and 7.10.

The vibration signal amplitude has obviously increased and the level of vibration is almost doubled when the motor is 80% loaded compared to no load situation.

As in Figure 7.10, the vibration signal of outer race defect has ahigher amplitude compared to the abrasive or generalized defect if compared at the same loading condition. Though it is expensive and not always easy to implement, vibration is the best medium to detect bearing faults.

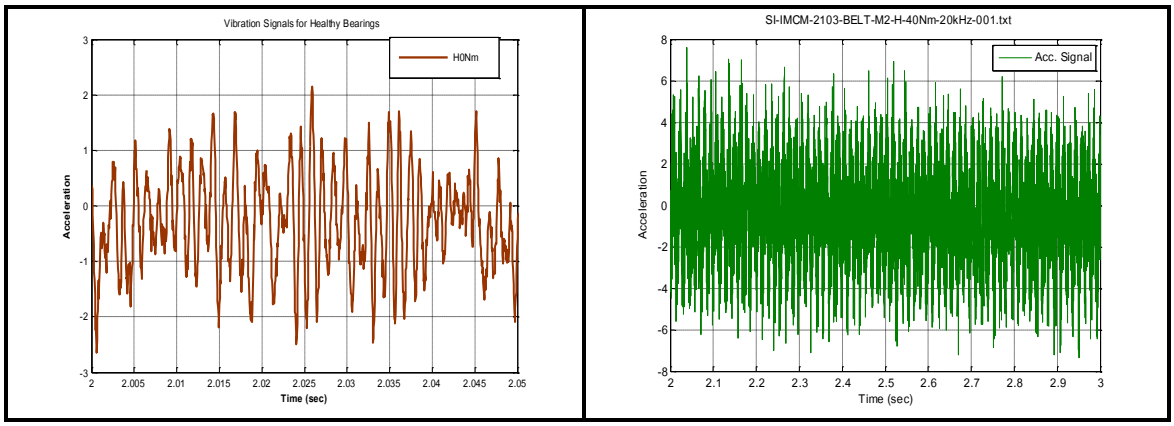

Figure 7.9 Vibration Signals of Healthy Motor at 0 and 40 Nm Loads

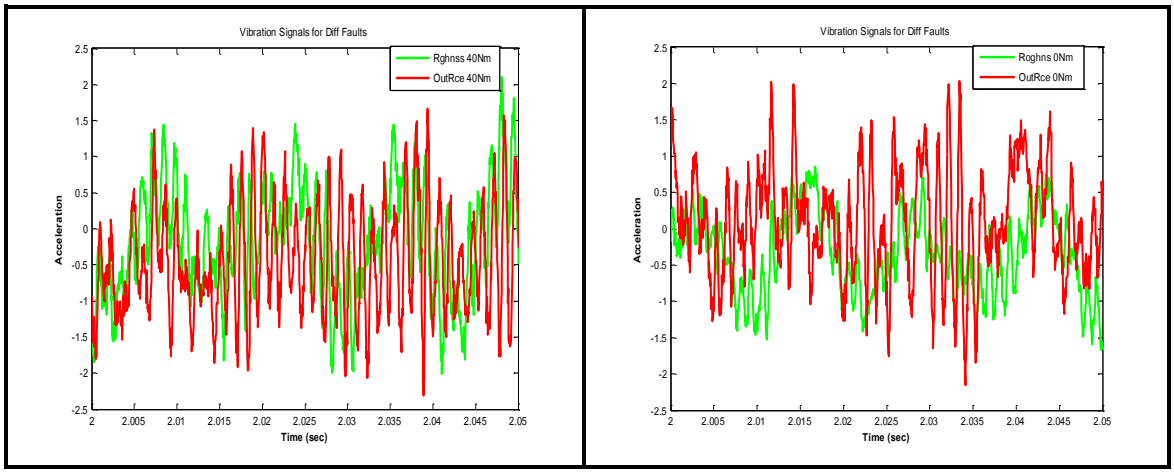

Figure 7.10 Vibration Signals for Bearing Defects at Different Loads

7.3 Inter-Turns Stator Fault

In this section, figures of motor currents during shorted turns fault testing are presented. The line currents, as in Figure 7.11 show a real linear change with the increment of the number of shorted stator turns.

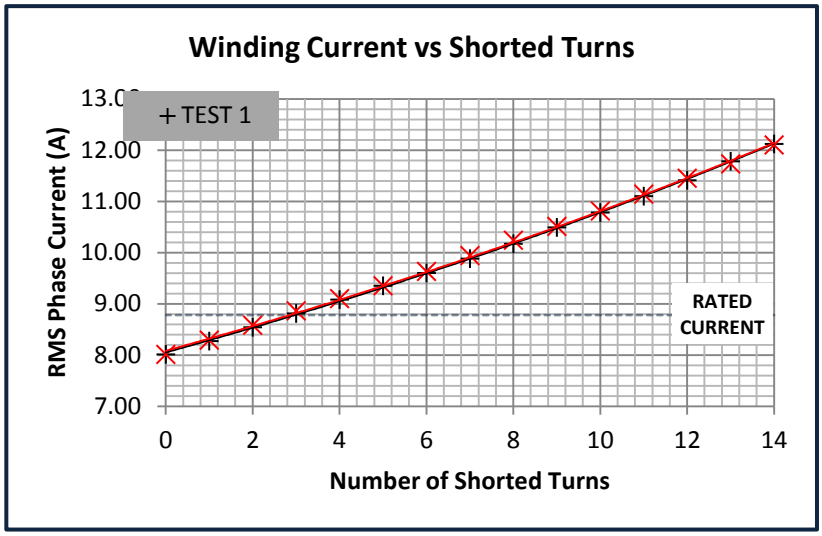

Figure 7.11 Number of Shorted Turns Versus Phase Current

The plots of Figure 7.12 show that the change in current is not noticeable when the motor is loaded with equal loadings even the shorted turns varied from 0 to 14 stator turns. In fact, there is a change in some current parameters that can be calculated like negative sequence currents and current imbalance values.

For currents, as the testing was done at 45 Nm load, there was no change in the current that can be detected by eye, but in fact the RMS value of the currents changes with the change of number of shorted turns.

7.4 Eccentricity Fault

The signals of two types of eccentricity are illustrated and compared to those of the healthy cases in the following sections.

7.4.1 Voltage Responses

Figure 7.13 shows the voltage time responses of the healthy and faulty motor with dynamic eccentricity at different loading conditions.

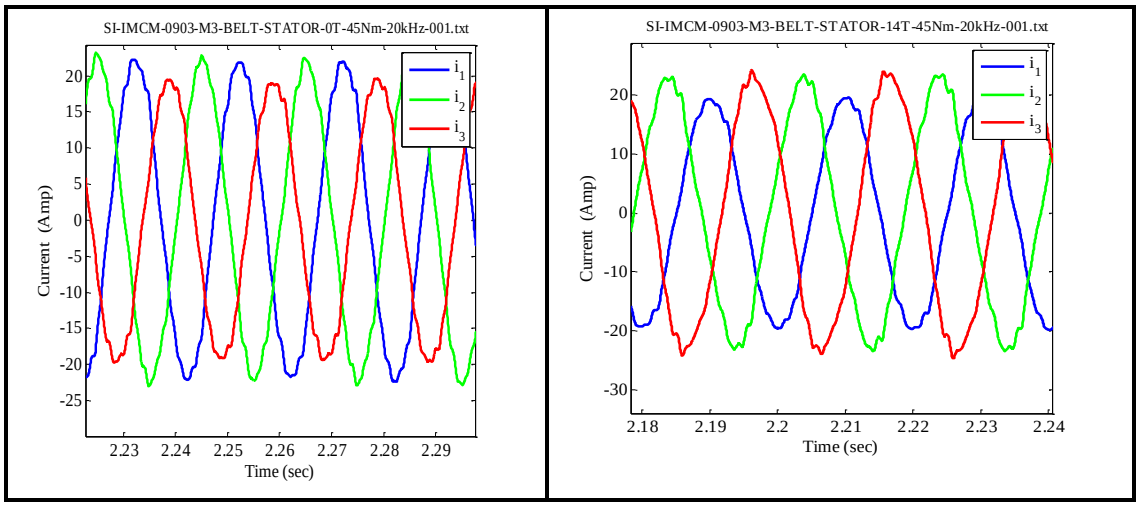

Figure 7.12 Motor Line Current of 0, and14 Shorted Turns

Voltages have exhibited no changes for faulty motors compared to the healthy ones at different levels of loadings.

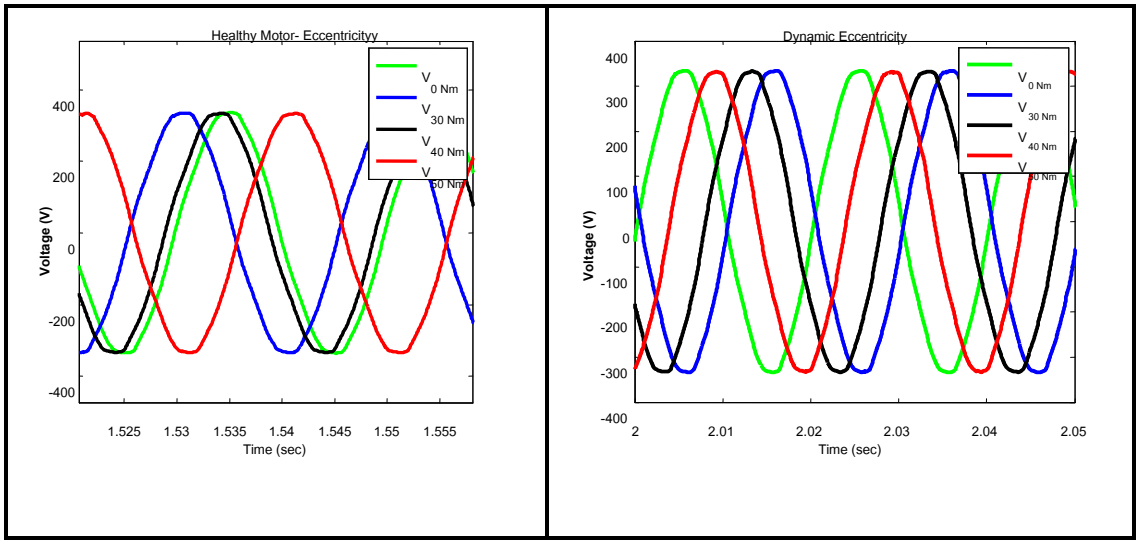

Figure 7.13 Motor Phase Voltages at Different Eccentricities and Loadings

7.4.2 Eccentricity Current Signals

Figure 7.14 illustrates the current responses for the healthy motor and for both static and dynamic eccentricities with different loadings.

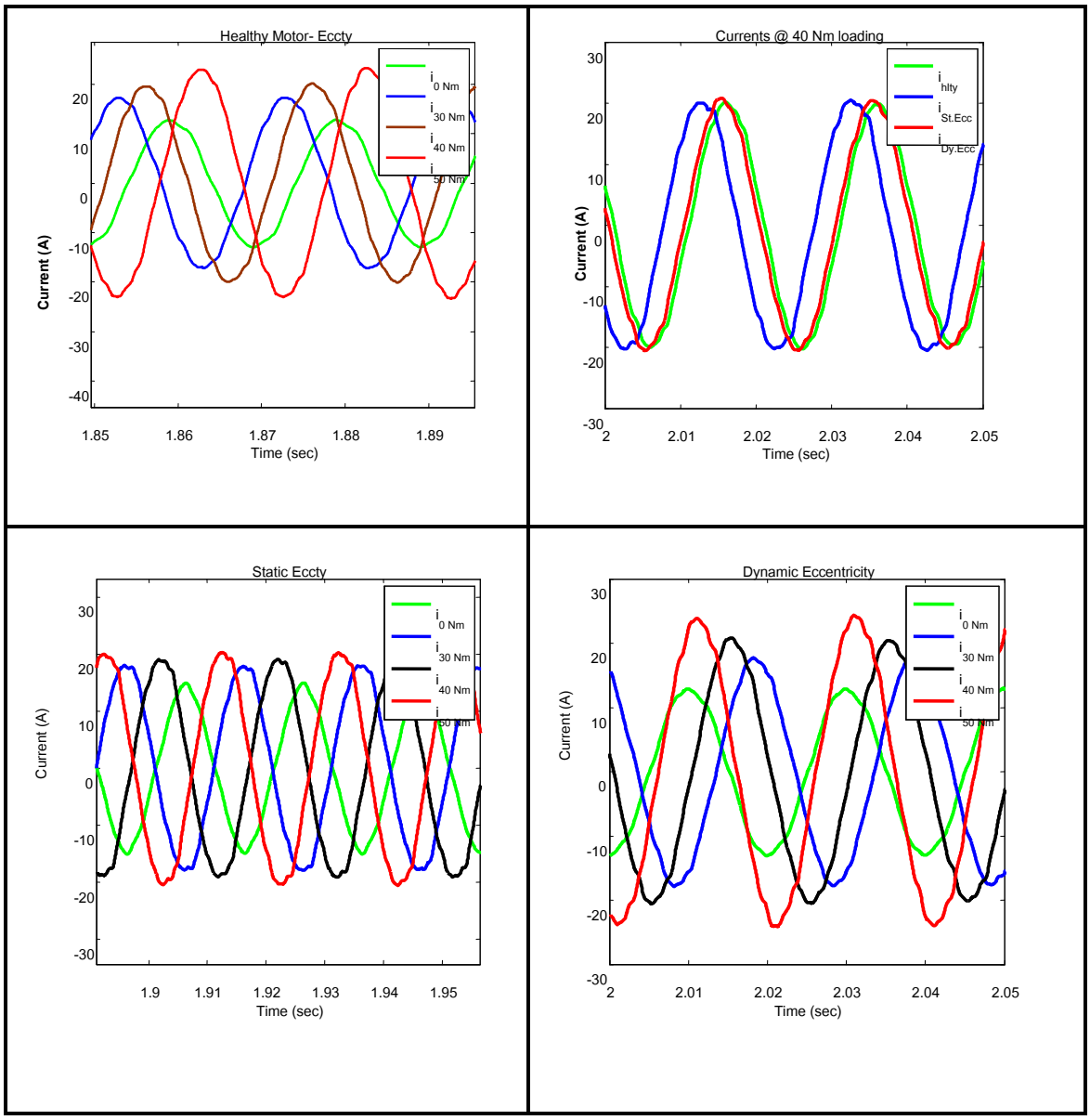

Figure 7.14 Motor Line Currents with Different Types of Eccentricity and Loads

Eccentricity currents are not exceptional from their counterparts of other faults. They are only affected by the loading amount not the fault type when viewing them with the eye.

7.4.3 Vibration Signals

Figure 7.15 shows different cases of vibration signals for two eccentricity types at different loading conditions.

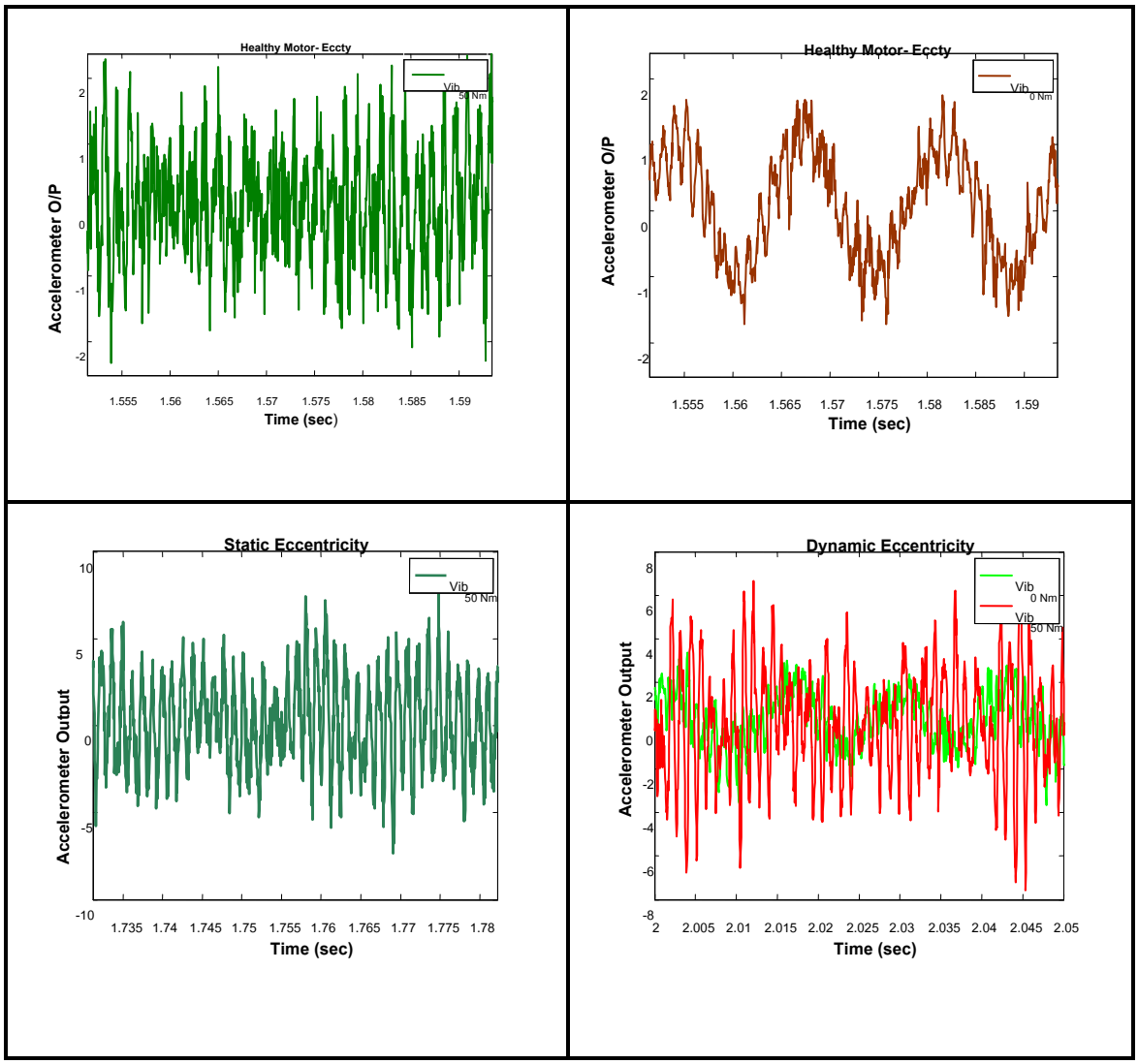

Figure 7.15 Accelerometer Outputs of Healthy and Eccentric Motor

The amplitudes of the acceleration signal increases with the increment of the load applied to the motor and it got even higher when the rotor gets eccentric dynamically compared to the static eccentricity at the same load. The difference is noticeable between unloaded and fully loaded motors signals especially for the dynamic eccentricity fault.

7.4.4 Speed Signals

The speed of the motor has a direct proportion with the load and line current. As the load of the motor increases, an increase in the current follows which result in an increase in speed slip which means a decrease of the rotor speed. In Figure 7.16, it is noticeable that the oscillation of the rotor speed for a full loaded motor (red coloured) is higher compared to that of the unloaded machine (green coloured).

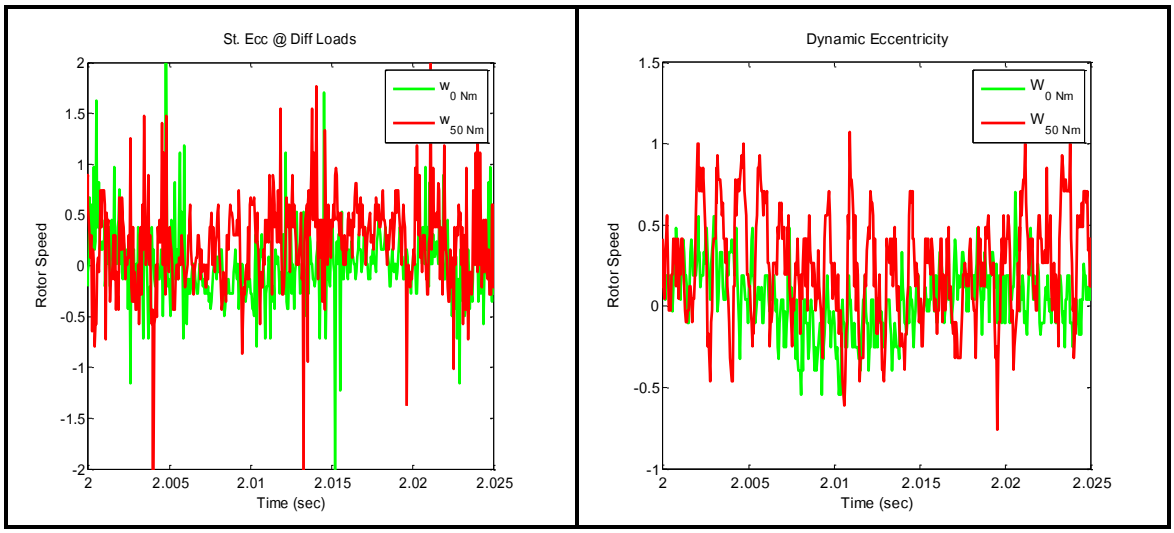

Figure 7.16 Speed Signals for Static and Dynamic Eccentricities at Different Loads

7.5 Power spectral Density Plot

As the effect of faults cannot be noticed by the eye, signals are taken through different signal processing in order to investigate the fault presence.

The spectra include data signatures directly related to the faults under observation. There are also some statistical features can be extracted from frequency domain such as frequency centre, root mean square frequency and root variance frequency.

Power spectral density (PSD) analysis is widely used technique for IMs fault detection. The PSD provides the power content of different frequencies and their amplitudes in a signal. It describes how the power of a signal or time series is distributed with frequency. It is a positive real function of a frequency variable associated with a stationary stochastic process, or a deterministic function of time, which has dimensions of power per hertz (Hz), or energy per hertz [181]. As the subject of the thesis is devoted to solely using motor currents signature techniques for condition monitoring, the spectrums plotted here are of current signals.

7.5.1 Rotor Fault

The spectrums of the motor line current for healthy and faulty rotors are presented in Figure 7.17. The fault harmonics on the spectrum are located according to the following equation:

$$f_{SB} = (1 \pm 2KS)f_s \quad \textbf{7.1}$$

$$S=(N_S-N_R)/N_S \quad \textbf{7.2}$$

$$N_S= 120* f_s/P \quad \textbf{7.3}$$

Where:

f_{SB}: harmonic fault frequency, K=1, 2, 3 ..., S: per unit slip, N_S : motor synchronous speed, N_R : rotor mechanical speed, f_s : supply frequency (50 Hz), and P: number of the stator poles.

The tested motor is a 4 pole, and runs at speed of 1442 rpm and 49.6 Nm load. For *K=7*, the faults harmonics are located at 46 Hz and 54 Hz.

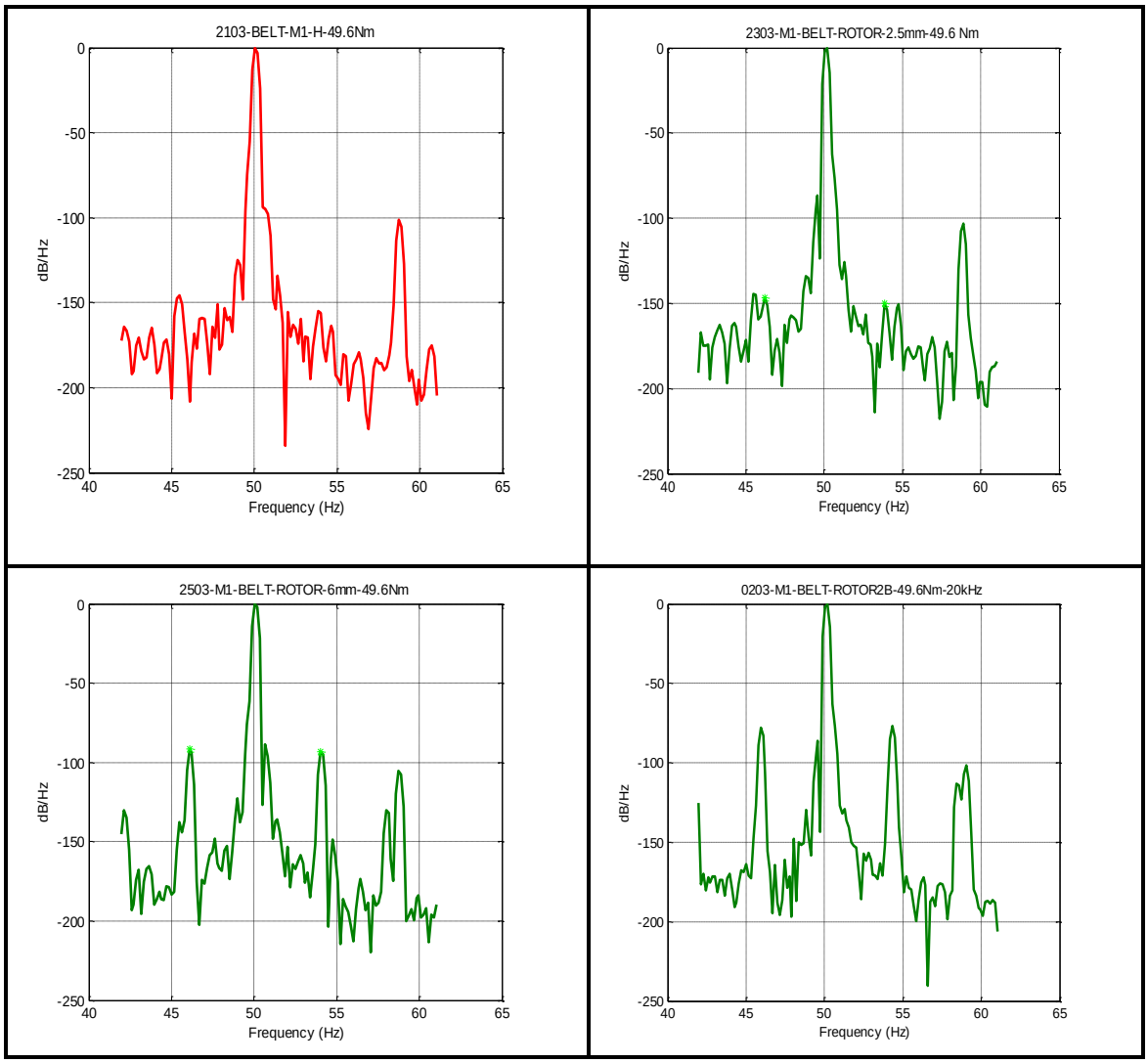

Figure 7.17 Spectrum For Different Rotor Fault Degrees at Full Load

It is apparent that the amplitude corresponding to both frequencies in a direct proportionality with the severity of the fault. For a 1 bar with a hole of 2.5 mm hole, the amplitude is peaking at -150 dB/ Hz to jump to (-120) dB/Hz, for 2 defected bar fault.

For better comparison, three plots were put on the same graph. Figure 7.18 shows the difference in amplitude between the healthy and faulty cases and same load is applied.The response to the fault is noticable.

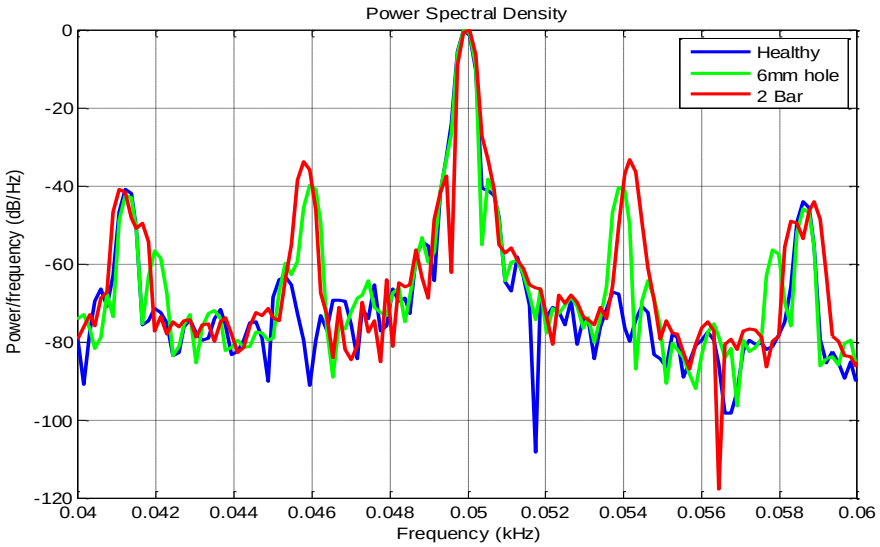

Figure 7.18 Spectrum For Healthy and Brorken Bars at 80% Load

It could be concluded that, the fault charaterstic amplitude inceeases when the either fault severity or load increases or both.

7.5.2 Bearings Fault

For the generalized roughness defect (abrasive test) is nearly unresearched even it is common fault in industry [70]. The reason behind that is this fault has no current or voltage characteristic frequencies [181]. Figure 7.19 shows spectra for such defect.

Figure 7.20 shows the spectrums of the motor line current for healthy and faulty bearing with outer race defect. The fault harmonics on the current spectrum in respect to the characteristic vibration frequency are calculated by Equations 7.4 and 7.5.

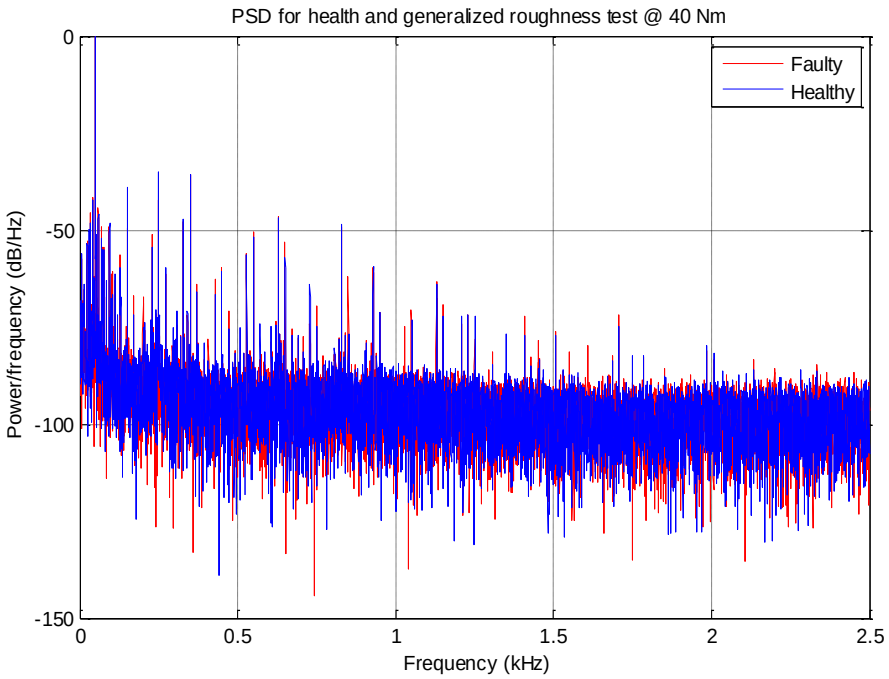

Figure 7.19 Current PSD of Healthy and Generalized Roughness Fault

$$f_{OD} = (n^* N_{R)}/2(1- BD^*\cos \alpha/PD) \quad \textbf{7.4}$$

$$f_{COD} = | f_s \pm m f_{OD} | \quad \textbf{7.5}$$

Where:

f_{od} : Harmonic outer race fault vibration frequency, n: Number of balls, N_R: Rotor speed in rpm, PD : Pitch diameter, BD : Ball Diameter, α: Ball contact angle (typically 0 degrees) [70], f_{cod}: fault characteristic current frequency, and m : Positive integer multiplier.

Bearing data needed for these equations is normally supplied by the manufacturer, but when such data is not available and for simplicity, the harmonic fault frequency in the current spectrum can be located according to equation 7.6 provided the number of the bearing balls is between 6 and 12

balls. The used bearing is stainless steel deep groove SKF explorer 6208 which has 9 balls.

$$f_{OD} = 0.4 \times n \times N_R \quad \textbf{7.6}$$

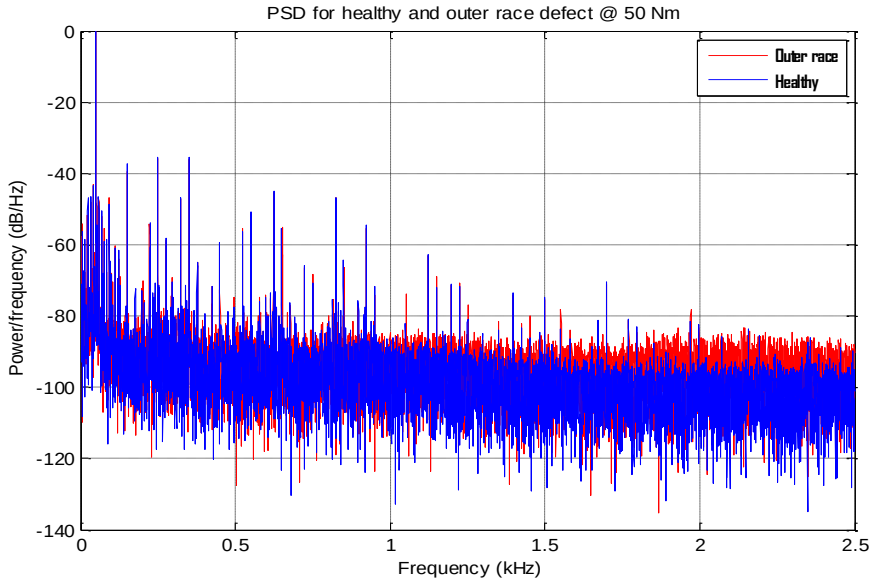

Figure 7.20 Spectrum For Healthy and Outer Race Way Bearing Fault at Full Load

7.6 Summary

The plots of some signals that were recorded during the testing phase of this project were presented in the time domain. The spectrums of the current for the healthy as well as the faulty motors were presented in the frequency domain as power spectral density plots. Such plots help having clear view of the location of the fault harmonics. Current is the medium to be used for monitoring the motor health and hence the plots were limited to this method.

Chapter 8. Monitoring System

In this study, stator current data from the units under test is collected from both healthy and faulty same model set of induction machines. The faults include broken rotor bars, bearing faults, inter-turn stator fault, and rotor eccentricity.

The dc component was removed from the recorded current data. The detailed implementation of the detection system is discussed. The method combines statistical calculations for features generation and machine learning for fault detection and diagnosis.

The application investigated here is the case when the motors run at steady state and don't experience any harsh change of speed or loading.

In this chapter, a technique to detect faults in induction machines by statistical analysis of stator currents is presented. By referring changes in relevant statistical features values to certain faults, defects in induction motors can be detected.

8.1 Methodology

The architecture of the proposed system is shown in Figure 8.1. The original stator current signals are obtained from the motor supplying lines through current sensors of the four induction machines.

The features to be used for classifications are extracted from the database using statistical and frequency domain parameters, that is mean, RMS, quadratic mean, median, variance, standard deviation, peak value, standard

error of the mean deviation, kurtosis, skewness, crest factor, minimum value, maximum value, sum, range, imbalance current magnitude, and maximum deflection. The normalized PSD magnitude is used for rotor fault only.

The role of SVM is to decide on which faults arise from measurable quantities and how severe that faults depending on the classification results.

8.2 Feature Extraction

Feature extraction of the monitored signal is a crucial step in any fault detection and diagnosis system. The final diagnosis results depend upon how precise and accurate the features are. Thus, the feature extraction should preserve the decisive information about the fault that helps in precise decision making [182].

On-line diagnosis systems' popularity comes from their ability to detect incipient faults at the very first moments of their build up. However, every care must be taken in choosing an adequate sampling rate, since a small sampling rate is usually deficient for diagnosis, and a large sampling rate is a burden for transferring and calculation and time consuming [182]. As the feature extraction is the leading step of the detection process, it is a critical initial step in any monitoring and fault diagnosis system.

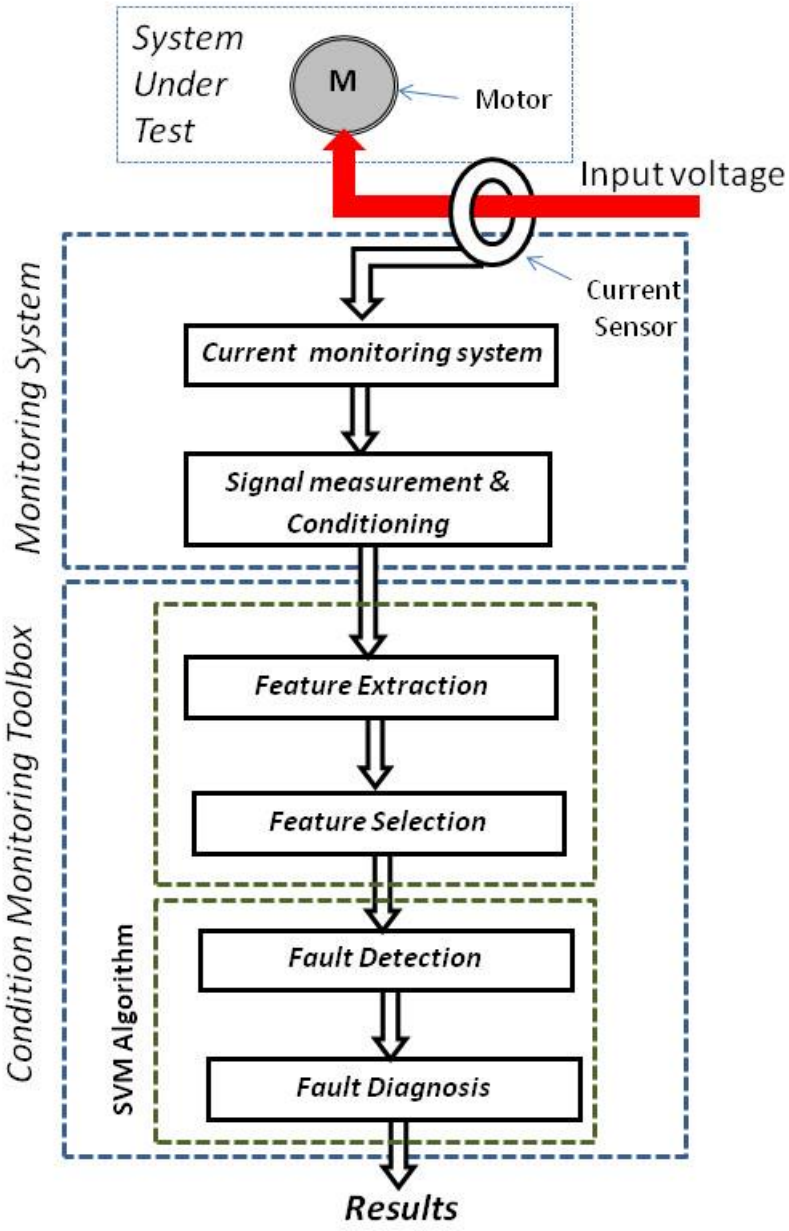

Figure 8.1 Architecture of The Designed Monitoring System

In conventional condition monitoring, current is the most commonly used for induction machines condition monitoring analysis in frequency domain through Fast Fourier Transform (FFT) which is suited for stationary processes. In this

work, the statistical features of the signals are extracted from the motor current time domain.

A time domain signal can be used for fault detection and diagnosis. In the condition monitoring field, statistical methods have been widely used and they can reflect the physical content of time domain data [16]. Statistical analysis of motor current signals provides good indicators that help in estimating the machine health. The following statistical features are extracted and used for the monitoring process:

1. Mean (μ): is the arithmetic average of a series of samples X, where n is the size of samples.

$$\mu = \sum X/n \quad \textbf{8.1}$$

2. Root Mean Squared Value (RMS): is the square root of the mean of the squared values of samples.

$$RMS = \left(\sqrt{(\sum(X^2)/n}\right) \quad \textbf{8.2}$$

3. Quadratic Mean (QM): is the mean of the squared root of the summation of the squared series values.

$$QM = \left(\sqrt{\sum(X^2)}\right)/n \quad \textbf{8.3}$$

4. Median (MD): is the middle point of the data array after arranging the data in an order, from low to high or high to low.

5. Variance (Sigma squared): is the average of the squares of the distance each value is from the mean. The shortcut formulas for both variance and standard deviation are given by [183]:

$$var = \frac{n\sum X^{2} - (\sum X)^{2}}{n(n-1)} \quad \textbf{8.4}$$

6. Standard Deviation (Sd): a measure of the effective energy or power content of the signal and clearly indicates deterioration in the monitored condition. It is the square root of the variance.

$$Sd{=}\sigma = var^{1/2} = [\,variance]^{1/2} \quad \textbf{8.5}$$

7. The peak value is calculated as the mean of the two peaks (the max and min) of the whole cycles in the samples series.

$$Xpeak = \sum_{N=1}^{N} \left(\frac{|max_l| + |max_l|}{2N} \right), \qquad l = 1,2,\dots,N \quad \textbf{8.6}$$

N (number of cycles) = supply freq x length of sampling time.

N= 50 (cycles/sec) X 5 (sec) = 250 cycles.

8. Standard Error of the Mean (Sdm): The standard error of the mean is the standard deviation for the distribution of errors or random fluctuations that are likely to occur in estimating the mean from sample means in a particular situation. the following formula is used to estimate the standard error of the mean from a single sample [184]:

$$Sdm{=}Sd/(n^{1/2}) \quad \textbf{8.7}$$

9. Kurtosis: Kurtosis indicates the flatness or the spikiness of the signal. Its value is very low for normal condition of the motor and high for faulty condition due to the spiky nature of the signal.

$$Kurtosis = \left\{\frac{n(n+1)}{(n-1)(n-2)(n-3)}\sum\frac{n(x-\mu)^4}{Sd}\right\} - \frac{3(n-1)^2}{(n-2)(n-3)} \quad \textbf{8.8}$$

10. Skewness (SK): It characterises the degree of asymmetry of a distribution around its mean. The following formula was used for computation of skewness:

$$Skewness\ (SK) = \frac{n}{(n-1)}\sum\frac{(x-\mu)^3}{Sd} \quad \textbf{8.9}$$

11. Crest Factor (CF): It is the ratio of peak value to the RMS value [185]

$$Crest\ Factor\ (CF) = \frac{Xpeak}{RMS} \quad \textbf{8.10}$$

12. Minimum value: It refers to the minimum signal point value in a given signal.
13. Maximum value: It refers to the maximum point value in a given signal.
14. Sum: It is the sum of all signal point values in a given signal.
15. Range: It refers to the difference between maximum and minimum signal point values for a given signal.
16. Imbalance Current Magnitude (I_{imb}): Calculates the imbalance magnitude between the different phases of a 3 phase motor currents.
17. Max Deflection (DelMax): indicates the maximum deflection magnitude of the current lines from the average RMS current value.

8.3 Features Selection

Features selection means eliminating features that do not contribute to the accuracy of the classifier or have negligible effect on the SVM success classifying rate. It is claimed that features selection doesn't improve the accuracy of the SVMs, but its importance is mainly lay in obtaining better understanding of the data [186].

A feature is considered as good or relevant when its discriminating ability is high among the classes. Ideally a good feature is characterised by its value does not vary much within a class, but It varies much among the different classes [16]. Good features are having the largest information contents about the fault compared to their counterparts.

The number of features to be chosen for fault classification is not limited as SVM classification efficiency does not depend on the number of features of the classified entities. This property enables SVM to be a promising approach for fault diagnostics [16]. A full flow chart of the proposed diagnostic engine is illustrated in Figure 8.2.

During this work, it has been found that feature selection is equally important as feature extraction. By choosing the relevant features that truly represent certain fault(s), the classification accuracy can be increased in most cases by certain degrees as high as the double.

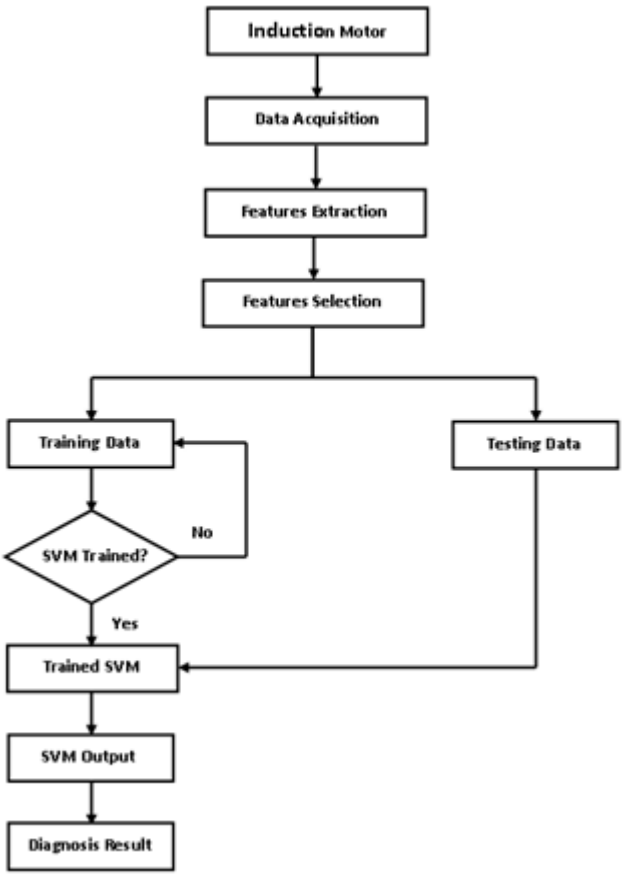

Figure 8.2 Flow Chart of The Proposed Diagnostic System

8.4 Support Vector Machines

Based on results from statistical learning theory and as a state-of-the-art classification method, SVM is introduced in 1992 by Boser, Guyon, and Vapnik.

SVMs are gaining popularity in many fields and disciplines from bioinformatics to science and engineering due to many attractive features such as accuracy and efficiency in modelling and empirical performance [187-189]. SVMs are replacing neural networks in a variety of fields, including engineering, information retrieval, and bioinformatics [189], and they belong to the general category of kernel methods [189].

According to [190], SVMs are defined as learning systems that use a hypothesis space of linear functions in a high dimensional feature space. This learning strategy is a principled and very powerful method that in the few years since its introduction in the 90's has already outperformed most other systems in a wide variety of applications.

Support Vector Machine has the ability to process data without losing previous knowledge. This property makes SVM suitable for online condition monitoring and fault diagnosis in real time applications. Moreover, due to improved computing power and the development of fast learning algorithms, it is now possible to train SVM in real-world applications [191].

SVMs have a drawback of having the attitude of black boxes in their performance that they do not provide the user much information on why a particular prediction was made [186].

The work represented in this chapter is based on using LIBSVM toolbox [192] for SVM classification and regression. It solves many classifications. This software provides an automatic model selection tool for Cross-SVM classification.

8.5 Principle of SVMs

SVM is considered as a binary output classifier where classification depends on the separating the tested data into two main classes. The two sets of data that can be separated using different linear hyperplanes are shown in Figure 8.3. Out of the many separating hyperplanes, only one (the dotted line) can provide

the maximum margin for separation; finding this hyperplane is the basic working principle of SVMs. i.e. finding the hyperplane that provides the maximum separating distance between the two data sets under test. Margin represents the distance between the nearest training point and the separating hyperplane.

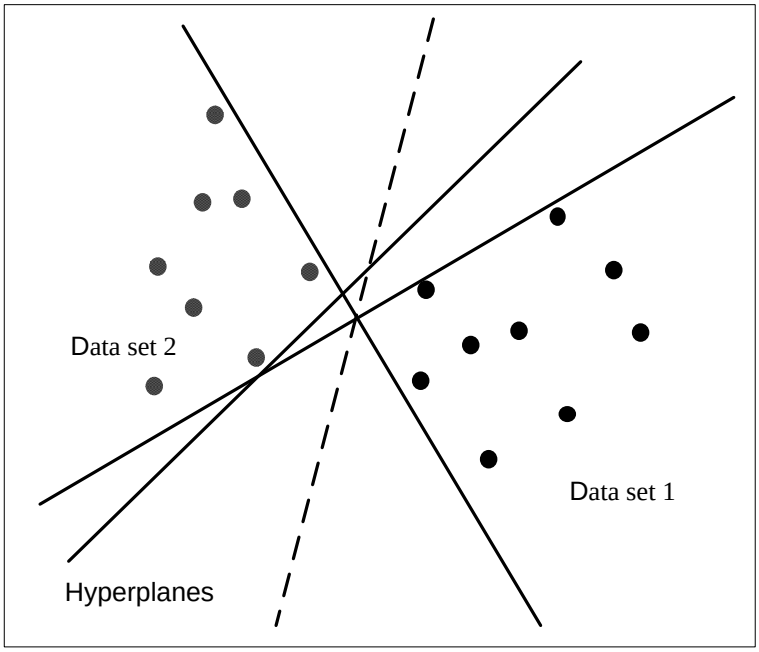

Figure 8.3 Two Data Sets with Different Hyperplanes

The classification task usually involves utilization of two sets of data that is training and testing data. Raw data is divided into two sets of training and testing data. SVM finds the optimal separating hyperplane that provides the best separation of the data and then maximizes the margin between these two classes. It takes the closest vectors of both classes and then maximizes the gap between them assuming that they are linearly separated, as in Figure 8.4.

Training data consists of data samples which besides their attributes or feature values are assigned one target value called class label. The ultimate goal of the

SVM algorithm is to produce a model that predicts the class label of the testing data instances when only it is fed with the data features.

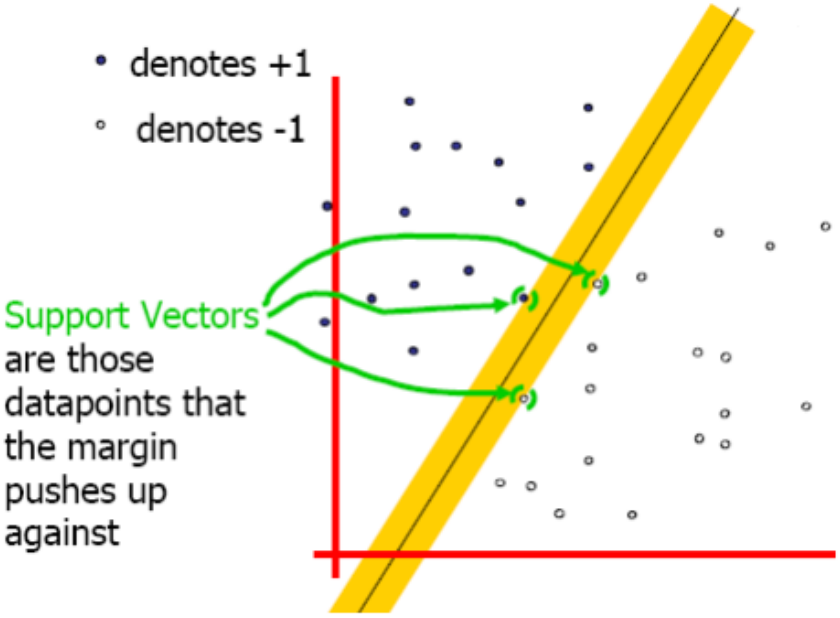

Figure 8.4 A Linear Support Vector Machine

Given a training data set with *n* training examples, ($\mathbf{x}_i$, y_i), i= 1, 2, …, *n*, where each example has d inputs i.e. each $\mathbf{x}_i$ is a list of d real numbers; ($\mathbf{x}_i \in \mathbf{R}^d$) and y=±1 , and y_i are the labels or targets of the samples, (**R**) is real numbers. The hyperplanes are characterized by a vector (**w**), which is orthogonal to the hyperplane, and a constant (b). The hyperplane that separates the data is expressed by:

$$\mathbf{w}.\mathbf{x} + b = 0 \qquad \textbf{8.11}$$

The canonical hyperplane which separates the data from the hyperplane expressed by Equation 8.11 by a distance of at least 1 should satisfy the following conditions.

$\mathbf{W} \cdot \mathbf{x_i} + b \geq +1$ when $y_i = +1$ **8.12**

$\mathbf{W} \cdot \mathbf{x_i} + b \leq -1$ when $y_i = -1$ **8.13**

The training vectors are mapped into high dimensional space. A separation hyper plane is found which maximizes the margin between the two separated classes. The process requires the solution of the following optimization problem:

$$min_{w,b,\check{z}} \frac{1}{2}||W|| + C \sum_{i=1}^{N} \zeta_i \quad \textbf{8.14}$$

Subject to: $y_i (w^T \Phi(x_i) - b \geq 1 - \zeta_i, \ \zeta_i \geq 0$

The training vectors are mapped into a higher dimensional (feature) space by the function (Φ) in which the separation of these training samples is linear and easies than the separation in the original dimensional (input) space. C is called the penalty parameter of the error or the soft margin and ζ_i is the margin error or slack. The final decision function will be in the form:

$$f(x) = \sum_{i=1}^{N} \alpha_i \ y_i \ K\left(x, x_i\right) + b \quad \textbf{8.15}$$

Where α is a coefficient associated with each training sample and known as the dual representation of the decision boundary. The parameters α, b and *w* are obtained through the optimization process. *(x)* is the new sample to be classified.

8.6 SVM Kernels

SVMs are built around the concept of SVMs-kernels. Kernel machines provide a modular framework that can be adapted to different tasks and domains by the choice of the kernel function and the base algorithm.

SVM uses kernels for solving the learning issues. SVM utilises few types of kernels such as linear, polynomial and radial basis function (RBF). Nonlinear kernels functions are used to map the input data to a high dimensional feature space, where the data can become linearly separable [189]. Choosing the best kernel type is a crucial part of the classification process and that is done experimentally i.e. by trying different kernels and choosing the one offers the best results.

SVMs are considered as an excellent classifier for binary classes, but can be used in solving multi-class problems with multi-class extensions where the multiclass problem is divided in a series of two class projects and that is known as multilevel or multiclass classification.SVM can be upgraded to be multiclass classifier.

The kernel function in Equation 8.15 is extremely important to achieve good SVM classification. Choosing the right kernel and tuning its parameters, which is done experimentally, has a direct impact on the final result. There are many available kernel functions. Here are three of the most used kernels:

- Linear: $K(x,x_i) = x^T x_i$

- Polynomial: $K(x,x_i) = (\gamma x^T x_i+1)^d, \gamma>0$

- Radial Basis Function (RBF): $K(x,x_i) = exp(-\gamma | |x- x_i||^2), \gamma>0$

  Where: d is the degree of the polynomial and equals 1 for the linear kernel. The parameter γ controls the width of the Gaussian and ||x|| is the norm of **x**.

8.7 SVM Testing

For testing, the following two methods are used. Leave-One-Out (LOO) and *N*-Fold Cross-Validation

In N-fold cross-validation, the data sample set is divided into complementary N-subsets. The first subset is used for testing the model that trained on the remaining subsets N-1 subsets. The analysis is performed upon one subset which called the training set. Validation analysis is performed on the other subset which is called the validation set or testing set.

The process is repeated for next subset and so. To reduce variability, the above procedure is run for multiple iterations upon the different N partitions of the whole set, and the validation results are averaged over the rounds. This process is repeated for N rounds.

LOO is a special case of this method. When N equals the number of total samples, then the method becomes LOO technique. Despite its simplicity, it remains the method of choice [193].

8.8 Confusion Matrix

Confusion matrix is a table-format layout that allows the user to have a clear picture of the algorithm performance. The matrix columns represent the instance of the predicted class, while each row represents the instances in an actual class. It shows the accuracy of the classification especially when the classes are unbalanced (instances of the classes are unequal).

For example, if the result of 3 classes classification A, B, and C is as follows: Classes A, B, and C have 10, 4 and 10 samples respectively. Out of 10 samples of class A, only 5 were classified as A, 4 as B and 1 as C. For class B, 3 are correctly classified, and 1 as A. For class C, only 60% (6 out of 10) of its samples were correctly classified, 30% as B and 10% as A. The confusion matrix will appear as in Figure 8.5

Actual Class				
	A	5	4	1
	B	1	3	0
	C	1	3	6
		A	B	C
			Predicted Class	

Figure 8.5 Example Confusion Matrix

8.9 Summary

The chapter has given an overview of the designed detection and diagnosis system components. The statistical features and SVM and its principle of work were reviewed. The chapter ends with a brief description of confusion matrix as an indicator of the classification result accuracy.

Chapter 9. Experimental Results

This chapter looks into the classification results of four types of faults which were seeded in belt coupled motors. First, rotor broken bars result is introduced. Next, bearing fault classification is discussed. Then, stator inter-turn short circuit, and air gap eccentricity faults SVM outputs are reviewed.

Part of the contribution of this work is to propose a toolbox; that can detect the presence of a fault and determine its severity when possible. The classification results of the belt couples motor are compared with those of direct coupled motor for verification.

9.1 Graphic User Interface

Wikipedia has defined Graphic User Interface (GUI) as an interface that allows easy interaction between user and electronic devices in general and where the information are available to the user through graphical icons and visual indicators opposed to text-based interfaces or typed command labels.

For easier usage of CBM, a GUI was implemented using Matlab. The GUI allows the user to choose the fault to be checked for, the classifier and class to use, and the type of kernels to be applied.

9.2 Current Based Monitoring Toolbox

One of the aims of the project is to build an induction motor Current Based Monitoring (CBM) toolbox which receives three phase motor current and

outputs the condition of the motor of being healthy or having one of four faults. The process goes through the following four phases:

Birth data; first time that the motor is installed and connected and set by the operator, the tool records the healthy signal. This is the condition monitoring starting point.

Running time; in prescribed intervals and depending on the operating conditions, the current signal is monitored and a set of current signals are recorded for processing.

Feature generation: Through using time domain features of the input current signals, the toolbox generates the relevant features of all the faults under observation.

Fault detection and diagnosis: The toolbox determines the type of the fault that has been detected. The fault that can be detected would be assigned ultimately to one of four categories, broken rotor bars, bearing fault, air gap eccentricity, or inter-turn stator fault. When possible, the toolbox determines the fault severity.

Figure 9.1 shows a snapshot of the toolbox screen where it allows the choice of the fault to be tested, the number of classes, classifier, kernel, and the testing mode to use. It provides also the success rate, table of features, and the classifier predicted result. Depending on the success rates through the confusion matrix, the operator can decide on the condition of the motor monitored.

9.3 Toolbox Features

1. Using current makes the tool reliable and the system is non intrusive to the motor. Such application is realized in offshore oil stations or in certain situation where the motor is situated in harsh environments or in places with very limited space or where the motor is not easily accessible.
2. Using one type of signals i.e. current makes the system cheaper as no expensive sensors, transducers, or extra components are required.
3. Fast as the running time of the algorithm takes few minutes. This allows the user to decide the right time for the required maintenance as the fault is detected immediately.

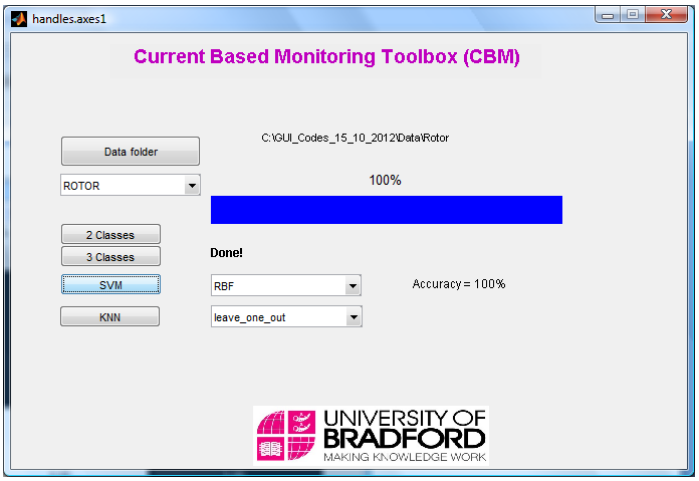

Figure 9.1 Snapshot of The Toolbox Screen

9.4 Diagnosis Process

Detecting the incipient fault alarms the need for the right maintenance action to be taken and that is the main purpose of the monitoring. Detecting the fault presence represents the core of the process and that is fulfils the target, but

determination of the fault severity enables the user to have a precise view of the machine health which helps in the repair scheduling.

The detection and diagnosis is done through the following steps.

1. Healthy readings are recorded to be used as a reference and labelled as class1 samples.

2. For monitoring, samples are recorded and labelled as class 2.

3. If the SVM output shows high success rate for class 2 that shows a high probability of fault presence. For example, for the rotor case the success rate for class 2 is 100% which indicates a definite rotor fault. And can be read directly from the rotor confusion matrix.

4. In case of detecting a fault and monitor the progress of it, another set of data is recorded in a later time and labelled as class3. The classification success rate for this class. Two classes classification is fine enough to prove the presence of a fault and begin maintenance scheduling.

5. During each cycle of monitoring, the process has to be run 6 times for the 6 monitored faults.

9.5 Rotor Fault Results

The DC component of the three current signals was stripped off, and the different features listed in section 8.3 were calculated. Each feature is calculated for every line current of the three. For each fault the most relevant features were chosen.

For a better representation and to avoid variability, the mean value of the three currents features is calculated and considered as the main feature as in equation 9.1.

$$RMS = (RMS_{(i1)} + RMS_{(i2)} + RMS_{(i3)}) / 3 \quad 9.1$$

Figure 9.2 and Figure 9.3 show the stacked plot of range and RMS as rotor fault features respectively. Five samples or examples are used for each of the classes. The fault is a one broken bar with 2.5 mm diameter hole. The linearity of the features behavior in the first figure of the features values is noticeable, where the features are changing within the same class due to the loading effect. Both of the features maintained a linear relation with the load value.

An adequate margin occurs when features' values for both classes are compared which leads to an easy differentiation between the healthy and faulty classes. Hence, both of these features are considered as good representatives of the BRB fault. The behavior of the PSD feature in Figure 9.4 is nonlinear so the feature was expelled from those chosen to represent the broken rotor bars fault.

The total of 12 features was used for the classification methods which are: Maximum value, range, peak, QM, variation, standard deviation, standard error, RMS, crest factor, kurtosis, imbalance value, max deflection from the RMS. A sample of the rotor fault features values are shown in Table 9.1.

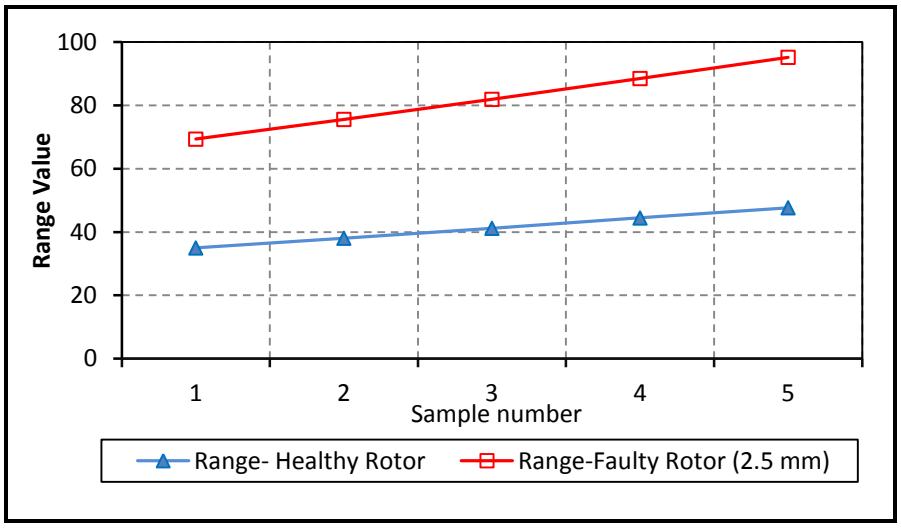

Figure 9.2 The "Range" Feature For Rotor Fault

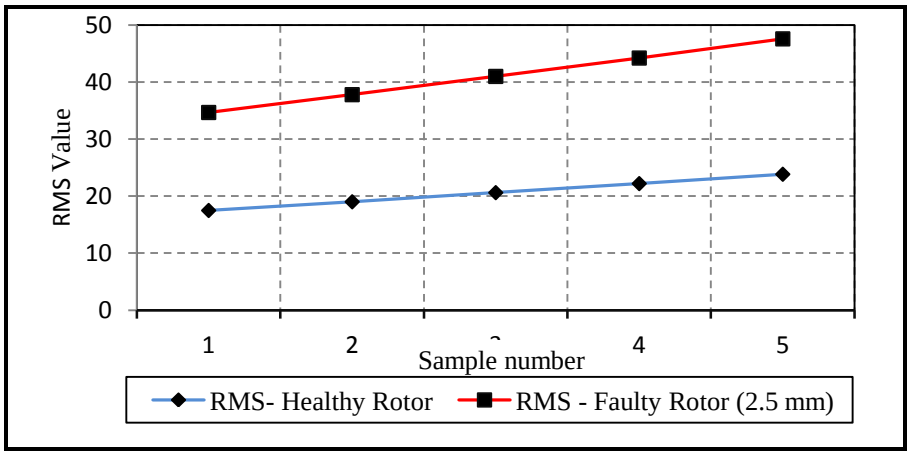

Figure 9.3 The RMS Feature For Rotor Fault

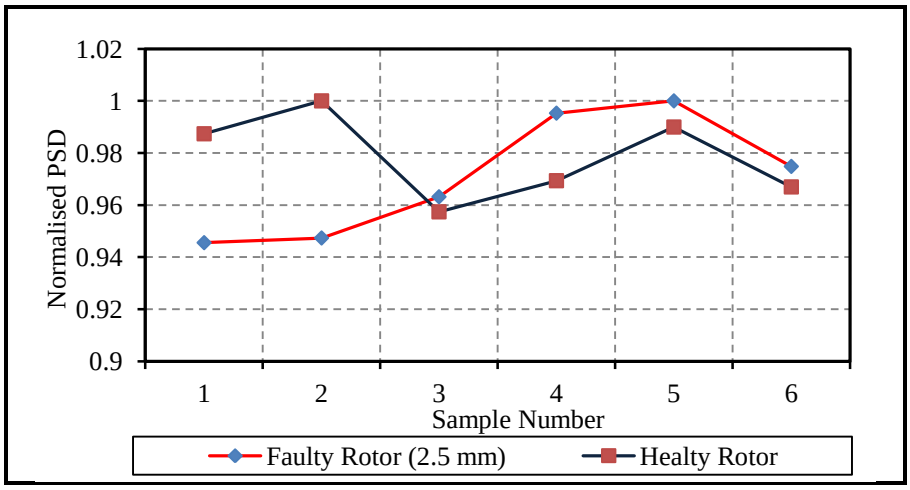

Figure 9.4 The Normalized PSD Feature for Rotor Fault

Table 9.1 Sample of The Features for Rotor Fault

Sample Names	Max	Min	Sum	Range	Peak value	Median	QM	Variation	Std Deviation
2103_BELT_M1_H_0Nm_20kHz_001	13.2793	-13.2388	-3.8E-11	26.5181	11.8622	0.0006	0.0283	80.5595	8.9621
2103_BELT_M1_H_30Nm_20kHz_001	17.5033	-17.5007	1.11E-10	35.0039	15.6244	-0.0021	0.0384	147.6414	12.1396
2103_BELT_M1_H_35Nm_20kHz_001	19.0248	-19.0599	1.08E-10	38.0848	16.9370	-0.0075	0.0414	171.5801	13.0903
2103_BELT_M1_H_40Nm_20kHz_001	20.6317	-20.5744	2.63E-10	41.2061	18.3589	-0.0072	0.0447	199.7264	14.1222
2103_BELT_M1_H_45Nm_20kHz_001	22.2160	-22.2615	4.97E-11	44.4775	19.8137	-0.0025	0.0482	232.4093	15.2368
2103_BELT_M1_H_49.6Nm_20kHz_001	23.8578	-23.8411	8.32E-11	47.6989	21.2597	-0.0160	0.0516	266.1460	16.3054
2403_M1_BELT_ROTOR_3.5mm_0Nm_20kHz_001	12.8893	-12.8667	-2.3E-10	25.7560	11.5452	0.0052	0.0276	76.0179	8.7188
2403_M1_BELT_ROTOR_3.5mm_30Nm_20kHz_001	17.1840	-17.1997	-7.3E-13	34.3837	15.4029	-0.0099	0.0377	142.1421	11.9220
2403_M1_BELT_ROTOR_3.5mm_35Nm_20kHz_001	18.7865	-18.7469	-6.8E-11	37.5335	16.7566	-0.0005	0.0408	166.5086	12.9037
2403_M1_BELT_ROTOR_3.5mm_40Nm_20kHz_001	20.3786	-20.3681	5.73E-11	40.7467	18.1813	-0.0049	0.0440	193.8139	13.9213
2403_M1_BELT_ROTOR_3.5mm_45Nm_20kHz_001	22.0185	-22.0387	-9.5E-11	44.0573	19.6855	-0.0027	0.0476	226.1952	15.0393
2403_M1_BELT_ROTOR_3.5mm_49.6Nm_20kHz_001	23.7405	-23.7976	8.13E-12	47.5381	21.1261	-0.0130	0.0510	260.0795	16.1264
2403_M1_BELT_ROTOR_4.5mm_0Nm_20kHz_001	13.2443	-13.2373	-1.4E-10	26.4816	11.8259	-0.0006	0.0284	80.8732	8.9925
2403_M1_BELT_ROTOR_4.5mm_30Nm_20kHz_001	17.2434	-17.2862	-1E-10	34.5296	15.4389	0.0070	0.0378	142.8486	11.9512
2403_M1_BELT_ROTOR_4.5mm_35Nm_20kHz_001	18.8430	-18.8472	8.47E-11	37.6902	16.8066	-0.0069	0.0411	168.8429	12.9932
2403_M1_BELT_ROTOR_4.5mm_40Nm_20kHz_001	20.2656	-20.2865	-5.7E-12	40.5521	18.0954	0.0057	0.0440	193.2471	13.9000
2403_M1_BELT_ROTOR_4.5mm_45Nm_20kHz_001	22.0362	-21.9441	1.52E-10	43.9803	19.5548	0.0109	0.0474	224.6086	14.9860
2403_M1_BELT_ROTOR_4.5mm_49.6Nm_20kHz_001	23.6371	-23.6321	1.68E-10	47.2692	21.0401	-0.0064	0.0509	258.6481	16.0821

For choosing the right kernel, the experimental results of using different kernels are compared. Results illustrated in Table 9.2 are for 2 and 3 classes using rotor balanced samples, and LOO validation using 3 different kernels.

It has been found that the RBF is the best among the three kernels and that applies to the rest of faults. It is important to note that the SVM and kernel parameters C and gamma (ɣ) are set to unity.

Table 9.2 Rotor Classification Results Using Different Kernels

Kernel		**Linear**	**Polynomial**	**RBF**
Accuracy Rate	**2 Classes**	100%	100%	100%
	3 Classes	33.33%	33.33%	66.67%

The results for 2 classes with balanced and unbalanced samples are shown in Table 9.3. An accuracy rate of 100% was achieved for both cases using SVM and LOO validation approach.

Results represent 18 samples; 6 samples per class; Healthy as class 1, one BRB with 2.5 mm hole as class 2, and one BRB with 6mm hole as class 3.

Figure 9.5 shows the confusion matrix for the rotor fault result. It shows that all the healthy samples are correctly classified and the faulty samples also have been 100% predicted which indicates a definite presence of a rotor fault.

Usually and in most cases RBF provides the best results among the three kernels. Even the accuracy has decreased for the 3 classes' case, but RBF is still produces the best results. The result of 3 classes' classification could be

considered as a confirmation index or an indication of the fault progression. But the fault presence is indicated by the 2 classes result.

Table 9.3 Classification Result for Rotor Fault

	Balanced Samples		Unbalanced Samples	
Sample Names	**Class**	**Predicted Labels**	**Class**	**Predicted Labels**
2103_BELT_M1_H_0Nm_20kHz_001	1	1	1	1
2103_BELT_M1_H_30Nm_20kHz_001	1	1	1	1
2103_BELT_M1_H_35Nm_20kHz_001	1	1	1	1
2103_BELT_M1_H_40Nm_20kHz_001	1	1	1	1
2103_BELT_M1_H_45Nm_20kHz_001	1	1	1	1
2103_BELT_M1_H_49.6Nm_20kHz_001	1	1	1	1
2303_M1_BELT_ROTOR_2.5mm_0Nm_20kHz_001	2	2	2	2
2303_M1_BELT_ROTOR_2.5mm_30Nm_20kHz_001	2	2	2	2
2303_M1_BELT_ROTOR_2.5mm_35Nm_20kHz_001	2	2	2	2
2303_M1_BELT_ROTOR_2.5mm_40Nm_20kHz_001	2	2	2	2
2303_M1_BELT_ROTOR_2.5mm_45Nm_20kHz_001	2	2	2	2
2303_M1_BELT_ROTOR_2.5mm_49.6Nm_20kHz_001	2	2	2	2
2503_M1_BELT_ROTOR_6mm_0Nm_20kHz_001			2	2
2503_M1_BELT_ROTOR_6mm_30Nm_20kHz_001			2	2
2503_M1_BELT_ROTOR_6mm_35Nm_20kHz_001			2	2
2503_M1_BELT_ROTOR_6mm_40Nm_20kHz_001			2	2
2503_M1_BELT_ROTOR_6mm_45Nm_20kHz_001			2	2
2503_M1_BELT_ROTOR_6mm_49.6Nm_20kHz_001			2	2

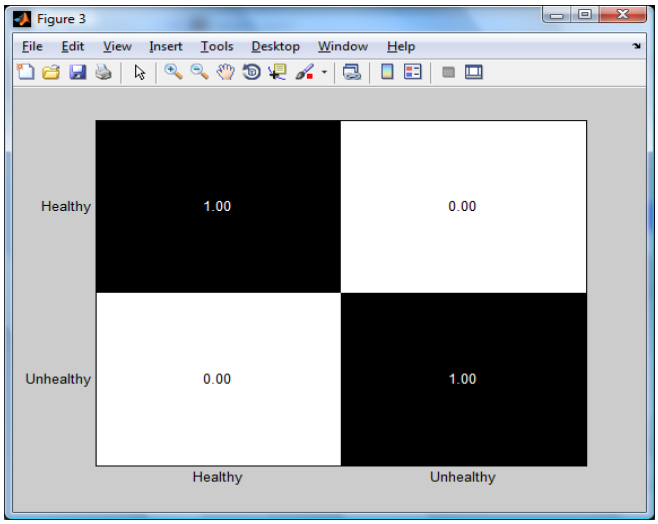

Figure 9.5 Confusion Matrix for Rotor Fault

9.6 Bearings Fault Results

Bearings faults are known for being difficult to detect using MCSA. Two types of faults are studied in this section, roughness and outer race defects. Ten relevant features were chosen for the classification process which are: Maximum value, minimum value, range, peak value, quadratic mean, variance, standard deviation, standard error, kurtosis, and RMS.

Bearings roughness is almost still a virgin area of research which is not explored. With SVM and LOO technique, an overall accuracy rate of 60% was achieved, as in Table 9.4, which could be considered as a good result as it is not common to use MCSA in bearings fault detection and especially for roughness. While the classification accuracy rate for the healthy samples is 20%, 80% of the faulty samples were correctly classified. The features for both types of defects studied are displayed in Table 9.5. It worth noting that, the

sample may include some irrelevant features which were calculated before the features selection has taken place and that applies to all the faults.

While it has been admitted in [181] that there is no characteristic frequency for this fault, the authors of [194] concluded that there is no possibility to detect roughness through current or vibration monitoring.

The recognition of the presence of the outer race fault is poor and the overall accuracy rate is about 10%. This result matches other references in the context that the current based FDD for this fault using MCSA cannot reach a significant level of detection [194].

Table 9.4 Results for Roughness Fault

Sample Names	Class	Predicted Labels
SI_IMCM_0703_M2_BELT_50minsAbrasive_0Nm_20kHz_001	2	2
SI_IMCM_0703_M2_BELT_50minsAbrasive_30Nm_20kHz_001	2	2
SI_IMCM_0703_M2_BELT_50minsAbrasive_40Nm_20kHz_001	2	2
SI_IMCM_0703_M2_BELT_50minsAbrasive_45Nm_20kHz_001	2	2
SI_IMCM_0703_M2_BELT_50minsAbrasive_49.6Nm_20kHz_001	2	1
SI_IMCM_2103_BELT_M2_H_0Nm_20kHz_001	1	2
SI_IMCM_2103_BELT_M2_H_30Nm_20kHz_001	1	1
SI_IMCM_2103_BELT_M2_H_40Nm_20kHz_001	1	2
SI_IMCM_2103_BELT_M2_H_45Nm_20kHz_001	1	1
SI_IMCM_2103_M2_BELT_H_49.6Nm_20kHz_001	1	2

Table 9.5 Sample Feaures for The Bearing Fault

Sample Names	Max	Range	Peak	QM	Variance	Std Devtn	Std Error	RMS	Crest Factor	Kurtosis
SI_IMCM_0703_M2_BELT_50minsAbrasive_0Nm_20kHz_001	13.1534	26.3398	11.8155	0.0285	81.7134	9.0277	0.0285	9.0277	1.4597	1.11E+28
SI_IMCM_0703_M2_BELT_50minsAbrasive_30Nm_20kHz_001	17.4743	34.9661	15.7501	0.0385	148.4048	12.1745	0.0385	12.1744	1.4374	2.72E+28
SI_IMCM_0703_M2_BELT_50minsAbrasive_35Nm_20kHz_001	18.9876	38.0145	17.0642	0.0416	173.3201	13.1566	0.0416	13.1566	1.4462	3.43E+28
SI_IMCM_0703_M2_BELT_50minsAbrasive_40Nm_20kHz_001	20.4876	40.9778	18.4307	0.0448	200.5584	14.1538	0.0448	14.1537	1.4484	4.27E+28
SI_IMCM_0703_M2_BELT_50minsAbrasive_45Nm_20kHz_001	22.1071	44.1910	19.8606	0.0482	232.4052	15.2381	0.0482	15.2380	1.4508	5.32E+28
SI_IMCM_0703_M2_BELT_50minsAbrasive_49.6Nm_20kHz_001	23.6415	47.2732	21.1844	0.0515	265.5578	16.2896	0.0515	16.2895	1.4520	6.5E+28
SI_IMCM_1403_BELT_M2_1.5mm_0Nm_20kHz_001	13.1717	26.3965	11.7621	0.0282	79.4987	8.9153	0.0282	8.9152	1.4854	1.07E+28
SI_IMCM_1403_BELT_M2_1.5mm_30Nm_20kHz_001	17.3753	34.9580	15.5395	0.0381	145.2253	12.0496	0.0381	12.0496	1.4595	2.64E+28
SI_IMCM_1403_BELT_M2_1.5mm_35Nm_20kHz_001	18.8947	37.9834	16.8872	0.0412	169.6456	13.0231	0.0412	13.0231	1.4652	3.33E+28
SI_IMCM_1403_BELT_M2_1.5mm_40Nm_20kHz_001	20.4256	40.8319	18.2229	0.0443	196.5312	14.0167	0.0443	14.0166	1.4574	4.15E+28
SI_IMCM_1403_BELT_M2_1.5mm_45Nm_20kHz_001	22.0863	44.1762	19.7105	0.0478	228.9580	15.1295	0.0478	15.1294	1.4629	5.21E+28
SI_IMCM_1403_BELT_M2_1.5mm_49.6Nm_20kHz_001	23.6358	47.3124	21.1546	0.0512	262.3462	16.1965	0.0512	16.1964	1.4617	6.39E+28
SI_IMCM_2103_BELT_M2_H_0Nm_20kHz_001	12.6063	25.1993	11.2711	0.0270	72.7998	8.5304	0.0270	8.5303	1.4776	9.36E+27
SI_IMCM_2103_BELT_M2_H_30Nm_20kHz_001	17.0123	34.0135	15.2439	0.0375	140.6150	11.8557	0.0375	11.8556	1.4353	2.51E+28
SI_IMCM_2103_BELT_M2_H_40Nm_20kHz_001	20.1269	40.2697	18.0468	0.0439	192.9680	13.8884	0.0439	13.8883	1.4503	4.04E+28
SI_IMCM_2103_BELT_M2_H_45Nm_20kHz_001	22.1152	44.1086	19.6225	0.0476	226.5384	15.0499	0.0476	15.0499	1.4789	5.13E+28
SI_IMCM_2103_M2_BELT_H_49.6Nm_20kHz_001	23.5384	47.1016	21.0731	0.0511	260.9171	16.1521	0.0511	16.1520	1.4594	6.34E+28

9.7 Inter-Turn Stator Fault Results

Stator turns faults are known to be fast progressing, so the faster the fault is detected, the better result is. Fourteen different cases of shorted turns were studied which were divided into two groups; class 1 and class 2.

Eleven features were used for the classification process which are: Mean, RMS, quadratic mean, variance, standard deviation, standard error of the mean deviation, kurtosis, minimum value, maximum value, imbalance current magnitude, and maximum deflection.

Four healthy samples and seven faulty samples (with 1 to 7 shorted turns) are used for the 2 classes SVM. The stator phase is consisted of 210 turns which means the fault has to be detected if 3% or less of the phase turns are faulty. The overall classification accuracy rate is 63.63%. A sample of the stator fault features is shown in Table 9.6.

The confusion matrix of Figure 9.6 shows that all the healthy samples were misclassified; whereas all the faulty samples have been correctly classified which indicates the presence of a fault and that should alarm the need for immediate check of motor stator.

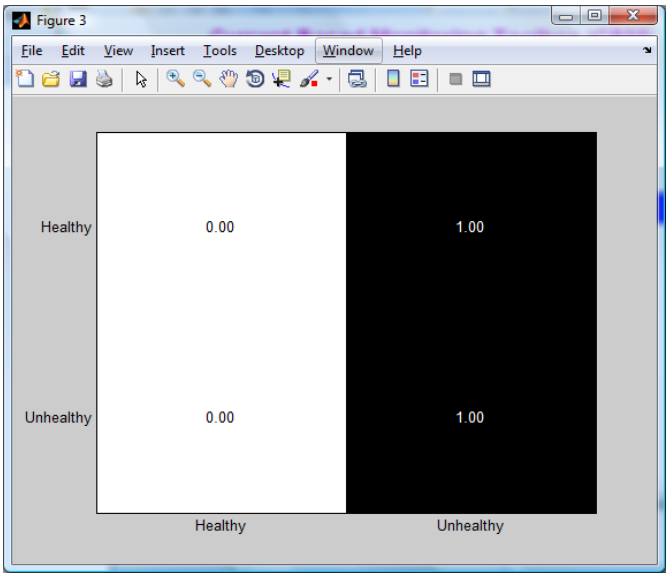

Figure 9.6 Confusion Matrix for 2-ClassesStator Fault

For 3 classes, four healthy and 14 faulty samples (with 1 to 14 shorted turns) are used. The overall accuracy rate has decreased to 50%. The 3 classes output is shown in Table 9.7.

In general, the 2 classes result is a good measure for the presence of a fault and that requires the need for immediate checking of the motor especially in the case of stator where the fault progresses very fast

Table 9.6 Sample of The Inter-Turn Stator Fault Features

Sample Names	Max	Min	Range	QM	Variation	Standard Deviation	Standard Error	RMS	imb	Del Max
00 SI_IMCM_0903_M3_BELT_STATOR_0T_45Nm_20kHz_001	22.032	-21.959	43.991	0.048	228.745	15.102	0.048	15.102	7.678	14.494
00 SI_IMCM_0903_M3_BELT_STATOR_NOBOX_45Nm_20kHz_001	22.105	-22.053	44.159	0.048	228.583	15.100	0.048	15.100	6.989	13.192
00 SI_IMCM_1003_M3_BELT_STATOR_0T_45Nm_20kHz_001	21.965	-21.919	43.884	0.048	227.379	15.076	0.048	15.076	2.635	4.965
00 SI_IMCM_1003_M3_BELT_STATOR_NOBOX_45Nm_20kHz_001	21.971	-21.931	43.902	0.048	227.207	15.071	0.048	15.070	2.677	5.043
01 SI_IMCM_0903_M3_BELT_STATOR_1T_45Nm_20kHz_001	22.062	-22.023	44.084	0.048	229.020	15.116	0.048	15.116	6.832	12.909
02 SI_IMCM_0903_M3_BELT_STATOR_2T_45Nm_20kHz_001	22.083	-22.079	44.161	0.048	229.499	15.136	0.048	15.136	5.851	11.069
03 SI_IMCM_0903_M3_BELT_STATOR_3T_45Nm_20kHz_001	22.095	-22.067	44.161	0.048	229.414	15.137	0.048	15.137	4.841	9.159
04 SI_IMCM_0903_M3_BELT_STATOR_4T_45Nm_20kHz_001	22.168	-22.157	44.325	0.048	230.264	15.167	0.048	15.167	4.294	8.140
05 SI_IMCM_0903_M3_BELT_STATOR_5T_45Nm_20kHz_001	22.259	-22.264	44.522	0.048	231.504	15.210	0.048	15.210	3.304	6.282
06 SI_IMCM_0903_M3_BELT_STATOR_6T_45Nm_20kHz_001	22.312	-22.264	44.576	0.048	232.518	15.245	0.048	15.244	3.192	6.083
07 SI_IMCM_0903_M3_BELT_STATOR_7T_45Nm_20kHz_001	22.326	-22.322	44.648	0.048	233.353	15.273	0.048	15.273	2.737	5.224

Table 9.7 SVM Output for 3 Classes Stator Fault

Sample Names	Class	Predicted labels
00_SI_IMCM_0903_M3_BELT_STATOR_0T_45Nm_20kHz_001	1	3
00_SI_IMCM_0903_M3_BELT_STATOR_NOBOX_45Nm_20kHz_001	1	3
00_SI_IMCM_1003_M3_BELT_STATOR_0T_45Nm_20kHz_001	1	2
00_SI_IMCM_1003_M3_BELT_STATOR_NOBOX_45Nm_20kHz_001	1	2
01_SI_IMCM_0903_M3_BELT_STATOR_1T_45Nm_20kHz_001	2	3
01_SI_IMCM_0903_M3_BELT_STATOR_2T_45Nm_20kHz_001	2	3
01_SI_IMCM_0903_M3_BELT_STATOR_3T_45Nm_20kHz_001	2	2
01_SI_IMCM_0903_M3_BELT_STATOR_4T_45Nm_20kHz_001	2	2
01_SI_IMCM_0903_M3_BELT_STATOR_5T_45Nm_20kHz_001	2	2
01_SI_IMCM_0903_M3_BELT_STATOR_6T_45Nm_20kHz_001	2	2
01_SI_IMCM_0903_M3_BELT_STATOR_7T_45Nm_20kHz_001	2	2
02_SI_IMCM_0903_M3_BELT_STATOR_10T_45Nm_20kHz_001	3	2
02_SI_IMCM_0903_M3_BELT_STATOR_11T_45Nm_20kHz_001	3	3
02_SI_IMCM_0903_M3_BELT_STATOR_12T_45Nm_20kHz_001	3	3
02_SI_IMCM_0903_M3_BELT_STATOR_13T_45Nm_20kHz_001	3	3
02_SI_IMCM_0903_M3_BELT_STATOR_14T_45Nm_20kHz_001	3	3
02_SI_IMCM_0903_M3_BELT_STATOR_8T_45Nm_20kHz_001	3	2
02_SI_IMCM_0903_M3_BELT_STATOR_9T_45Nm_20kHz_001	3	2

9.8 Eccentricity Fault Results

The eccentricity fault was studied as two separated faults which are static and dynamic eccentricity. Nine features were chosen for classification which are: Maximum value, minimum value, range, peak value, quadratic mean, variation, standard deviation, standard error of the mean deviation, and RMS. Table 9.8 shows the calculated values of these features.

For static eccentricity, the classification result is poor (16.67%). Besides it is being difficult to detect the static eccentricity, the result could be attributed to the technology used to produce the static eccentricity fault with a fraction of a

millimeter. In addition, the assembling method of the eccentric bearing within the motor could have an effect on the process. Static eccentricity can be detected easily when it progresses to a dynamic eccentricity fault.

In dynamic eccentricity, with the all 17 features, the accuracy rate was only 50% which has increased to 91.67% after using only the good features. Table 9.9 contains the SVM output for the dynamic eccentricity.

The confusion matrix of Figure 9.7 shows that 83% of the healthy samples were correctly classified. It also indicates the definite presence of a dynamic eccentricity fault with 100% accuracy rate for faulty samples classification. Table 9.10 shows a summary of the belt coupled motor results.

Table 9.8 Features of The Eccentricity Fault

Sample Names	Max	Min	Range	Peak	QM	Variance	Standard Deviation	Standard Error	RMS
SI_IMCM_0803_M4_BELT_H_0Nm_20kHz_001	12.6439	-12.6257	25.2696	11.4178	0.0276	76.4320	8.7304	0.0276	8.7304
SI_IMCM_0803_M4_BELT_H_30Nm_20kHz_001	17.2981	-17.2788	34.5770	15.5119	0.0378	142.9254	11.9452	0.0378	11.9452
SI_IMCM_0803_M4_BELT_H_35Nm_20kHz_001	18.7467	-18.7084	37.4551	16.7893	0.0409	167.4865	12.9340	0.0409	12.9339
SI_IMCM_0803_M4_BELT_H_40Nm_20kHz_001	20.1936	-20.1653	40.3589	18.1219	0.0441	194.8161	13.9478	0.0441	13.9477
SI_IMCM_0803_M4_BELT_H_45Nm_20kHz_001	21.8331	-21.7877	43.6208	19.5735	0.0476	226.9854	15.0593	0.0476	15.0592
SI_IMCM_0803_M4_BELT_H_49.6Nm_20kHz_001	23.4214	-23.4005	46.8219	21.0210	0.0510	260.2203	16.1254	0.0510	16.1253
SI_IMCM_1103_M4_BELT_SE_0Nm_20kHz_001	13.6573	-13.6824	27.3397	12.2652	0.0296	88.0685	9.3701	0.0296	9.3701
SI_IMCM_1103_M4_BELT_SE_30Nm_20kHz_001	17.5163	-17.5376	35.0539	15.7810	0.0387	149.8146	12.2271	0.0387	12.2271
SI_IMCM_1103_M4_BELT_SE_35Nm_20kHz_001	19.0090	-18.9501	37.9591	17.0135	0.0416	173.5336	13.1632	0.0416	13.1632
SI_IMCM_1103_M4_BELT_SE_40Nm_20kHz_001	20.4085	-20.4125	40.8210	18.2918	0.0447	199.8241	14.1263	0.0447	14.1262
SI_IMCM_1103_M4_BELT_SE_45Nm_20kHz_001	22.0886	-22.1024	44.1910	19.7937	0.0481	231.6972	15.2121	0.0481	15.2120
SI_IMCM_1103_M4_BELT_SE_49.6Nm_20kHz_001	23.7213	-23.7168	47.4381	21.1932	0.0514	265.0210	16.2691	0.0514	16.2691
SI_IMCM_1503_BELT_M4_DE_0Nm_20kHz_001	13.1139	-13.1070	26.2209	11.8150	0.0285	81.1121	9.0057	0.0285	9.0056
SI_IMCM_1503_BELT_M4_DE_30Nm_20kHz_001	17.5737	-17.5924	35.1661	15.7411	0.0384	147.2521	12.1324	0.0384	12.1324
SI_IMCM_1503_BELT_M4_DE_35Nm_20kHz_001	19.0428	-19.0298	38.0726	16.9969	0.0414	171.6421	13.0993	0.0414	13.0992
SI_IMCM_1503_BELT_M4_DE_40Nm_20kHz_001	20.4904	-20.4536	40.9440	18.3207	0.0446	199.1735	14.1122	0.0446	14.1121
SI_IMCM_1503_BELT_M4_DE_45Nm_20kHz_001	22.2413	-22.1984	44.4397	19.8258	0.0481	231.6270	15.2177	0.0481	15.2177
SI_IMCM_1503_BELT_M4_DE_49.6Nm_20kHz_001	23.8804	-23.8604	47.7408	21.2896	0.0515	265.6888	16.2981	0.0515	16.2980

Table 9.9 Results For Dynamic Eccentricity Fault With LOO SVM

Sample Name	Class	Predicted label
SI_IMCM_0803_M4_BELT_H_0Nm_20kHz_001	1	1
SI_IMCM_0803_M4_BELT_H_30Nm_20kHz_001	1	1
SI_IMCM_0803_M4_BELT_H_35Nm_20kHz_001	1	1
SI_IMCM_0803_M4_BELT_H_40Nm_20kHz_001	1	1
SI_IMCM_0803_M4_BELT_H_45Nm_20kHz_001	1	1
SI_IMCM_0803_M4_BELT_H_49.6Nm_20kHz_001	1	2
SI_IMCM_1503_BELT_M4_DE_0Nm_20kHz_001	2	2
SI_IMCM_1503_BELT_M4_DE_30Nm_20kHz_001	2	2
SI_IMCM_1503_BELT_M4_DE_35Nm_20kHz_001	2	2
SI_IMCM_1503_BELT_M4_DE_40Nm_20kHz_001	2	2
SI_IMCM_1503_BELT_M4_DE_45Nm_20kHz_001	2	2
SI_IMCM_1503_BELT_M4_DE_49.6Nm_20kHz_001	2	2

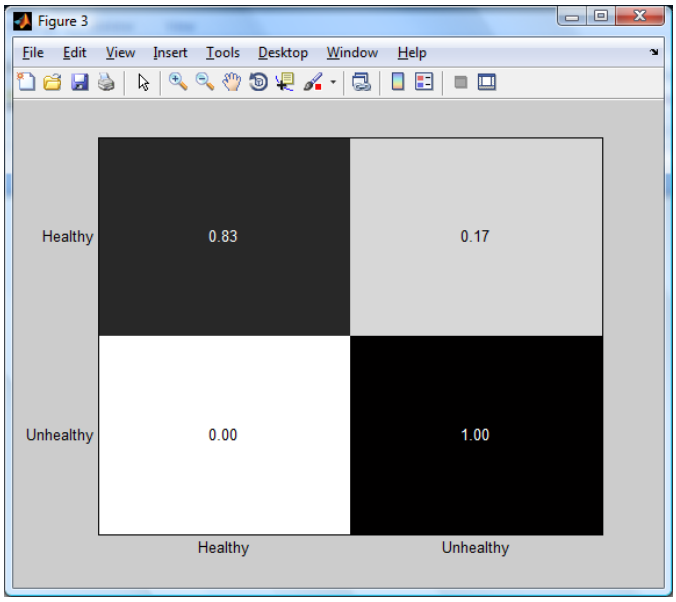

Figure 9.7 Confusion Matrix for Dynamic Eccentricity

Table 9.10 Summary of Results

SN	Fault		No. of Classes	No. of Relevant Features	Classifier	Kernel	N	No. of Samples	Overall Accuracy Rate %
1	Rotor		2	12	SVM - LOO	RBF	-	12	100
			3		SVM - LOO	RBF		18	66.67
2	Bearings	Roughness	2	10	SVM - LOO	RBF	-	10	60
		Outer Race	2	10	SVM - LOO	RBF	-	10	10
					SVM – N-Fold	RBF	5	10	9.09
3	Stator		2	11	SVM - LOO	RBF	-	11	63.63
			3	11	SVM - LOO	RBF	-	18	50
4	Eccentricity	Static	2	9	SVM - LOO	RBF	-	12	16.67
		Dynamic	2	9	SVM – N-Fold	RBF	3	12	16.67
					SVM - LOO	RBF	-	12	91.67

9.9 Results Verifications

For verification, the data collected during the direct coupling of the motor-load phase of testing is used for classifications. The same features are calculated and used for the classification. The kernel and parameters are kept unchanged. LOO is chosen for SVM testing. The rotor, stator, and eccentricity faults are chosen for the verification process. The results are comparable to those of the belt coupled motor results.

As in Table 9.11, ten samples are used for the classification process. The overall classification accuracy rate is 80%. Only one healthy sample is misclassified. All the faulty samples are correctly classified which indicates the explicit presence of a rotor broken bar fault.

Table 9.11 Rotor Fault Calssification Results (Direct Coupled Motor)

Sample Names	Class	Predicted Labels
KTP-SI-2203-M1-H-0 Nm-20k-001	1	1
KTP-SI-2203-M1-H-12.5 Nm-20k-001	1	1
KTP-SI-2203-M1-H-25-20k-001	1	2
KTP-SI-2203-M1-H-37.5 Nm-20k-001	1	1
KTP-SI-2203-M1-H-50 Nm-20k-001	1	1
KTP-SI-2303-M1-1BAR-0 Nm-20k-001	2	2
KTP-SI-2303-M1-1BAR-12.5 Nm-20k-001	2	2
KTP-SI-2303-M1-1BAR-25 Nm-20k-001	2	2
KTP-SI-2303-M1-1BAR-37.5 Nm-20k-001	2	2
KTP-SI-2303-M1-1BAR-50 Nm-20k-001	2	2

The results of the stator tests and dynamic eccentricity are shown in Table 9.12 and Table 9.13 respectively. Fourteen samples are used for the stator classification.

Table 9.12 SVM Output for Stator Fault (Direct Coupled Motor)

Sample Names	Class	Predicted labels
KTP_SI_M3_H(1)_40Nm_20k_001	1	1
KTP_SI_M3_H(2)_40Nm_20k_001	1	2
KTP_SI_M3_H(3)_40Nm_20k_001	1	1
KTP_SI_M3_H(4)_40Nm_20k_001	1	1
KTP_SI_M3_H(5)_40Nm_20k_001	1	1
KTP_SI_M3_H(6)_40Nm_20k_001	1	2
KTP_SI_M3_H(7)_40Nm_20k_001	1	1
KTP_SI_M3_1T_40Nm_20k_001	2	2
KTP_SI_M3_2T_40Nm_20k_001	2	2
KTP_SI_M3_3T_40Nm_20k_001	2	2
KTP_SI_M3_4T_40Nm_20k_001	2	1
KTP_SI_M3_5T_40Nm_20k_001	2	2
KTP_SI_M3_6T_40Nm_20k_001	2	2
KTP_SI_M3_7T_40Nm_20k_001	2	2

Table 9.13 SVM Results for Dynamic Eccentricity Fault (Direct Coupled Motor)

Sample Name	Class	Predicted label
KTP_SI_M4_H_25Nm_20k_001	1	1
KTP_SI_M4_H_30Nm_20k_001	1	1
KTP_SI_M4_H_35Nm_20k_001	1	2
KTP_SI_M4_H_40Nm_20k_001	1	1
KTP_SI_M4_H_45Nm_20k_001	1	1
KTP_SI_M4_H_50Nm_20k_001	1	2
KTP_SI_1806_M4_DE_00Nm_20kHz_001	2	1
KTP_SI_1806_M4_DE_30Nm_20kHz_001	2	2
KTP_SI_1806_M4_DE_35Nm_20kHz_001	2	2
KTP_SI_1806_M4_DE_40Nm_20kHz_001	2	2
KTP_SI_1806_M4_DE_45Nm_20kHz_001	2	2
KTP_SI_1806_M4_DE_50Nm_20kHz_001	2	2

The success classification rate for the healthy samples is 71%, and the overall accuracy rate is approximately 79%. Only one faulty sample is misclassified, making the accuracy rate for this class as high as 86%. Such high accuracy indicates the high probability of fault existence and the need for immediate stator check.

Twelve samples are used for testing the dynamic eccentricity fault. The overall accuracy and classes rates are 83% which is high enough to indicate the fault presence.

9.10 Summary

As the SVM has a good reputation in classification field, it has been adapted for this work. In fact, it has been difficult to compare the results of this work with the outcomes of other similar researches as much of the reported works are either using different samples of data or different ways of features generation and extraction and that all make direct comparison is not the best way to judge the outcome of this work.

The results in illustrate acceptable to very good classification and detection results for, rotor, stator, dynamic eccentricity, and general bearing roughness.

The static eccentricity and bearing defects have low rates which coincide with current research findings. When progresses, static eccentricity becomes dynamic and then can easily be detected.

For the outer race bearing fault, the fault signature is masked by other harmonics within the current signal as the changes of the motor air gap can be a result of a number of other sources like the machine vibration or misalignment.

Results show that a multi fault monitoring system can be developed for induction motors faults using current as a sensed signal and statistical features along with SVMs for detection and diagnosis.

Chapter 10. Conclusions and Future Work

Condition monitoring means the continuous evaluation of the health of plant and equipment throughout its serviceable life [1]. As a simple fault may lead to a very costly damage, the idea of detecting a fault, confronting it and relating it to ideally one cause before it deteriorates is the main concern of engineers and researchers.

Early detection and diagnosis of process faults while the plant is still operating in a controllable region can help avoid abnormal event progression and reduce productivity losses which in turn can help avoid major system breakdowns and catastrophes.

Bearing and stator faults are the major problem makers in induction machines and to them are 80% of the faults attributed. Though bearings are inexpensive to replace, their problems are difficult to detect and their failures can cause significant losses. Stator faults are fast progressive and should be detected early to avoid losses. Rotor faults though are rarely occurring and withstandable for a while, if not detected at the right time they may lead to a catastrophe.

In this thesis, several faults creation and monitoring of a squirrel cage rotor induction motor system operations were performed through the machine current waveforms. The method has used statistical calculations for features generation. Machine learning is used as detection and diagnosis mechanism, choosing support vector machines as a tool for that. The application of the

proposed method has shown to provide a useful diagnosis for the faults studied.

10.1 Summary

Maintenance types, induction machines, and machine learning are introduced in chapter one. A thorough literature survey is done in Chapters two to four which cover the faults types, features, and detection techniques.

The background information on squirrel cage induction motors construction, principle of work, and modelling was provided in Chapter five. While Chapter six includes a description of the rig used for testing the motors and seeding the faults onto them, Chapter seven has presented plots of the signals retrieved in both time and frequency domains.

The basis and theory of proposed method for detection and diagnosis is described in Chapter eight. The work results have been discussed in Chapter nine which showed that the proposed method produces reasonable classification results. Since not all IMs are identical, their characteristic may vary from one model to another and the working environments and conditions may also vary, as a result, the proposed method must be carried-out on each individual drive in order to accurately detect the studied faults in different systems.

The proposed system uses statistical techniques to extract the features from the stator current signal of the electric motor. Then the motor input current features are used for SVM training and testing. The proposed system was

tested using signals obtained from four induction motors under healthy and faulty states with different loading conditions. The motors were subjected to the following faults: broken rotor bar, faulty bearing, stator turn-to-turn fault, and eccentricity. Though improvement is always required, the test results are promising for the real time applications.

10.2 Conclusions and Contributions

The following conclusions and contributions can be drawn from the work done throughout the different phases of the project.

1. The proposed system managed to detect and diagnose three faults out of four to certain acceptable degree. It has been shown that MCSA, statistical parameters and support vector machines provide a good method for some IM faults detection and diagnosis.

2. Rotor and dynamic eccentricity faults are the easiest to detect. Static eccentricity can be detected when it progresses to dynamic eccentricity.

3. One of the aims of this project is to study in influences in stator currents from various faults. Characteristic features of each fault type are presented and studied. The background from the study is used to decide on the monitoring system.

4. Extracting faults features is the first and vital phase of detection and diagnosis process, but choosing the relevant ones is not less important

than generating them. Choosing the right features can even, in certain cases, double the classification accuracy rate.

5. SVM has a good classification capability even when the number of samples of each class doesn't exceed the number of a hand fingers.

6. A toolbox has been produced for four different faults of the induction motor where it is only needed to provide the current signals of the motor to have the results of whether any of the faults exists or not.

7. To have a reliable data, it is suggested that data recorded for zero to full load in small steps of loading for healthy and all faulty situations when possible.

8. To implement IM fault detection using the proposed method in commercial monitors, the SVM classifier for each fault type needs to be pre-determined. Since the features mostly affected by the corresponding faults are known, it is easy to choose the most viable ones, and the SVM classifier can be designed.

9. It can be concluded that MCSA approach is an effective method of monitoring the condition of electric induction motors because of its simplicity to implement and cost effectiveness. Furthermore it has a considerable degree of accuracy and there is no interruption to the motor whilst being monitored.

10. The application of machine learning for fault diagnosis is becoming more dominant compared to conventional methods and that is

attributed to the increased availability of computational resources and the vast algorithmic developments [16].

11. The proposed system that combines MCSA, statistical generated features and SVM has high effectiveness. Features are easily extracted from raw current data and the best SVM kernel has been chosen experimentally. The system can be easily extended to any other faults and number of classes.

10.3 Suggestions for Future Work

Future work could possibly be focused on:

1. The study could be extended to include other faults like misalignment fault or other parts within the same fault such as, inner race way, balls, and cages.
2. Future research may look into studying multiple faults of a motor that are happening at the same time.
3. To have more consolidated monitoring results, multiple signals can be used such as current and voltage as both methods are cost effective.
4. Detecting bearing and static eccentricity faults using MCSA is not an easy task, so the detection capability could be improved by using different features extraction techniques and combined artificial intelligence methods.

5. The area of research for the general roughness defect in bearings is still almost blank, so it is a good opportunity for researches to concentrate upon such a corner.

6. In this project, only one set of drives was used for the experimental work. The characteristics of different motor machines are different, and that results in different features and, thus, different SVM classifiers. SVM classifiers must be determined for each motors combination. This is not very effective for the method to be commercially deployed. It is more desirable to have SVM classifiers that can classify induction motors of different models for different power rates and sizes. For this, further study is required.

7. A number of approaches that utilizes MCSA have been developed to detect and diagnose induction motors faults and these have produced several commercially viable techniques, which are currently used to monitor drive systems. However, still there is a need to develop new techniques to overcome problems, such as when the motor is running at no load or during transient stages.

8. Line-neutral voltage signature has been used for Rotor Bars fault detection. It is not only preserves the advantage and simplicity of MCSA, but also it is more sensitive to motor failures [46]. However, the analysis of line-neutral voltage signatures still remains far from being fully researched. More efforts are needed to improve the overall fault diagnosis of induction motors using this technique.

References

1. Tavner, P.J., *Condition Monitoring of Electrical Machines*1988: Research Studies Press Ltd.

2. Nimmo, I., *Adequately address abnormal situation operations.* Chemical Engineering Progress, 1995. **91**(9): p. 36-45.

3. Venkat, V., et al., *A review of process fault detection and diagnosis. Part I: Quantitative model-based methods.* Computers and Chemical Engineering, 2003. **27**: p. 293-311.

4. Lacey, S.J., *The role of vibration monitoring in predictive maintenance-Part 1: Principle and Practice.* Maintenance & Engineering (incorporating: maintenance and asset management Journal), 2010. **10**: p. 36-45.

5. Singh, G.K. and S.A.S. Al Kazzaz, *Induction machine drive condition monitoring and diagnostic research - A survey.* Electric Power Systems Research, 2003. **64**(2): p. 145-158.

6. Gertler, J.J., *Survey of model-based failure detection and isolation in complex plants.* Control Systems Magazine, IEEE, 1988. **8**(6): p. 3-11.

7. Gertler, J., *Fault Detection and Diagnosis in Engineering Systems*. 1 ed1998: CRC; 1 edition 504.

8. Yang, Q., *Model-Based And Data Driven Fault Diagnosis Methods With Applications To Process Monitoring*, 2004, Case Western Reserve University / Ohio.

9. Humphrey, D.W. *Less is more*. Industry Journal, 2009. **01**, 07-21.

10. Boldea, I. and S.A. Nasar, *The Induction Machine Handbook*2002: CRC Press.

11. Yong, T., et al. *Efficiency optimization of induction motors using genetic algorithm and Hybrid Genetic Algorithm*. in *Electrical Machines and Systems (ICEMS), 2011 International Conference on*. 2011.

12. Phumiphak, T. and C. Chat-uthai. *Estimation of induction motor parameters based on field test coupled with genetic algorithm*. in *Power System Technology, 2002. Proceedings. PowerCon 2002. International Conference on*. 2002.

13. M.Peltola, *Slip of ac Induction Motors and How to Minimize It*, in *Drives magazine*2002.

14. Thomson, W.T. and M. Fenger, *Current signature analysis to detect induction motor faults.* Industry Applications Magazine, IEEE, 2001. **7**(4): p. 26-34.

15. Wikipedia, t.f.e. *Machine learning*. 2010 [cited 2010 9/9]; Available from: http://en.wikipedia.org/wiki/Machine_learning.

16. Sakthivel, N.R., V. Sugumaran, and S. Babudevasenapati, *Vibration based fault diagnosis of monoblock centrifugal pump using decision tree.* Expert Systems with Applications, 2010. **37**(6): p. 4040-4049.

17. Cortes C., V.V., *Support Vector Networks.* Learning Machines, 1995. **20**: p. 273-297.

18. Madden, M.G. and P.J. Nolan, *Generation of Fault Trees from Simulated Incipient Fault Case Data*, in *Ninth International Conference on Artificial Intelligence in Engineering*1994: Pennsylvania, U.S.A.

19. Wikipedia, t.f.e. *Support vector machines*. 2012; Available from: http://en.wikipedia.org/wiki/Machine_learning#Support_vector_machines.

20. Habetler, T.G., et al. *Complete current-based induction motor condition monitoring: stator, rotor, bearings, and load*. in *Power Electronics Congress, 2002. Technical Proceedings. CIEP 2002. VIII IEEE International*. 2002.

21. Isermann, R., *Supervision, fault-detection and fault-diagnosis methods - an introduction.* Control Engineering Practice, 1997. **5**(5): p. 639-652.

22. Willsky, A.S., *A Survey of Design Methods for Failure Detection in Dynamic Systems.* Automatica, 1976. **12**: p. 601-611.

23. Mohamed, L. and A.S. Ibrahim, *Model-based fault diagnosis via parameter estimation using knowledge based and fuzy logic approach*, in *IEEE MELECON*2002.

24. John, H., *Model-based fault detection in information poor plants.* Automatica, 1994. **30**(6): p. 929-943.

25. Krishnan, M., S. Das, and S.A. Yost, *A 10-Year Mechatronics Curriculum Development Initiative: Relevance, Content, and Results—Part II.* Education, IEEE Transactions on, 2010. **53**(2): p. 202-208.

26. Harihara, P.P., K.d. Kim, and A.G. Parlos, *Signal-based versus Model-based Fault Diagnosis—A Trade-off in Complexity and Performance*, in *4th IEEE International Symposium on Diagnostics For Electric Machines, Power Electronics and Drives*2003. p. 277-282.

27. Duffuaa, S.O., A. Raouf, and J.D. Campbell, *Planning and Control of Maintenance Systems: Modeling and Analysis*1999: John Wiley and Sons. 400 pages.

28. Wilson, A., *Asset Maintenance Management: A Guide to Developing Strategy & Improving Performance*5 Jan 2002: Industrial Press.

29. Nejjari, H. and M.E.H. Benbouzid, *Monitoring and diagnosis of induction motors electrical faults using a current Park's vector pattern learning approach.* Industry Applications, IEEE Transactions on, 2000. **36**(3): p. 730-735.

30. Welch, D.E., et al., *Elctrical signture analysis (ESA) as a diagnostic maintenance technique for detecting the high consequence fuel pump filure modes*, 2002.

31. Kryter, R.C. and H.D. Haynes, *Condition monitoring of machinery using motor current signature analysis.* S V Sound and Vibration, 1989. **23**(9): p. 14-21.

32. Elkasabgy, N.M., A.R. Eastham, and G.E. Dawson, *Detection of broken bars in the cage rotor on an induction machine.* Industry Applications, IEEE Transactions on, 1992. **28**(1): p. 165-171.

33. Peck, J.P. and J. Burrows, *On-line condition monitoring of rotating equipment using neural networks.* ISA Transactions, 1994. **33**(2): p. 159-164.

34. Lin, J.-L., et al., *Motor shaft misalignment detection using multiscale entropy with wavelet denoising.* Expert Systems with Applications, 2010. **37**(10): p. 7200-7204.

35. Boskoski, P., et al., *Detection of lubrication starved bearings in electrical motors by means of vibration analysis.* Tribology International, 2010. **43**(9): p. 1683-1692.

36. Thorsen, O.V. and M. Dalva, *Failure identification and analysis for high-voltage induction motors in the petrochemical industry.* Industry Applications, IEEE Transactions on, 1999. **35**(4): p. 810-818.

37. Leonard, R.A. and W.T. Thomson, *Vibration and stray flux fault monitoring for unbalanced supply and inter-turn winding diagnosis in induction motors.* Br. J. NDT, 1986: p. 211–215.

38. Riley, C.M., et al. *A method for sensorless on-line vibration monitoring of induction machines*. in *Industry Applications Conference, 1997. Thirty-Second IAS Annual Meeting, IAS '97., Conference Record of the 1997 IEEE*. 1997.

39. Oumaamar, M.E.K., et al. *Neutral Voltage Analysis for Broken Rotor Bars Detection in Induction Motors Using Hilbert Transform Phase*. in *Industry Applications Conference, 2007. 42nd IAS Annual Meeting. Conference Record of the 2007 IEEE*. 2007.

40. Khezzar, A., et al., *Induction Motor Diagnosis Using Line Neutral Voltage Signatures.* Industrial Electronics, IEEE Transactions on, 2009. **56**(11): p. 4581-4591.

41. Farahani, H.F., et al. *Investigation of unbalance supplying voltage on the thermal behavior of Squirrel Cage Induction motor using monitoring system*. in *Universities Power Engineering Conference, 2007. UPEC 2007. 42nd International*. 2007.

42. Elkasabgy, N.M., A.R. Eastham, and G.E. Dawson. *The detection of broken bars in the cage rotor of an induction machine*. in *Industry Applications Society Annual Meeting, 1988., Conference Record of the 1988 IEEE*. 1988.

43. Milimonfared, J., et al., *A novel approach for broken-rotor-bar detection in cage induction motors.* Industry Applications, IEEE Transactions on, 1999. **35**(5): p. 1000-1006.

44. Cupertino, F., et al., *Analysis techniques for detection of IM broken rotor bars after supply disconnection.* Industry Applications, IEEE Transactions on, 2004. **40**(2): p. 526-533.

45. Supangat, R., et al. *Detection of Broken Rotor Bar Faults and Effects of Loading in Induction Motors during Rundown*. in *Electric Machines & Drives Conference, 2007. IEMDC '07. IEEE International*. 2007.

46. Mehrjou, M.R., et al., *Rotor fault condition monitoring techniques for squirrel-cage induction machine—A review.* Mechanical Systems and Signal Processing, 2011. **25**(8): p. 2827-2848.

47. Alfayez, L., D. Mba, and G. Dyson, *The application of acoustic emission for detecting incipient cavitation and the best efficiency point of a 60 kW centrifugal pump: case study.* NDT & E International, 2005. **38**(5): p. 354-358.

48. Loutas, T.H., et al., *Condition monitoring of a single-stage gearbox with artificially induced gear cracks utilizing on-line vibration and*

acoustic emission measurements. Applied Acoustics, 2009. **70**(9): p. 1148-1159.

49. Tandon, N., G.S. Yadava, and K.M. Ramakrishna, *A comparison of some condition monitoring techniques for the detection of defect in induction motor ball bearings.* Mechanical Systems and Signal Processing, 2007. **21**(1): p. 244-256.

50. Tandon, N., K.M. Ramakrishna, and G.S. Yadava, *Condition monitoring of electric motor ball bearings for the detection of grease contaminants.* Tribology International, 2007. **40**(1): p. 29-36.

51. Gaylard, A., A. Meyer, and C. Landy. *Acoustic evaluation of faults in electrical machines*. in *Electrical Machines and Drives, 1995. Seventh International Conference on (Conf. Publ. No. 412)*. 1995.

52. Ellison, A.J. and S.J. Yang, *Effects of rotor eccentricity on acoustic noise from induction machines.* Electrical Engineers, Proceedings of the Institution of, 1971. **118**(1): p. 174-184.

53. Sasi, A.Y.B., et al., *A validated model for the prediction of rotor bar failure in squirrel-cage motors using instantaneous angular speed.* Mechanical Systems and Signal Processing, 2006. **20**(7): p. 1572-1589.

54. Sasi, A., B. Payne, and F. Gu, *The Exploitation of Instantaneous Angular Speed for Condition Monitoring of Electric Motors*, in *14th International Congress on Condition Monitoring and Diagnostic Engineering Management (COMADEM),* 2001: Manchester, UK. p. 311-318.

55. Gu, F., et al., *An investigation of the effects of measurement noise in the use of instantaneous angular speed for machine diagnosis.* Mechanical Systems and Signal Processing, 2006. **20**(6): p. 1444-1460.

56. Kliman, G.B. and J. Stein, *Methods of Motor Current Signature Analysis.* Electric Machines & Power Systems, 1992. **20**(5): p. 463-474.

57. Sang-Bin, L. and T.G. Habetler, *An online stator winding resistance estimation technique for temperature monitoring of line-connected induction machines.* Industry Applications, IEEE Transactions on, 2003. **39**(3): p. 685-694.

58. Bonnett, A.H. and G.C. Soukup, *Cause and analysis of stator and rotor failures in three-phase squirrel-cage induction motors.* Industry Applications, IEEE Transactions on, 1992. **28**(4): p. 921-937.

59. Hafezi, H. and A. Jalilian. *Design and Construction of Induction Motor Thermal Monitoring System*. in *Universities Power Engineering Conference, 2006. UPEC '06. Proceedings of the 41st International*. 2006.

60. Beguenane, R. and M.E.H. Benbouzid, *Induction motors thermal monitoring by means of rotor resistance identification.* Energy Conversion, IEEE Transactions on, 1999. **14**(3): p. 566-570.

61. Cheng, S., et al., *A Nonintrusive Thermal Monitoring Method for Induction Motors fed by Closed-loop Inverter Drives.* Power Electronics, IEEE Transactions on, 2012. **PP**(99): p. 1-1.

62. Zhi, G., et al. *A novel online rotor temperature estimator for induction machines based on a cascading motor parameter estimation scheme*. in *Diagnostics for Electric Machines, Power Electronics and Drives, 2005. SDEMPED 2005. 5th IEEE International Symposium on*. 2005.

63. Salisbury, R. *Thermal imaging and predictive maintenance: what the future has in store*. in *Cement Industry Technical Conference, 2000 IEEE-IAS/PCA*. 2000.

64. Benhaddadi, M., R. Khaldi, and M. Benghanem. *Experimental study of heating in induction motor fed by PWM inverter*. in *Instrumentation and Measurement Technology Conference, 1997. IMTC/97. Proceedings. Sensing, Processing, Networking., IEEE*. 1997.

65. Yahoui, H. and G. Grellet. *Measurement of physical signals in rotating part of electrical machine by means of optical fibre transmission*. in *Instrumentation and Measurement Technology Conference, 1996. IMTC-96. Conference Proceedings. 'Quality Measurements: The Indispensable Bridge between Theory and Reality'., IEEE*. 1996.

66. Filho, E.R., R.R. Riehl, and E. Avolio. *Automatic three-phase squirrel-cage induction motor test assembly for motor thermal behaviour studies*. in *Industrial Electronics, 1994. Symposium Proceedings, ISIE '94., 1994 IEEE International Symposium on*. 1994.

67. Eltabach, M. and A. Charara. *Comparative investigation of electrical diagnostic procedures in induction motors*. in *Power Electronics, Electrical Drives, Automation and Motion, 2006. SPEEDAM 2006. International Symposium on*. 2006.

68. Drif, M., et al. *Squirrel cage rotor faults detection in induction motor utilizing stator power spectrum approach*. in *Power Electronics, Machines and Drives, 2002. International Conference on (Conf. Publ. No. 487)*. 2002.

69. Cruz, S.M.A. and A.J.M. Cardoso. *Rotor cage fault diagnosis in three-phase induction motors by the total instantaneous power spectral analysis*. in *Industry Applications Conference, 1999. Thirty-Fourth IAS Annual Meeting. Conference Record of the 1999 IEEE*. 1999.

70. Zhenxing, L., et al., *Online rotor mixed fault diagnosis way based on spectrum analysis of instantaneous power in squirrel cage induction motors.* Energy Conversion, IEEE Transactions on, 2004. **19**(3): p. 485-490.

71. Legowski, S.F., A.H.M. Sadrul Ula, and A.M. Trzynadlowski, *Instantaneous power as a medium for the signature analysis of induction motors.* Industry Applications, IEEE Transactions on, 1996. **32**(4): p. 904-909.

72. Bin, L. and M. Paghda. *Induction motor rotor fault diagnosis using wavelet analysis of one-cycle average power*. in *Applied Power Electronics Conference and Exposition, 2008. APEC 2008. Twenty-Third Annual IEEE*. 2008.

73. Isermann, R., *Model-Based Fault Detection and Diagnosis - Status and Applications.* Annual Reviews in Control, 2005. **29**: p. 71-85.

74. Andrews, J.J. and B. Moss, *Reliability and Risk Assessment (Hardcover)*. 2nd Edition ed2002 Wiley Blackwell.

75. Albrecht, P.F., et al., *Assessment of the Reliability of Motors in Utility Applications.* Power Engineering Review, IEEE, 1987. **PER-7**(9): p. 41-41.

76. Kliman, G.B., et al., *Noninvasive detection of broken rotor bars in operating induction motors.* Energy Conversion, IEEE Transactions on, 1988. **3**(4): p. 873-879.

77. Nandi, S., et al. *Study of three phase induction motors with incipient rotor cage faults under different supply conditions*. in *Industry Applications Conference, 1999. Thirty-Fourth IAS Annual Meeting. Conference Record of the 1999 IEEE*. 1999.

78. Bonnett, A.H., *Root cause AC motor failure analysis with a focus on shaft failures.* Industry Applications, IEEE Transactions on, 2000. **36**(5): p. 1435-1448.

79. Saleh, A.F., *Detection and Diagnosis of Electrical Faults in Induction Motors Using Instantaneous Phase Variation*, in *School of Mechanical, Aerospace and Civil Engineering.*2005, University of Manchster.

80. Pennacchi, P., et al., *Use of modal representation for the supporting structure in model-based fault identification of large rotating machinery: part 1—theoretical remarks.* Mechanical Systems and Signal Processing, 2006. **20**(3): p. 662-681.

81. Pennacchi, P., et al., *Use of modal representation for the supporting structure in model-based fault identification of large rotating machinery: Part 2—application to a real machine.* Mechanical Systems and Signal Processing, 2006. **20**(3): p. 682-701.

82. Mini, V.P., S. Setty, and S. Ushakumari. *Fault detection and diagnosis of an induction motor using fuzzy logic*. in *Computational Technologies in Electrical and Electronics Engineering (SIBIRCON), 2010 IEEE Region 8 International Conference on*. 2010.

83. Thomson, W.T. *On-line MCSA to diagnose shorted turns in low voltage stator windings of 3-phase induction motors prior to failure*. in *Electric Machines and Drives Conference, 2001. IEMDC 2001. IEEE International*. 2001.

84. Thomson, W.T. and D. Morrison. *On-line diagnosis of stator shorted turns in mains and inverter fed low voltage induction motors*. in *Power Electronics, Machines and Drives, 2002. International Conference on (Conf. Publ. No. 487)*. 2002.

85. Zoubek, H., S. Villwock, and M. Pacas, *Frequency Response Analysis for Rolling-Bearing Damage Diagnosis.* Industrial Electronics, IEEE Transactions on, 2008. **55**(12): p. 4270-4276.

86. Blodt, M., et al., *Models for Bearing Damage Detection in Induction Motors Using Stator Current Monitoring.* Industrial Electronics, IEEE Transactions on, 2008. **55**(4): p. 1813-1822.

87. Nandi, S., H.A. Toliyat, and L. Xiaodong, *Condition monitoring and fault diagnosis of electrical motors-a review.* Energy Conversion, IEEE Transactions on, 2005. **20**(4): p. 719-729.

88. Bonnett, A.H. *Cause and analysis of anti-friction bearing failures in AC induction motors*. in *Pulp and Paper Industry Technical Conference, 1993., Conference Record of 1993 Annual*. 1993.

89. Devaney, M.J. and L. Eren, *Detecting Motor Bearing Faults.* Instrumentation & Measurement Magazine, IEEE, 2004. **7**(4): p. 30-50.

90. Ilonen, J., et al., *Diagnosis tool for motor condition monitoring.* Industry Applications, IEEE Transactions on, 2005. **41**(4): p. 963-971.

91. Akin, B., et al., *Low Order PWM Inverter Harmonics Contributions to the Inverter-Fed Induction Machine Fault Diagnosis.* Industrial Electronics, IEEE Transactions on, 2008. **55**(2): p. 610-619.

92. Jee-Hoon, J., L. Jong-Jae, and K. Bong-Hwan, *Online Diagnosis of Induction Motors Using MCSA.* Industrial Electronics, IEEE Transactions on, 2006. **53**(6): p. 1842-1852.

93. Stack, J.R., T.G. Habetler, and R.G. Harley, *Bearing fault detection via autoregressive stator current modeling.* Industry Applications, IEEE Transactions on, 2004. **40**(3): p. 740-747.

94. Nandi, S., et al., *Parameter Independent Detection of Eccentricity Faults in Induction Machines.* Industrial Electronics, IEEE Transactions on, 2010. **PP**(99): p. 1-1.

95. Awadallah, M.A. and M.M. Morcos, *Application of AI tools in fault diagnosis of electrical machines and drives-an overview.* Energy Conversion, IEEE Transactions on, 2003. **18**(2): p. 245-251.

96. Faiz, J. and M. Ojaghi, *Different indexes for eccentricity faults diagnosis in three-phase squirrel-cage induction motors: A review.* Mechatronics, 2009. **19**(1): p. 2-13.

97. Sin, M.L., W.L. Soong, and N. Ertugrul, *Induction Machine On-line Condition Monitoring and Fault Diagnosis - A Survey*, 2003, Univeristy of Adelaide: Adelaide.

98. Nandi, S., R.M. Bharadwaj, and H.A. Toliyat, *Performance analysis of a three-phase induction motor under mixed eccentricity condition.* Energy Conversion, IEEE Transactions on, 2002. **17**(3): p. 392-399.

99. DeBortoli, M.J., et al., *Effects of rotor eccentricity and parallel windings on induction machine behavior: a study using finite element analysis.* Magnetics, IEEE Transactions on, 1993. **29**(2): p. 1676-1682.

100. Sribovornmongkol, T., *Evaluation of Motor Online Diagnosis by FEM Simulations*, in *School of Electrical Engineering,* 2006, Royal Institute of Technology: Stockholm.

101. Nandi, S., et al., *Detection of Eccentricity Faults in Induction Machines Based on Nameplate Parameters.* Industrial Electronics, IEEE Transactions on, 2011. **58**(5): p. 1673-1683.

102. Cruz, S.M.A., *An Active-Reactive Power Method for the Diagnosis of Rotor Faults in Three-Phase Induction Motors Operating Under Time-Varying Load Conditions.* Energy Conversion, IEEE Transactions on, 2012. **27**(1): p. 71-84.

103. Long, W., et al. *Improved online condition monitoring using static eccentricity-induced negative sequence current information in induction machines*. in *Industrial Electronics Society, 2005. IECON 2005. 31st Annual Conference of IEEE*. 2005.

104. Nagrani, S., S.S. Pathan, and I.H. Bhoraniya, *Misalignment Fault Diagnosis In Rotating Machinery Through The Signal Processing Technique – Signature Analysis.* International Journal of Advanced Engineering Research and Studies, 2012. **1**(2).

105. Rao, J.S., *Rotor Dynamics*. 3rd edition ed1996: New Age International.

106. Saavedra, P.N. and D.E. Ramírez, *Vibration Analysis of Rotors for the Identification of Shaft Misalignment Part 1: Theoretical AnalysisP N Saavedra and D E Ramírez.* Journal of Mechanical Engineering Science, 2004.

107. Obaid, R.R., T.G. Habetler, and D.J. Gritter. *A simplified technique for detecting mechanical faults using stator current in small induction motors*. in *Industry Applications Conference, 2000. Conference Record of the 2000 IEEE*. 2000.

108. Piotrowski, J., *Shaft Alignment Handbook* 2006: CRC Press.

109. Trzynadlowski, A.M. and E. Ritchie, *Comparative investigation of diagnostic media for induction motors: a case of rotor cage faults.* Industrial Electronics, IEEE Transactions on, 2000. **47**(5): p. 1092-1099.

110. Zhang, S., Y. Qu, and Q. Han. *Fault characteristics analysis for rotor systems with misalignment based on Wavelet Packet Decomposition and frequency-band energy ratio analysis*. in *Control Conference (CCC), 2011 30th Chinese*. 2011.

111. Nikranjbar, A., *Model-based mixed eccentricity fault diagnosis of cage induction motor using particle swarm optimization*, in *Engineering, Design and Technology*2008, University of Bradford: Bradford, UK. p. 337.

112. Cempel, C., *Vibroacoustic Condition Monitoring*1991, New York: Ellis Horwood.

113. Acosta, G.G., C.J. Verucchi, and E.R. Gelso, *A current monitoring system for diagnosing electrical failures in induction motors.* Mechanical Systems and Signal Processing, 2006. **20**(4): p. 953-965.

114. Cruz, S.M.A. and A.J.M. Cardoso, *Stator winding fault diagnosis in three-phase synchronous and asynchronous motors, by the extended Park's vector approach.* Industry Applications, IEEE Transactions on, 2001. **37**(5): p. 1227-1233.

115. Mehala, N. and R. Dahiya, *Detection of Bearing Faults of Induction Motor Using Park's Vector Approach.* International Journal of Engineering and Technology, 2010. **2**(4): p. 263-266.

116. Cruz, S.M.A. and A.J.M. Cardoso, *Rotor Cage Fault Diagnosis in Three-Phase Induction Motors by Extended Park's Vector Approach.* Electric Machines & Power Systems, 2000. **28**(4): p. 289 - 299.

117. Marques Cardoso, A.J., S.M.A. Cruz, and D.S.B. Fonseca, *Inter-turn stator winding fault diagnosis in three-phase induction motors, by Park's vector approach.* Energy Conversion, IEEE Transactions on, 1999. **14**(3): p. 595-598.

118. Silva, J.L.H. and A.J.M. Cardoso. *Bearing failures diagnosis in three-phase induction motors by extended Park's vector approach*. in *Industrial Electronics Society, 2005. IECON 2005. 31st Annual Conference of IEEE*. 2005.

119. Izzet, Ã.-n., K. Dalci, and Ã.Â.b. Senol, *Detection of bearing defects in three-phase induction motors using Park's transform and radial basis function neural networks.* Sadhana, 2006. **31**(3): p. 235-244-244.

120. Benbouzid, M.E.H., et al., *Induction motor asymmetrical faults detection using advanced signal processing techniques.* Energy Conversion, IEEE Transactions on, 1999. **14**(2): p. 147-152.

121. Cabal-Yepez, E., et al. *FPGA-Based Online Induction Motor Multiple-Fault Detection with Fused FFT and Wavelet Analysis*. in *Reconfigurable Computing and FPGAs, 2009. ReConFig '09. International Conference on*. 2009.

122. Durocher, D.B. and G.R. Feldmeier, *Predictive versus preventive maintenance.* Industry Applications Magazine, IEEE, 2004. **10**(5): p. 12-21.

123. Wang, H. and W. Yang. *Rotor bar fault feature extraction of induction motor base on FFT and MUSIC*. in *Mechatronic Science, Electric Engineering and Computer (MEC), 2011 International Conference on*. 2011.

124. Mahamad, A.K. and T. Hiyama. *Improving Elman Network using genetic algorithm for bearing failure diagnosis of induction motor*. in

Diagnostics for Electric Machines, Power Electronics and Drives, 2009. SDEMPED 2009. IEEE International Symposium on. 2009.

125. Ertan, H.B. and O. Keysan. *External search coil as a means of measuring rotor speed of an induction motor*. in *Advanced Electromechanical Motion Systems & Electric Drives Joint Symposium, 2009. ELECTROMOTION 2009. 8th International Symposium on*. 2009.

126. Qianxiang, L. and H. Jingtao. *A high accuracy FFT algorithm for induction motor sensor-less speed estimation*. in *Electrical Machines and Systems, 2008. ICEMS 2008. International Conference on*. 2008.

127. Brigham, E.O., *The Fast Fourier Transform And Its Applications*. Vol. 1. 1988: Prentice-Hall, Inc.

128. Hamidi, H., A.R. Nasiri, and F. Nasiri. *Detection and isolation of mixed eccentricity in three phase induction motor via wavelet packet decomposition*. in *Control Conference, 2004. 5th Asian*. 2004.

129. Zhongming, Y., W. Bin, and A. Sadeghian, *Current signature analysis of induction motor mechanical faults by wavelet packet decomposition.* Industrial Electronics, IEEE Transactions on, 2003. **50**(6): p. 1217-1228.

130. Antonino-Daviu, J., et al., *Application and optimization of the discrete wavelet transform for the detection of broken rotor bars in induction machines.* Applied and Computational Harmonic Analysis, 2006. **21**(2): p. 268-279.

131. Eren, L. and M.J. Devaney, *Bearing damage detection via wavelet packet decomposition of the stator current.* Instrumentation and Measurement, IEEE Transactions on, 2004. **53**(2): p. 431-436.

132. Douglas, H., P. Pillay, and A. Ziarani. *Detection of broken rotor bars in induction motors using wavelet analysis*. in *Electric Machines and Drives Conference, 2003. IEMDC'03. IEEE International*. 2003.

133. Sang-Hyuk, L., et al. *Fourier and wavelet transformations for the fault detection of induction motor with stator current*. in *Industrial Electronics Society, 2004. IECON 2004. 30th Annual Conference of IEEE*. 2004.

134. Barendse, P.S., et al. *The application of wavelets for the detection of inter-turn faults in induction machines*. in *Electric Machines and Drives Conference, 2009. IEMDC '09. IEEE International*. 2009.

135. Das, S., et al. *Wavelet aided SVM classifier for stator inter-turn fault monitoring in induction motors*. in *Power and Energy Society General Meeting, 2010 IEEE*. 2010.

136. Williamson, S. and K. Mirzoian, *Analysis of Cage Induction Motors with Stator Winding Faults.* Power Apparatus and Systems, IEEE Transactions on, 1985. **PAS-104**(7): p. 1838-1842.

137. Tallam, R.M., et al. *Neural network based on-line stator winding turn fault detection for induction motors*. in *Industry Applications Conference, 2000. Conference Record of the 2000 IEEE*. 2000.

138. Tallam, R.M., et al., *A Survey of Methods for Detection of Stator-Related Faults in Induction Machines.* Industry Applications, IEEE Transactions on, 2007. **43**(4): p. 920-933.

139. Wang, J. and R. Hamilton. *A review of negative sequence current*. in *Protective Relay Engineers, 2010 63rd Annual Conference for*. 2010.

140. Kliman, G.B., et al. *A new approach to on-line turn fault detection in AC motors*. in *Industry Applications Conference, 1996. Thirty-First IAS Annual Meeting, IAS '96., Conference Record of the 1996 IEEE*. 1996.

141. Bouzid, M. and G. Champenois. *A novel reliable indicator of stator windings fault in induction motor extracted from the symmetrical components*. in *Industrial Electronics (ISIE), 2011 IEEE International Symposium on*. 2011.

142. Janeiro, F.M., et al. *Induction Motor Broken Bars Online Detection*. in *Instrumentation and Measurement Technology Conference Proceedings, 2008. IMTC 2008. IEEE*. 2008.

143. Nise, N.S., *Control Systems Engineering*. 3rd ed2000: John Wiley and Sons.

144. Benbouzid, M.E.H., M. Vieira, and C. Theys, *Induction motors' faults detection and localization using stator current advanced signal processing techniques.* IEEE Transactions on Power Electronics, 1999. **14**(1): p. 14-22.

145. Tak Son, C. and Z. Linzheng. *A new prototype of diagnosis system of inner-faults for three-phase induction motors developed by expert system*. in *Electrical Machines and Systems, 2001. ICEMS 2001. Proceedings of the Fifth International Conference on*. 2001.

146. Li, B., et al., *Fuzzy lattice classifier and its application to bearing fault diagnosis.* Applied Soft Computing, 2012. **12**(6): p. 1708-1719.

147. Lasurt, I., A.F. Stronach, and J. Penman. *A fuzzy logic approach to the interpretation of higher order spectra applied to fault diagnosis in electrical machines*. in *Fuzzy Information Processing Society, 2000. NAFIPS. 19th International Conference of the North American*. 2000.

148. Schoen, R.R., et al., *An unsupervised, on-line system for induction motor fault detection using stator current monitoring.* Industry Applications, IEEE Transactions on, 1995. **31**(6): p. 1280-1286.

149. Goode, P.V. and C. Mo-Yuen, *Using a neural/fuzzy system to extract heuristic knowledge of incipient faults in induction motors: Part II-Application.* Industrial Electronics, IEEE Transactions on, 1995. **42**(2): p. 139-146.

150. Amari, S. and S. Wu, *Improving support vector machine classifiers by modifying kernel functions.* Neural Networks, 1999. **12**(6): p. 783-789.

151. Rojas, A. and A.K. Nandi, *Practical scheme for fast detection and classification of rolling-element bearing faults using support vector machines.* Mechanical Systems and Signal Processing, 2006. **20**(7): p. 1523-1536.

152. Samanta, B., *Gear fault detection using artificial neural networks and support vector machines with genetic algorithms.* Mechanical Systems and Signal Processing, 2004. **18**(3): p. 625-644.

153. Samanta, B., K.R. Al-Balushi, and S.A. Al-Araimi, *Artificial neural networks and support vector machines with genetic algorithm for bearing fault detection.* Engineering Applications of Artificial Intelligence, 2003. **16**(7–8): p. 657-665.

154. Samanta, B. and K.R. Al-Balushi, *Artificial neural network based fault diagnostics of rolling element bearings using time-domain features.* Mechanical Systems and Signal Processing, 2003. **17**(2): p. 317-328.

155. Widodo, A. and B.-S. Yang, *Support vector machine in machine condition monitoring and fault diagnosis.* Mechanical Systems and Signal Processing, 2007. **21**(6): p. 2560-2574.

156. Gordi Armaki, M. and R. Roshanfekr. *A new approach for fault detection of broken rotor bars in induction motor based on support vector machine*. in *Electrical Engineering (ICEE), 2010 18th Iranian Conference on*. 2010.

157. Kwak, J.-S. and M.-K. Ha, *Neural network approach for diagnosis of grinding operation by acoustic emission and power signals.* Journal of Materials Processing Technology, 2004. **147**(1): p. 65-71.

158. Hurdle, E.E., L.M. Bartlett, and J.D. Andrews, *Fault diagnostics of dynamic system operation using a fault tree based method.* Reliability Engineering & System Safety, 2009. **94**(9): p. 1371-1380.

159. Ericson, C.A., *Fault Tree Analysis- A History*, in *17th International System Safety Conference*1999.

160. Madden, M.G.M. and P.J. Nolan, *Monitoring and diagnosis of multiple incipient faults using fault tree induction.* Control Theory and Applications, IEE Proceedings -, 1999. **146**(2): p. 204-212.

161. R. SaravanaKumar, K., Vinoth Kumar, and K.K.Ray, *Fuzzy Logic Based Fault Detection in Induction Machines using Labview.* International Journal of Computer Science and Network Security, 2009. **9**(9): p. 226-243.

162. Benbouzid, M.E.H. and H. Nejjari. *A simple fuzzy logic approach for induction motors stator condition monitoring*. in *Electric Machines and Drives Conference, 2001. IEMDC 2001. IEEE International*. 2001.

163. Mini, V.P. and S. Ushakumari. *Incipient fault detection and diagnosis of induction motor using fuzzy logic*. in *Recent Advances in Intelligent Computational Systems (RAICS), 2011 IEEE*. 2011.

164. Pereira, L.A. and D. da Silva Gazzana. *Rotor broken bar detection and diagnosis in induction motors using stator current signature analysis and fuzzy logic*. in *Industrial Electronics Society, 2004. IECON 2004. 30th Annual Conference of IEEE*. 2004.

165. Pereira, L.A., D. da Silva Gazzana, and L.F.A. Pereira. *Motor current signature analysis and fuzzy logic applied to the diagnosis of short-circuit faults in induction motors*. in *Industrial Electronics Society, 2005. IECON 2005. 31st Annual Conference of IEEE*. 2005.

166. Karanayil, B., M.F. Rahman, and C. Grantham. *Stator and rotor resistance observers for induction motor drive using fuzzy logic and artificial neural networks*. in *Industry Applications Conference, 2003. 38th IAS Annual Meeting. Conference Record of the*. 2003.

167. Ghate, V.N. and S.V. Dudul, *Cascade Neural-Network-Based Fault Classifier for Three-Phase Induction Motor.* Industrial Electronics, IEEE Transactions on, 2011. **58**(5): p. 1555-1563.

168. Mohan, N., *Electric drives : an integrated approach*2003, Minneapolis: MNPERE.

169. Wildi, T., *Electrical Machines, Drives and Power Systems*2002: Prentice Hall.

170. Penman, J., et al., *Condition monitoring of electrical drives.* IEE Proceedings Part B : Electric Power Applications, 1986. **133**(3): p. 142-148.

171. Mohan, N., *Electric drives : an integrated approach*2001, Minneapolis: MNPERE.

172. Chalmers, B. and A. Williamson, *AC Machines: Electromagnetics and Design*. 1st Edition ed1991: Research Studies Press.

173. Chapman, S.J., *Electric Machinery Fundamentals*1999: McGraw-Hill.

174. Hughes, A., *Electric Motors and Drives-fundamentals, Types and Applications*. 5th ed2001: Newnes.

175. Mohan, N., *Advanced Electric Drives Analysis, Control and Modeling using Simulink*2006: Minneapolis, MN, MNPERE.

176. Sokolowski, J.A. and C.M. Banks, *Principles of Modeling and Simulation: A Multidisciplinary Approach*2009: John Wiley & Sons, Inc.

177. Ljung, L. and T. Glad, *Modeling of dynamic systems*1994, Upper Saddle River, N. J.: Prentice Hall

178. Switchgear & Instrumentation, S.I., *Motor Manager 6 User Guide*, 2005.

179. ABB, *ACS800 Hardware Manual*, 2005.

180. Powell, *3 Phase Sensor Box Electronic Manual.* 2009.

181. Stack, J.R., T.G. Habetler, and R.G. Harley, *Fault classification and fault signature production for rolling element bearings in electric machines.* Industry Applications, IEEE Transactions on, 2004. **40**(3): p. 735-739.

182. Han, T., et al., *Fault Diagnosis System of Induction Motors Based on Neural Network and Genetic Algorithm Using Stator Current Signals.* Internaional Journal of Rotating Machenary, 2006: p. 1-13.

183. Blumam, A.G., *Elementry Statistics*. 2nd Edition, ed2003: Mc Graw Hill.

184. Brown, J.D. *Standard error vs. Standard errrorr of measurement*. 1999.

185. Eltabach, M., et al. *Features Extracaction using vibration signals for condition monitoring of lifting cranes*.

186. Ben-Hur, A. and J. Weston, *A User's Guide to Support Vector Machines*.

187. Gunn, S.R., *Support Vector Machines for Classification and Regression*, 1998, University of Southampton. p. 66.

188. Boser, B.E., I.M. Guyon, and N.V. Vapnik, *A training algorithm for optimal margin classiers*, in *5th Annual ACM Workshop on COLT*1992, ACM Press: Pittsburgh, PA. p. 144-152.

189. Scholkopf, B. and A.J. Smola, *Learning With Kernels,* 2002, Cambridge, MA: MIT Press.

190. Cristianini, N. and J. Shawe-Taylor, *An Introduction to Support Vector Machines and Other Kernel-based Learning Methods*2000: Cambridge University Press.

191. Milgram, J., M. Cheriet, and R. Sabourin, *"One Against One" or "One Against All": Which One is Better for Handwriting Recognition with SVMs?*, in *Tenth International Workshop on Frontiers in Handwriting Recognition* 2006.

192. Chang, C. and L. CJ. *LIBSVM -- A Library for Support Vector Machines*. 2012 12 September 2012]; Available from: http://www.csie.ntu.edu.tw/~cjlin/libsvm/.

193. Rifkin, R. and A. Klautau, *In defense of one-vs-all classication.* Journal of Machine Learning Research, 2004. **5**: p. 101-104.

194. Zhenyu Yang, Z., et al., *A Study of Rolling-Element Bearing Fault Diagnosis Using Motor's Vibration and Current Signatures*, in *7th IFAC Symposium on Fault Detection, Supervision and Safety of Technical Processes*2009: Barcelona, Spain.

Appendices

Appendix-I: Fuzzy Logic

I.1 Introduction

Fuzzy logic is technique that is used to translate verbal ideas to some numbers and then uses these numbers to associate particular concepts. Fuzzy Logic is very helpful in the situation to make a decision where there is no clear difference between the true or false. So Fuzzy Logic can be used in condition where answer is present between this true and false. This usually happens in case of machines during the particular fault diagnosis. Practically it is not possible to classify a machine's conditions with respect to particular fault, so Fuzzy Logic is used by classifying a particular fault with its degree of severity. The most important feature of using Fuzzy Algorithm is that the human knowledge/experience can be combined into the system. The general case of Fuzzy Logic is shown in Figure I.1.

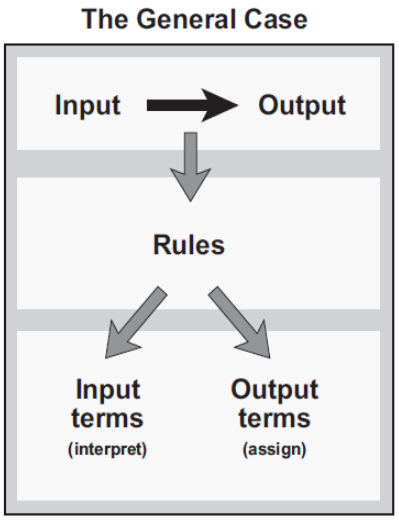

Figure I. 1: General case of fuzzy logic

In Fuzzy Logic precision is very much important. It is a suitable way which is used to map an input variable to an output variable. This is the starting point for Fuzzy Logic. Consider an example of tipping in a restaurant that is dependent on how much the service is good at a restaurant; Fuzzy Logic will decide what will be the tip. The graphical representation of this tipping example is shown in Figure I.2.

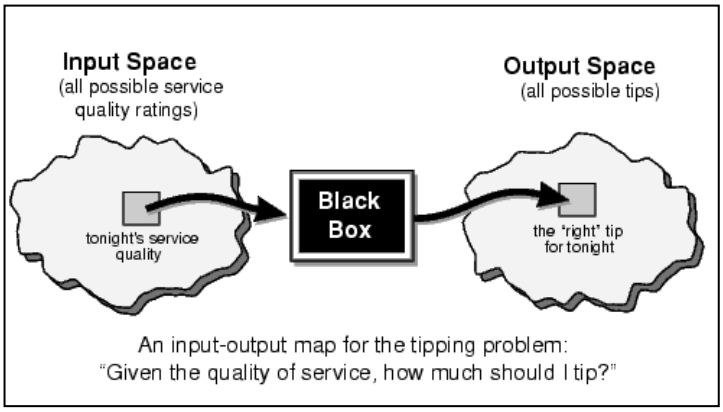

Figure I. 2**:** Example of tipping

I.2 Foundations of Fuzzy Logic

Fuzzy Logic is dependent on four things.

1. Fuzzy Sets
2. Membership Functions
3. Logical Operations
4. If-then Rules
5. Implication

I.2.1 Fuzzy Sets

The input and output functions of the Fuzzy Logic is fuzzy sets. In the example of tipping in the restaurant the input fuzzy sets will be the quality of food and quality of service and the output fuzzy set will be the tipping membership functions. This is shown in Figure I.3.

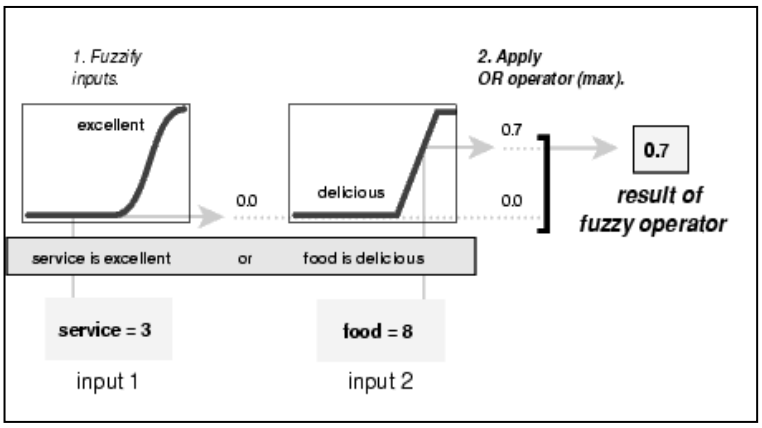

Figure I. 3**:** Input of fuzzy set

I.2.2 Membership Functions

Membership function is basically a curve that is used for mapping an input value to a membership value that is varying from 0 to 1. There are different types of curves that can be used as membership function; examples can be trapezoid, triangular, Sigmoid and double sigmoid as shown in Figure I.4.

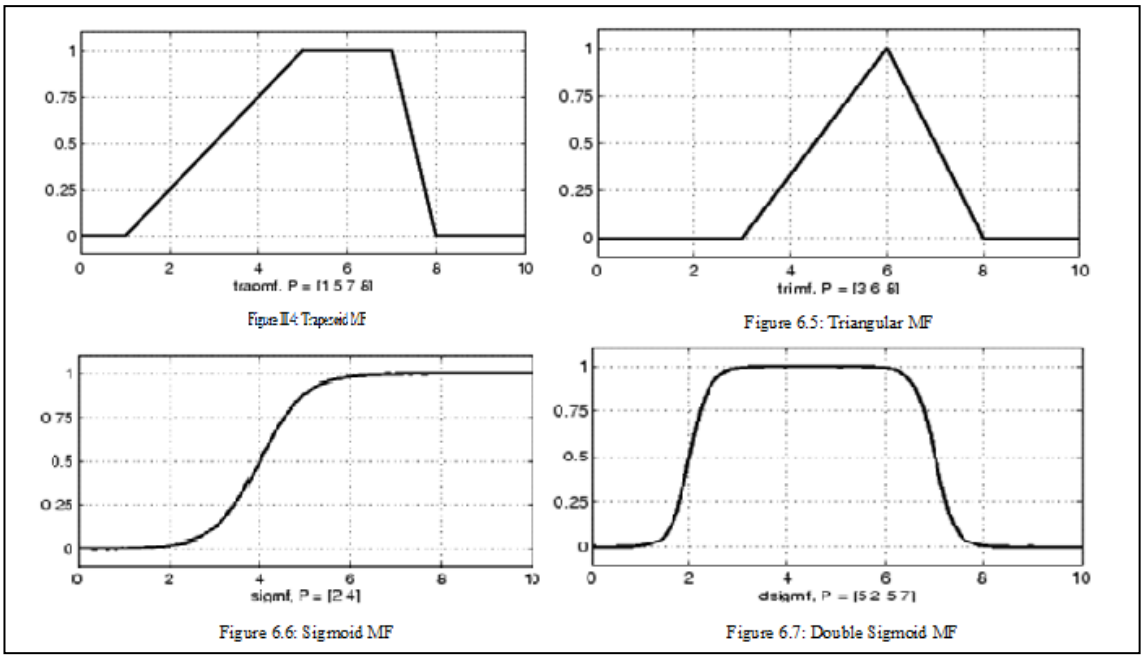

Figure II.4 Trapezoid MF

Figure 6.5: Triangular MF

Figure 6.6: Sigmoid MF

Figure 6.7: Double Sigmoid MF

Figure I. 4 Membership functions

I.2.3 Logical Operations

Normal Boolean logic is used in fuzzy reasoning. In Boolean logic there is number possibilities that can be used when implementing a fuzzy logic but commonly used one are the simplest one that is shown in Table I.1. Figure I.5 shows the logical operation used in tipping example.

Table I.1: Boolean Logic

AND			OR			NOT	
A	B	Min(A,B)	A	B	Max(A,B)	A	1-A
0	0	0	0	0	0	0	1
0	1	0	0	1	1	1	0
1	0	0	1	0	1		
1	1	1	1	1	1		

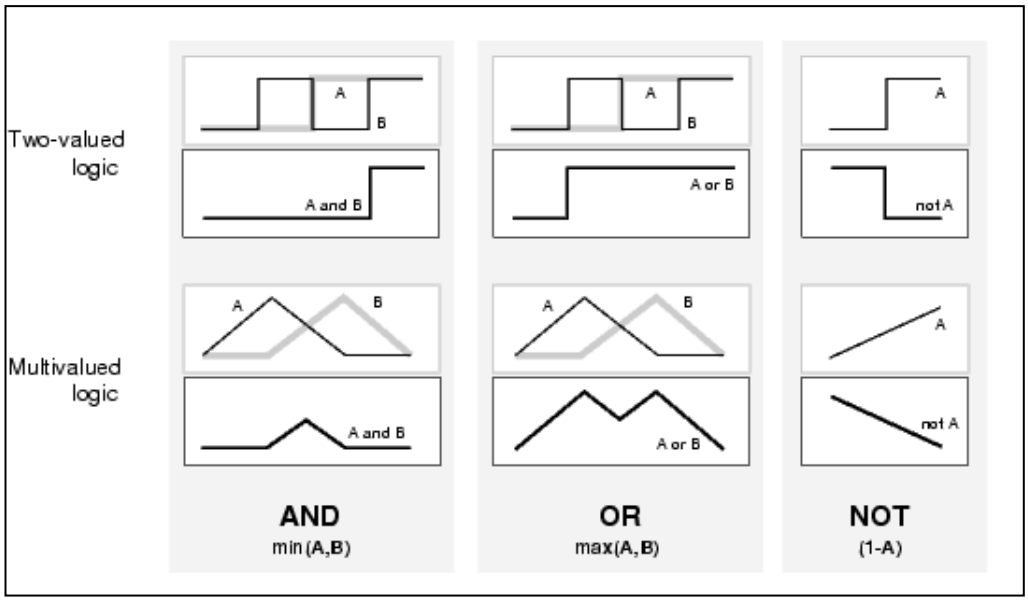

Figure I. 5: Logic Operations

I.2.4 If-Then Rules

If-then rules are used to interpret the knowledge in some form. This is the most popular form to represent the knowledge as the rules. These rules are basically the knowledge. These are used for the précised decision making. It is basically used to map the membership value to an output value. In the example of tipping some of the rules are given below.

- IF service is poor OR food is rancid
- THEN tip is cheap
- IF service is excellent OR food is delicious
- THEN tip is generous

I.2.5 Implications

There are two types of implications i.e. minimum implication and the product implications. In case of minimum implications the membership value was got from

input membership function; output membership function is truncated to that value. In case of product implications the result is simply the multiplication of input membership value and the output membership value. The difference is shown in Figure I.6.

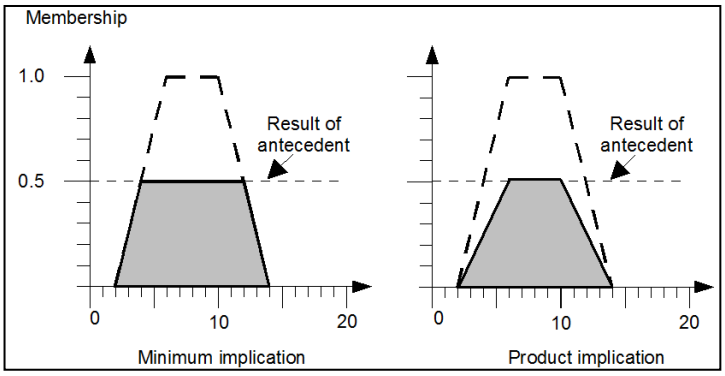

Figure I. 6: Implications

I.3 Fault Detection Process

By using the Fast Fourier Transform (FFT) rotor bar faults can be analysed using the current spectrum of Induction Motors. This technique depends on the analysis of particular harmonics in spectrum which are caused by the rotor bar faults. Figure I.7 shows the ideal spectrum. The sideband frequencies near the main frequency are due to broken bars. In idealized condition, rotating magnetic field produced in induction motor is given by:

$$n_1 = \frac{120\ f_1}{p} \tag{I-1}$$

Where: f_1 = Supply Frequency, p = Poles in the Induction Motor.

$$\text{slip } (s) = {}^{(n_1 - n)}/_{n_1} \tag{I-2}$$

Where: n = Synchronous speed of induction motor, n_1 = Actual speed of induction motor.

Side band frequencies will occur at ± 2s f_1 on both side of fundamental frequency

fb=(1±2s)f. (I.3)

I.4 Measured Data

Induction motor (M1) was tested in healthy working condition and for broken rotor bars. All the tests are done at same load that is of 49.6Nm. The frequency range is from 0 to 100 Hz, as it contains the fundament frequency and almost all the visible side band. In Figure I.7 the magnitude at 45.32 Hz is-63.32 dB/Hz. The figure shows that the side band frequencies are close to fundamental frequency with almost negligible in amplitude.

Figure I.7 shows the power spectrum of a motor with one bar broken. The figure clearly shows that the magnitude of side band frequency are increasing that is at 45.93 Hz the magnitude is increased to (- 39.82) dB/Hz.

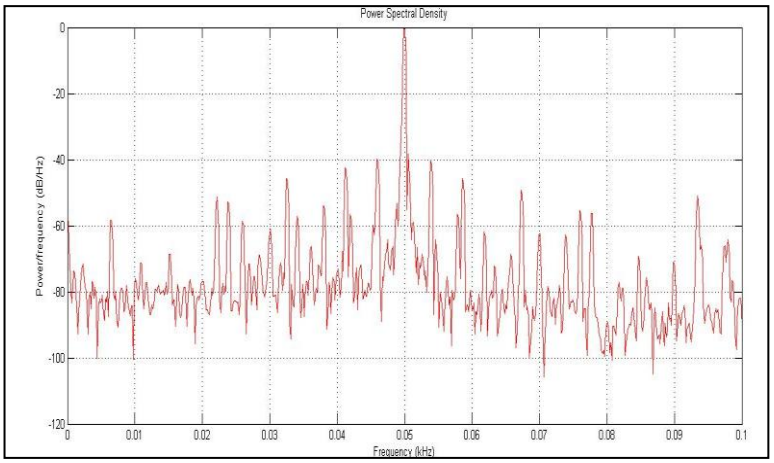

Figure I. 7: One bar Broken Spectrum

Now the side magnitude of side band frequency is increased due to increase in the number of bars broken. At 45.78 Hz the magnitude of power spectrum is -33.86 dB/Hz.

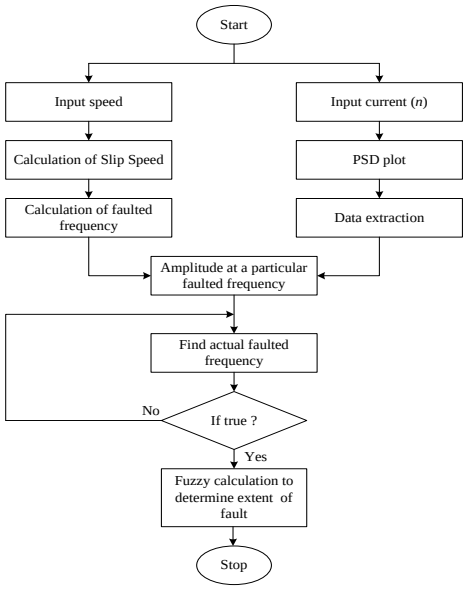

Figure I.8: Flow chart of fault detection algorithm

I.5 Amplitude at Particular Faulted Frequency

First calculate the slip speed of motor by putting the value of actual and synchronous speed of motor in equation I.2. This slip speed is used to calculate the particular faulted frequency in the spectrum by using the equation 7.7. The value of current (i1) is used to plot the spectrum of PSD.

I.6 Actual Faulted Frequency

The calculated faulted frequency is not the actual faulted frequency. The actual faulted frequency is slightly different from the calculated one. The program will check for actual faulted frequency by finding the highest amplitude in the range of -2 Hz from the calculated frequency this is done by finding all the bits of arrays that is greater than the calculated faulted frequency. Then applying for loop on this particular bit array which starts from 22 bits lesser to 3 bits higher and respectively check for highest amplitude corresponding to each bit.

I.7 Diagnosis Using Fuzzy Logic

Fuzzy Logic is used to determine how much fault is present in Induction Motor. Amplitude calculated is used along with Fuzzy Logic to determine how much fault or how many rotor bars are broken in a particular motor. The extracted amplitude from the PSD plot is the fuzzy sets. This fuzzy set of amplitude is divided into different ranges that are small, medium, large and very large. These ranges are basically for the input membership function. The input membership functions used are the triangular and trapezoid. The membership functions used for the output are also the triangular and trapezoid. This output membership function is also divided into small ranges that is healthy, cracked, one bar broken, two bars broken which are used to

determine the extent of fault present in induction motor. The Boolean Logic used for the reasoning of Fuzzy Logic is AND. The implication used for the defuzzification is product implication as it is more précised as compare to minimum implication. The decision made by fuzzy system is based on some rules. There are four different rules which are made for this fuzzy system as given below:

- If (amplitude is small) then (output is healthy)
- If (amplitude is medium) then (output is cracked)
- If (amplitude is large) then (output is one bar broken)
- If (amplitude is very large) then (output is two bar broken)

I.8 Results and Discussion - Healthy Motor

The PSD plot of a healthy motor is plotted using the current (i1) at 35 Nm and 49.6 Nm loads as shown in Figures I.9 and I.10 respectively. From the figure it is seen that for the healthy motor side band frequencies are very close to fundamental frequency. At 35Nm load the amplitude of side band frequencies is small as the current in rotor is small as shown in Figure I.9. At 49.6 Nm load the magnitude of side and frequencies is increased as the load is increased from 35 Nm to 49.6 Nm as shown in Figure I.4. From Figure I.3 and Figure I.4 it is observed as the load of motor was increased the amplitude of side band frequency also increased and the rotor bar faults are easy to determine at full load or at maximum load. Then fuzzy logic is used to determine how much fault is present in induction motor. The input and output membership functions of fuzzy system are shown in Figure I.11 and Figure I.12.

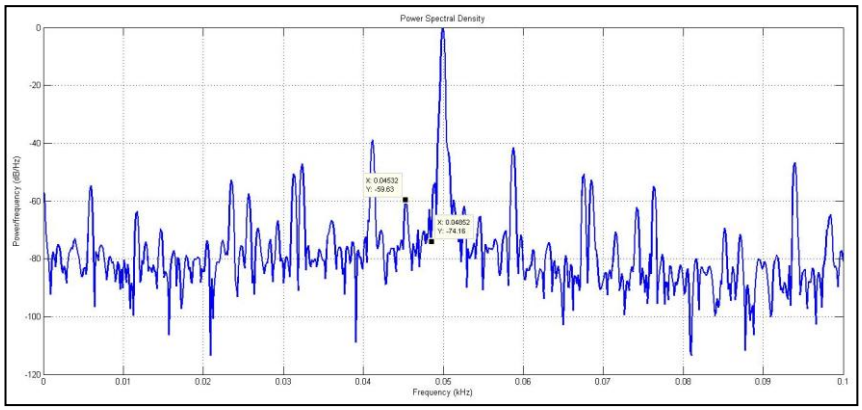

Figure I.9: PSD of Healthy Motor at 35 Nm Load

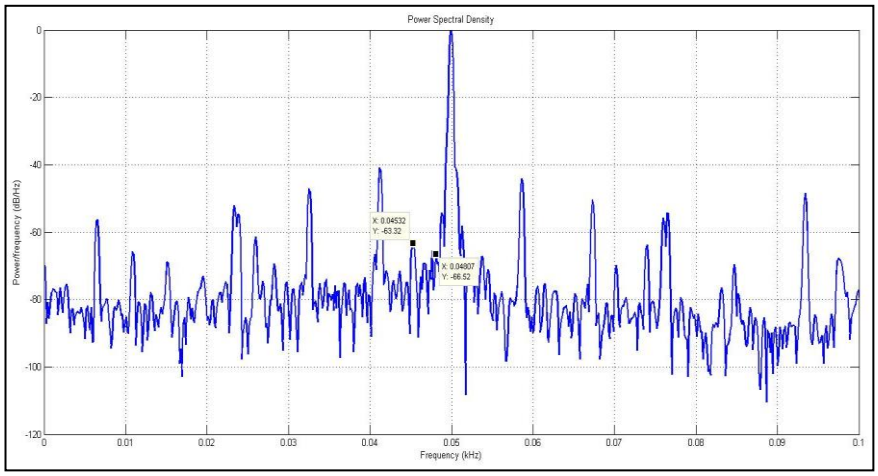

Figure I.10: PSD of Healthy Motor at 49.6 Nm Load

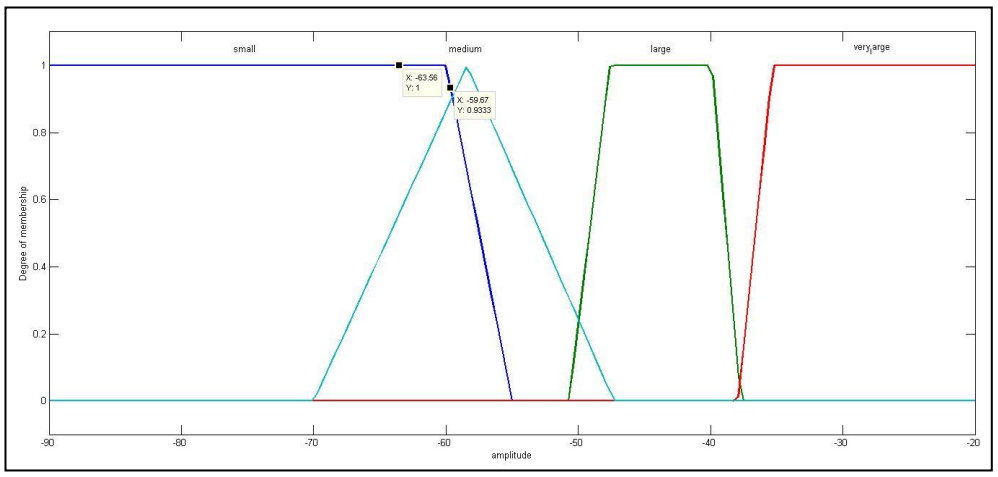

Figure I.11: Input MF of fuzzy logic of healthy motor

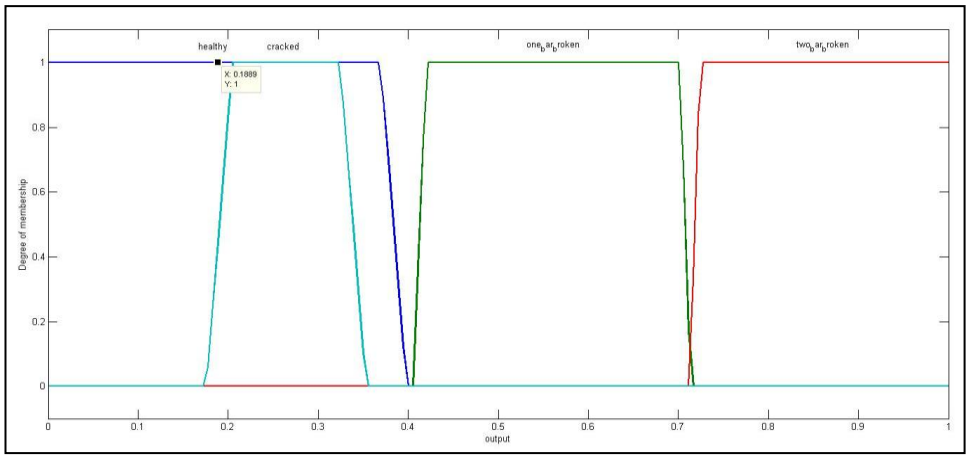

Figure I.12: Output MF of Fuzzy Logic of Healthy Motor.

All the observations and results of PSD plot and fuzzy system is shown in Table I.2.

Table I.2**:** Results and Observations of Healthy Motor

Load	35 Nm Load`	49.6 Nm Load
Synchronous speed (rpm)	1500	1500
Actual speed (rpm)	1459	1441
Slip	0.0273	0.0393
Faulted frequency (KHz)	0.0485	0.0480
Amplitude (dB/Hz)	-74.16	-66.52
Actual faulted frequency (KHz)	0.0453	0.0453
Amplitude (dB/Hz)	-59.67	-63.39
Input MF value	-59.67	-63.39
Output MF value	0.1889	0.1889

From the Figure I.1 and Table I.2 it is seen that the condition of a particular motor can be determined easily by using the fuzzy system. From the Figure I.2 it clearly shows that a motor is healthy with no rotor faults.

I.9 One Bar Broken Motor

A 6mm hole is made in one bar of the rotor which is equal to the one bar broken in the rotor.. The PSD is plotted for the induction motor whose one bar is broken at a load of 35 Nm and 49.6 Nm. The PSD spectrum at 35 Nm load is given in Figure I.13 and the spectrum of 49.6 Nm is given in Figure I.14. From these figures it is concluded that amplitude of side band frequencies are increasing as the fault in the IM is increasing. The calculated and actual frequency along with their amplitude is shown in these figures. The amplitude of side band frequency is fed to fuzzy logic system in order to determine intensity of fault present in motor. The input and output MF of fuzzy logic is shown in the Figure I.15 and Figure I.16 along with the results of motor.

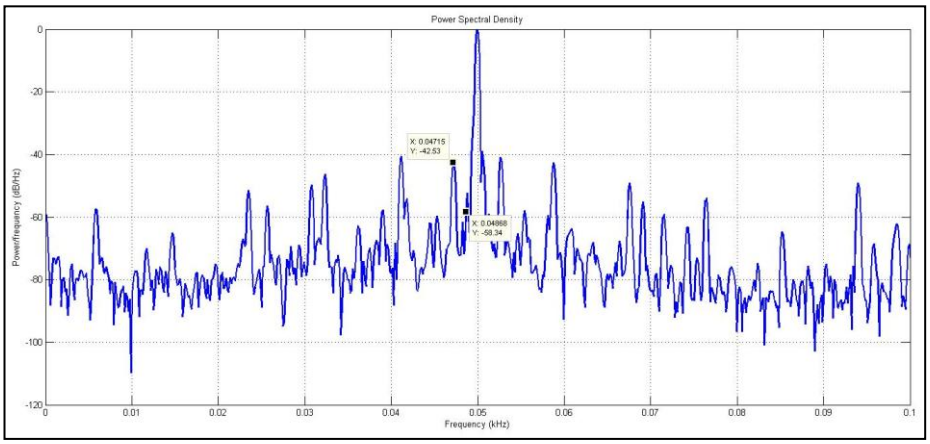

Figure I.13**:** PSD of One Rotor Bar Broken Motor at 35 Nm Load

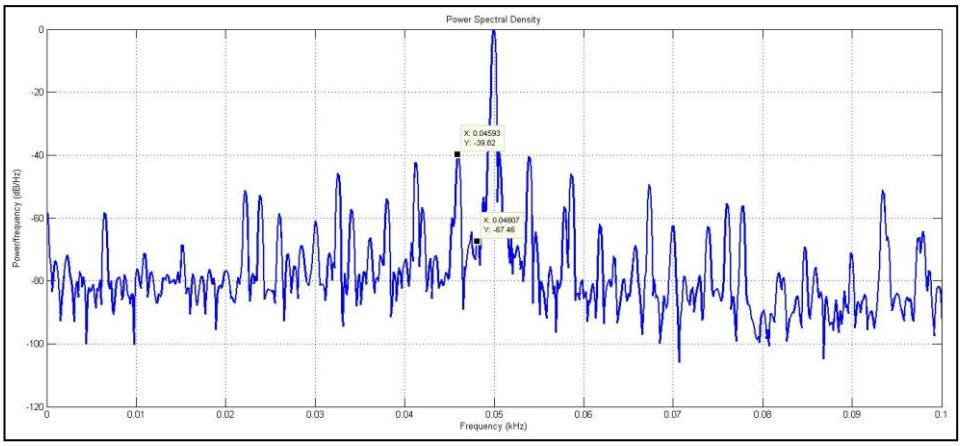

Figure I.14**:** PSD of One Rotor Bar Broken motor at 49.6 Nm Load

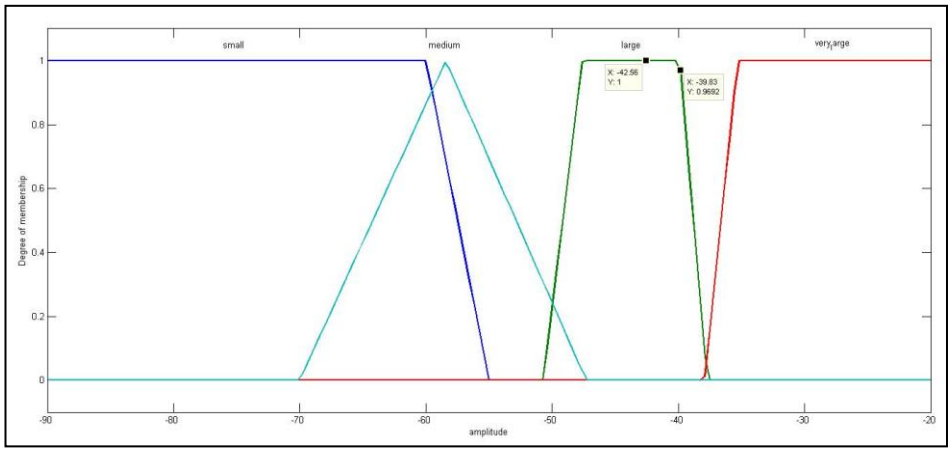

Figure I.15**:** Input MF of Fuzzy Logic of One Rotor Bar Broken

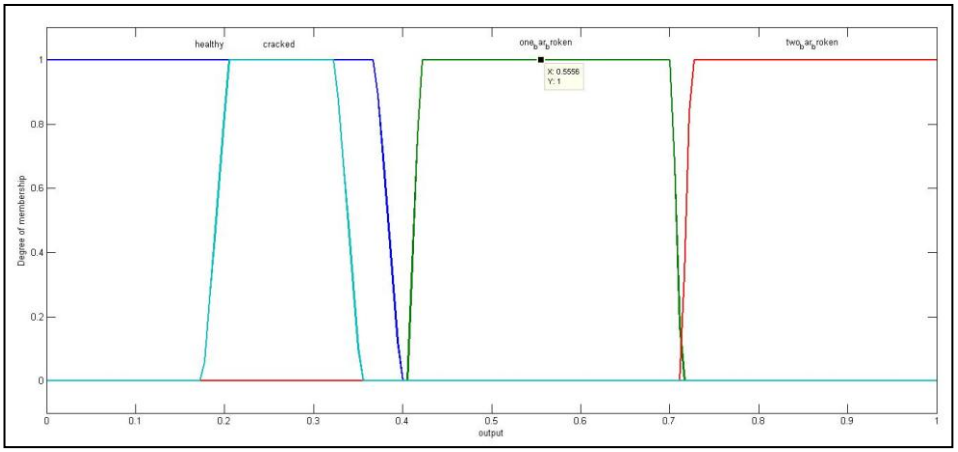

Figure I.16**:** Output MF of Fuzzy Logic of One Rotor Bar Broken

The result of one rotor bar broken is given in Table I.3.

Table I.3**:** Results and observations of one rotor bar broken motor

Load	35 Nm Load`	49.6 Nm Load
Synchronous speed (rpm)	1500	1500
Actual speed (rpm)	1457	1439
Slip	0.0287	0.0407
Faulted frequency (KHz)	0.0486	0.0480
Amplitude (dB/Hz)	-58.3667	-67.4569
Actual faulted frequency (KHz)	0.04715	0.04593
Amplitude (dB/Hz)	-42.5239	-39.8168
Input MF value	-42.5239	-39.8168
Output MF value	0.5599	0.5599

I.10 Conclusion

From the observation it is seen that the rotor bar faults only affect the two sideband frequency. At no load it is very difficult to detect the rotor bar faults as the current in motor is very small so the particular faulted frequency is very close to the fundamental 50Hz frequency. So the motor was test at two different loads that is 35 Nm and 49.6 Nm.

At 35 Nm load detection of rotor bar faults was slightly difficult because the motor works at low slip as compare to 49.6 Nm load. It is very much reliable to detect the rotor bars faults at 48.6 Nm load.

At 49.6 Nm load amplitude of faulted frequencies is very much high as compare to no load motor or with 35 Nm load. So the faulted frequency can easily be recognized at 49.6 Nm load. Results show that as the rotor bar faults is increasing, faulted frequency increases.

The advantage of detecting rotor bar faults using the FFT Technique is that it is very much suitable for high load condition and can be implemented easily. The disadvantage of this technique is that it has lost time information and not very much effective for the lightly loaded condition.

Appendix-II: Motor Data Sheet

ISO 9001
Certificate No.
Certificate No.
Certificate No.

BROOK CROMPTON

Tel. Fax.

EQUIVALENT CIRCUIT PARAMETERS

Supplied To:	Frame Ref. W-DA132MB		Serial Number
	Output 7.5 kW		Volts 400 Delta
Purchase Order / Enquiry Ref.	Hertz 50	IC 411	Amps 15.2A @ 400/50
Account No.	Rev/Min 1445		Poles 4
Note: All equivalent circuit parameters are in Ohms per phase referred to the stator	Duty/Rating S1		Sec. Volts / Sec. Amps
Slip is expressed as a per unit value	Phases 3	Insulation F	Cos ϕ 0.82 / IP 55
Reference temperature for locked rotor :- 20°C Reference temperatures for full load :- 75°C.			

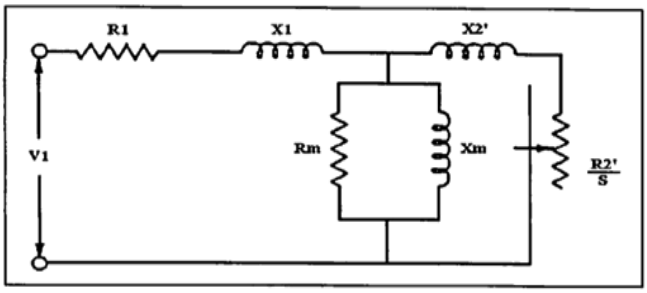

Machine parameter	Locked rotor	Full load
R1	1.71	2.08
X1	2.60	5.36
R2'	1.65	1.66
X2'	2.50	4.56
RM	2766	2766
XM	85.9	85.9

The induction Motor data supplied by manufacturer:

Nameplate Data of The Motor.

Parameter	Symbol	Value	Unit
Number of stator phases	m	3	-
Number of pole pairs	p	2	-
Stator winding connection	Δ	-	-
Rated power	P_{rated}	7.5	kW
Rated supply voltage (LL , rms)	V_{rated}	415	V
Line frequency	f	50	Hz
Rated current	I_{rated}	15.2	A
Rated speed	N_{rated}	1445	rpm
Rated electromagnetic torque	$T_{e,\ rated}$	49	$N.m$

Data Used for dq Modeling (Rated Values in 20° C)

Parameter	Symbol	Value	Unit
Stator phases' electrical resistance	R_s	1.71	Ω
Stator phases' electrical reactance	X_{ls}	5.36	Ω
Rotor electrical resistance	R_r	1.90	Ω
Rotor electrical reactance	X_{lr}	5.0	Ω
Magnetizing resistance	R_m	2284	Ω
Magnetizing reactance	X_m	81.9	Ω